

APPENDIX O

HYDRODYNAMIC MODEL DEVELOPMENT, CALIBRATION, VERIFICATION, AND EVALUATION OF FLOW REDUCTION AND SEA LEVEL RISE SCENARIOS IN AID OF MINIMUM FLOWS DEVELOPMENT FOR THE LOWER LITTLE MANATEE RIVER

Prepared for:
Southwest Florida Water Management District
2379 Broad Street
Brooksville, FL 34604-6899

Prepared by:

The logo for Janicki Environmental, Inc. features a stylized wave shape with a blue-to-green gradient. The company name is written in a sans-serif font across the middle of the wave.

Janicki Environmental, Inc.

Janicki Environmental, Inc.
1155 Eden Isle Drive NE
St. Petersburg, FL 33704

September 2023

Table of Contents

1.0 INTRODUCTION	1-1
1.1 Project Background and Objectives.....	1-1
1.2 Report Outline	1-1
2.0 HYDRODYNAMIC MODEL DEVELOPMENT	2-1
2.1 EFDC Model Description.....	2-1
2.2 Model Grid and Bathymetry	2-2
2.3 Available Data and Model Calibration and Verification Periods.....	2-10
3.0 HYDRODYNAMIC MODEL CALIBRATION AND VERIFICATION	3-1
3.1 Statistical Measures of Goodness of Fit	3-1
3.2 Calibration Results	3-3
3.3 Verification Results	3-10
4.0 BASELINE AND FLOW REDUCTION SCENARIOS	4-1
4.1 Description of Scenarios.....	4-1
4.2 Comparison of Results.....	4-2
4.3 Sensitivity Analysis.....	4-6
5.0 SEA LEVEL RISE SCENARIOS.....	5-1
6.0 SUMMARY AND CONCLUSIONS	6-1
7.0 REFERENCES	7-1
Attachment 1	A-1

1.0 INTRODUCTION

This report provides a description of an Environmental Fluid Dynamics Code (EFDC) hydrodynamic model developed to aid the District in evaluation and selection of a minimum flow for the tidal portion of the Little Manatee River. The project background and objectives are described below, followed by the outline of the report.

1.1 PROJECT BACKGROUND AND OBJECTIVES

The District has been working on developing minimum flows for the Lower Little Manatee River, defined as the portion of the river downstream of the US Highway 301 bridge and extending to the mouth of the river, over much of the last decade. Previous efforts included use of an EFDC model developed by Huang and Liu (2007). This model was used by Janicki Environmental, Inc. (JEI) to develop and update the recommended minimum flows for the Lower Little Manatee River (JEI 2018, Jacobs and JEI 2021). Peer review panel comments on the 2021 draft report (Peer Review Panel 2021; Appendix E of Main Report of which this document is Appendix K) called for improvements to the hydrodynamic model.

The objective of this effort was to revise the EFDC hydrodynamic model for the Lower Little Manatee River, complete appropriate model calibration and verification, and implement the model for a set of flow reduction and sea level rise scenarios, with comparisons of expected responses in salinity within the lower river to those of baseline conditions.

1.2 REPORT OUTLINE

The remainder of this report includes the following sections:

- Section 2 presents the description of the model development, including a general description of the EFDC hydrodynamic model utilized, the revised model grid and bathymetry for the grid derived from existing information, the model input data requirements and data sources used, and the periods chosen for model calibration and verification.
- Section 3 presents the model calibration and verification results, including graphical and statistical comparisons of simulated and observed data.
- Section 4 presents the set of flow reduction scenarios implemented and comparison of the results of these scenarios to those of the baseline condition with respect to salinity habitat metrics.
- Section 5 presents the set of sea level rise scenarios implemented for the baseline condition and proposed minimum flows for the lower river, with comparison of the results of the minimum flow scenarios for each sea level rise condition to those of the appropriate baseline scenario with sea level rise scenario.
- Section 6 summarizes the results of the model calibration and verification and the results of the flow reduction scenarios and the sea level rise scenarios.

2.0 HYDRODYNAMIC MODEL DEVELOPMENT

This section provides a detailed description of the hydrodynamic model for the Lower Little Manatee River, including an overview of the EFDC model itself, description of the model grid system developed for the lower river, and discussion of the availability of data needed for model development, including time periods for model calibration and verification.

2.1 EFDC MODEL DESCRIPTION

The EFDC model is a general-purpose modeling package for simulating two- and three-dimensional flow, transport, and biogeochemical processes in surface water systems including rivers, lakes, estuaries, reservoirs, wetlands, and nearshore to shelf-scale coastal regions. The model was developed by Dr. John Hamrick at the Virginia Institute of Marine Science (Hamrick, 1996), and is supported by the U.S. Environmental Protection Agency (EPA) Office of Research and Development (ORD), EPA Region 4, and EPA Headquarters. The Florida Department of Environmental Protection (FDEP) and the Florida water management districts have used this model extensively.

The physics of the EFDC model, and many aspects of the computational scheme, are equivalent to the widely used Blumberg-Mellor model (Blumberg and Mellor 1987). EFDC is an open source, public domain, surface water modeling system which can be used to model hydrodynamics, water quality, sediments, and contaminants, as described by Hamrick (1992) and Tetra Tech (2002, 2006a, 2006b, 2006c, 2006d, 2007). The hydrodynamic model is based on the first principles of conservation of mass and responses to physical forces (tides, winds, solar radiation, water inflows and outflows, and associated water movement). The EFDC model solves the three-dimensional, vertically hydrostatic, free surface, turbulent averaged equations of motions for a variable density fluid. Dynamically coupled transport equations for turbulent kinetic energy, turbulent length scale, salinity and temperature are also solved. The two turbulence parameter transport equations implement the Mellor-Yamada level 2.5 turbulence closure scheme (Mellor and Yamada 1982). The EFDC model uses a stretched or sigma vertical coordinate, and curvilinear orthogonal horizontal coordinates.

The following description of the EFDC model is taken largely from Tetra Tech (2007). The numerical scheme for the equations of motion uses second-order accurate spatial finite differencing on a staggered or C grid, and the time integration employs a second-order accurate three-time level finite difference scheme with an internal-external mode splitting procedure to separate the internal shear or baroclinic mode from the external free surface gravity wave or barotropic mode. The external mode solution is semi-implicit and simultaneously computes the two-dimensional surface elevation field by a preconditioned conjugate gradient procedure. The external solution is completed by the calculation of the depth-average barotropic velocities using the new surface elevation field. The model's semi-implicit external solution allows large time steps that are constrained only by the stability criteria of the explicit central difference or higher order upwind advection scheme used for the nonlinear accelerations. Horizontal boundary conditions for the external mode solution include

options for simultaneously specifying the surface elevation only, the characteristic of an incoming wave, free radiation of an outgoing wave, or the normal volumetric flux on arbitrary portions of the boundary (Tetra Tech 2007).

The model's internal momentum equation solution is implicit with respect to vertical diffusion and at the same time step as the external solution. The internal solution of the momentum equations is in terms of the vertical profile of shear stress and velocity shear. Time splitting inherent in the three-time level scheme is controlled by periodic insertion of a second-order accurate two time level trapezoidal step (Tetra Tech 2007).

The model implements a second-order accurate mass conservation fractional step solution scheme for the Eulerian transport equations at the same or twice the time step of the momentum equation solution (Smolarkiewicz and Margolin 1993). The advective step of the transport solution uses either the central difference scheme used in the Blumberg-Mellor model or a hierarchy of positive definite upwind difference schemes. The highest accuracy upwind scheme, second-order accurate in space and time, is based on a flux corrected transport version of Smolarkiewicz's multidimensional positive definite advection transport algorithm (Smolarkiewicz 1984; Smolarkiewicz and Clark 1986; Smolarkiewicz and Grabowski 1990). The horizontal diffusion step is explicit in time, with an implicit vertical diffusion step.

2.2 MODEL GRID AND BATHYMETRY

The spatial domain of the model grid system (Figure 2-1) extends from the upstream boundary at the US Highway 301 bridge crossing, coincident with the USGS Little Manatee River at US 301 near Wimauma, FL (No. 02300500) gage, located approximately 15 miles (24 km) upstream of the mouth of the river. Based on comments received as part of the Peer Review of the 2021 Draft Minimum Flows document, the downstream model domain extends into Tampa Bay proper. This provides a downstream boundary removed from the mouth of the river such that simulated flow reductions at the upstream end of the model domain are not expected to noticeably impact the downstream boundaries. The offshore boundary is approximately 3.4 miles (5.5 km) from the mouth of the river, with the northern and southern boundaries approximately 2.3 miles (3.7 km) and 3.4 miles (5.5 km) from the mouth of the river, respectively. Figure 2-2 provides additional views of zoomed in portions of the grid system to show how the grid system fits with the river's shoreline.

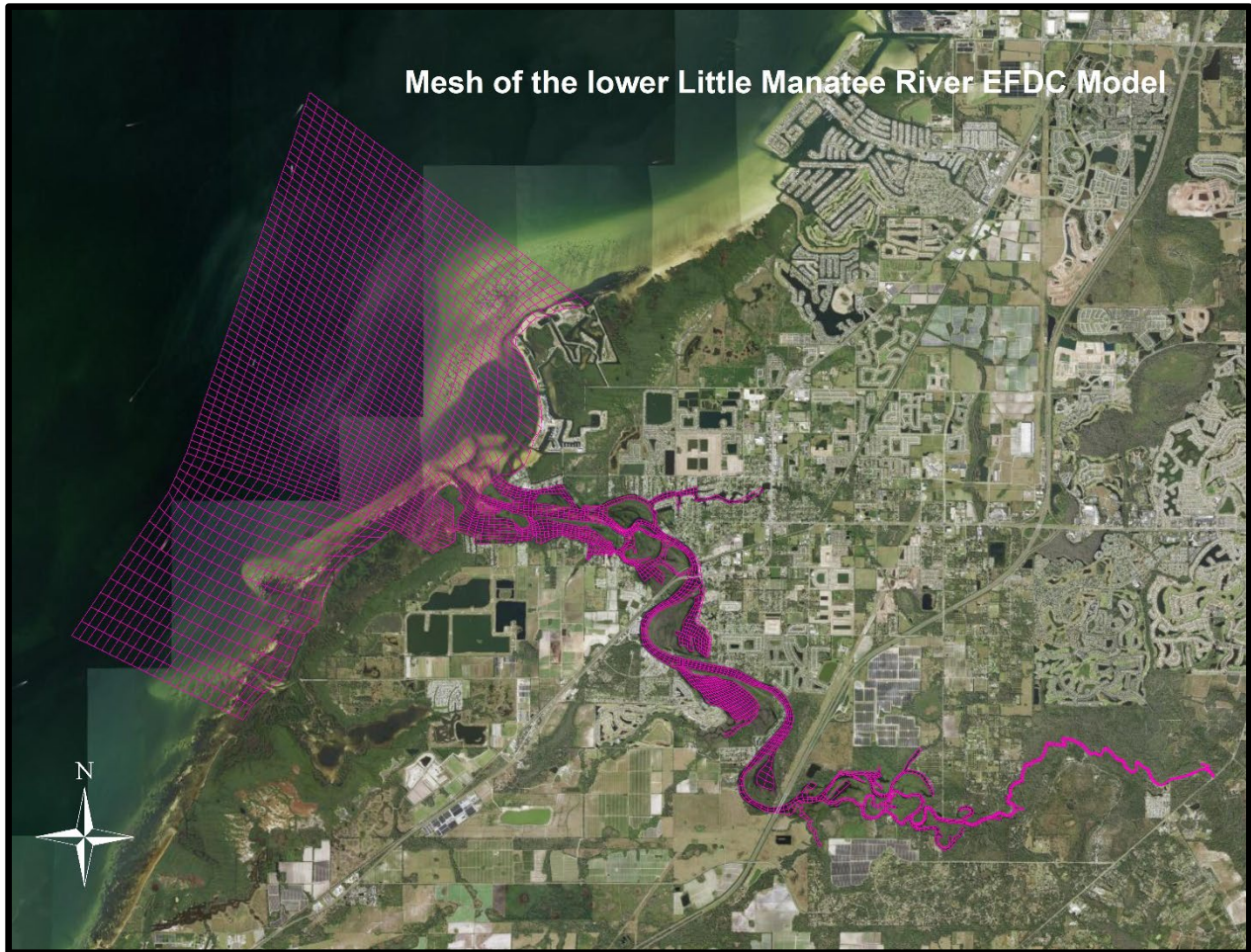


Figure 2-1. The orthogonal grid system (horizontal view) for the EFDC model of the Lower Little Manatee River.

The orthogonal grid system contains 4,542 grid cells, with 2850 cells within the river, with horizontal sizes ranging from ~6 m in the upper reaches of the river to as large as 450 m in Tampa Bay offshore regions. The vertical dimension is divided into four uniform sigma layers, each representing one-quarter of the water column depth, with this vertical structure adopted to resolve vertical mixing in this shallow water system, as much of the river bottom is less than 1.5 m below 0 elevation relative to the NAVD88 vertical datum. The EFDC model simulates wetting and drying in response to water surface elevation changes and runs at a timestep of 1 second.



Figure 2-2. Zoomed in views of the EFDC model grid system: Top Left - Near the mouth of the Little Manatee River; Top Right – 7 km upstream from the mouth; Bottom – Upstream braided portion.

Grid cell bathymetry was developed using a raster file generated from point bathymetric data collected in the river (Wang 2006) and developed for Tampa Bay from Tyler et al. (2007). The shoreline GIS coverage used to develop the grid system in the river was obtained from FDEP, with a portion of the FDEP shoreline compared to an aerial view of the river’s shoreline provided in Figure 2-3.

As part of the calibration process, initial grid cell bathymetry assignments were subject to revisions to more accurately simulate the river channel and associated movements of higher salinity water from Tampa Bay into and out of the river during tidal cycles. The final grid cell bathymetry, relative to the NAVD88 vertical datum, is shown on a grid cell map of the entire model domain in Figure 2-4, with the bathymetry zoomed to the river being provided in Figure 2-5.



Figure 2-3. FDEP shoreline GIS coverage in braided portion of the river compared to aerial photograph of the river.

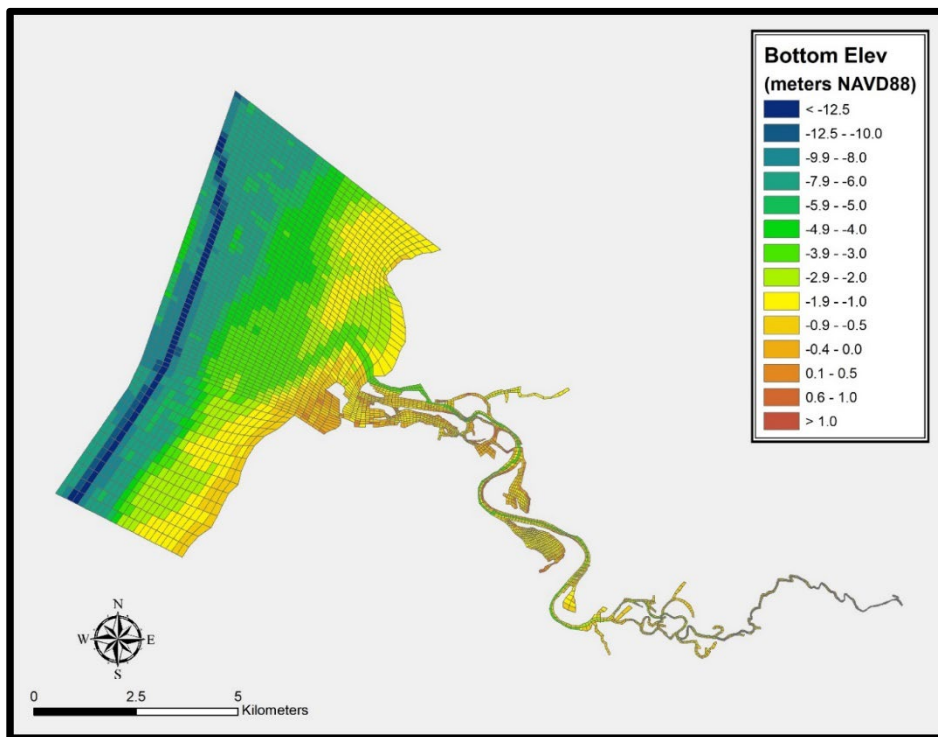


Figure 2-4. The orthogonal grid system (horizontal view) and bathymetry relative to NAVD88 vertical datum used by the EFDC model for the Lower Little Manatee River.

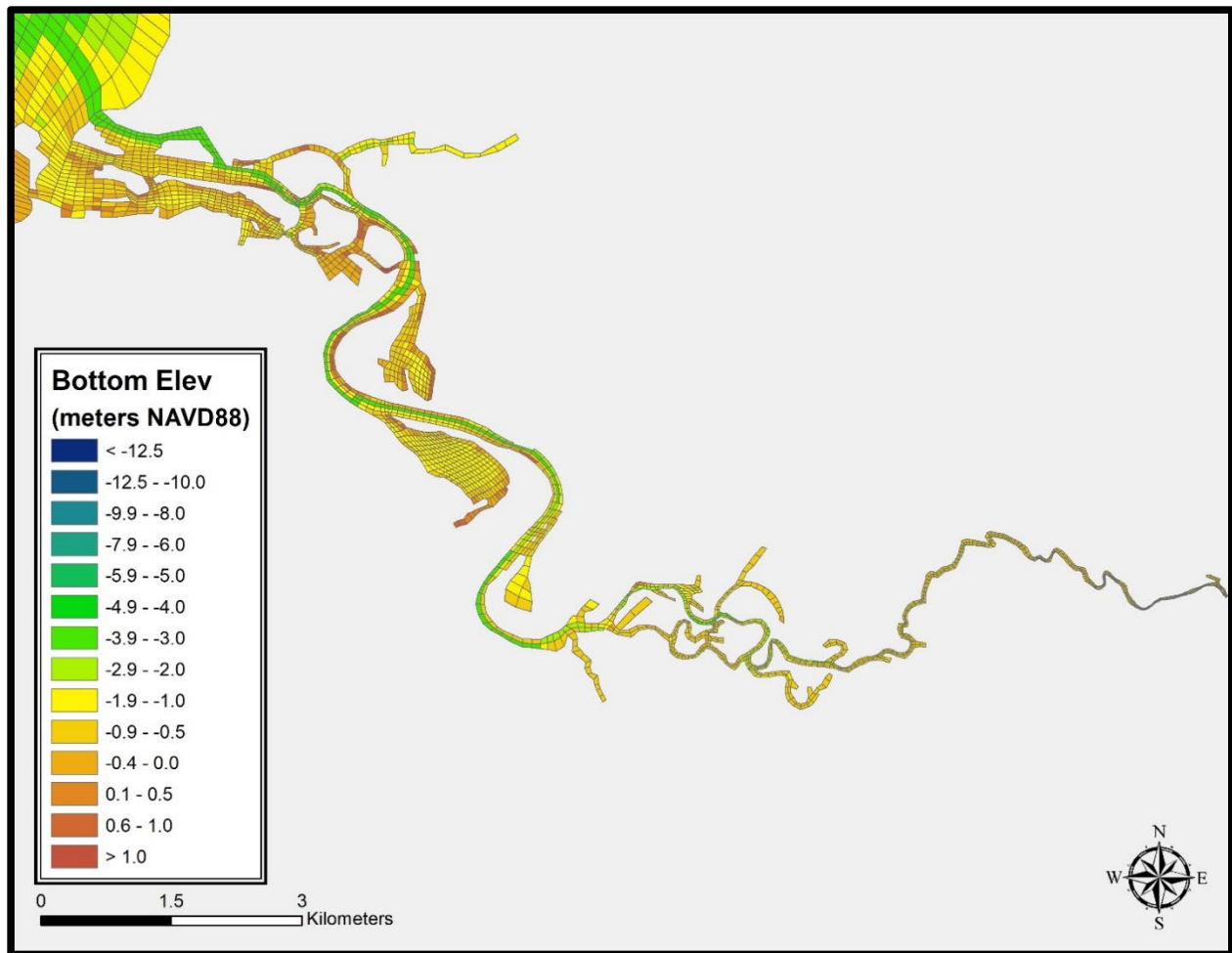


Figure 2-5. The orthogonal grid system (horizontal view) and bathymetry relative to NAVD88 vertical datum within the lower river used by the EFDC model for the Lower Little Manatee River.

Comparisons are provided of the model grid volumes and bottom areas within the river to those estimated from the raster file generated as part of the bathymetric data collection reporting (Wang 2006). This was done to ensure that the actual river bathymetry was reasonably represented in the model and less errors would occur in estimating the changes in habitat metrics expected resulting from flow reduction scenarios. The comparisons summed model grid volumes and bottom areas over sections of the river defined by the river kilometer system (Figure 2-6). The volumes for this comparison were estimated based on water surface elevations of 0 m relative to the NAVD88 vertical datum.

The comparison of river volume by river kilometer (Rkm) is provided in Figure 2-7, with Rkm 0 at the mouth of the river and Rkm 22 near the upstream boundary of the model domain. The Rkm markers shown in Figure 2-6 indicate the downstream border of the Rkm section, so that the volume for Rkm 1 is that between the marks for Rkm 1 and 2 in Figure 2-4.

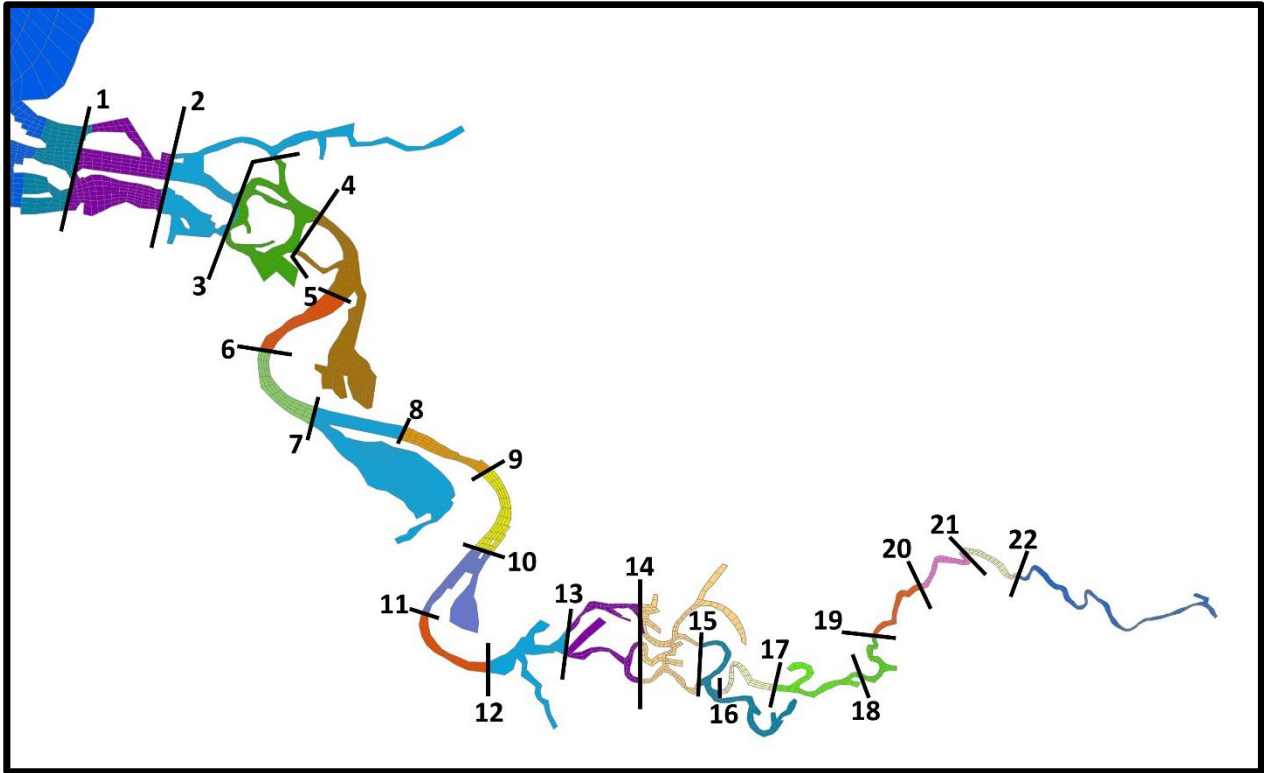


Figure 2-6. Model grid cells assigned to river kilometer for comparison of model and observed river system physiography.

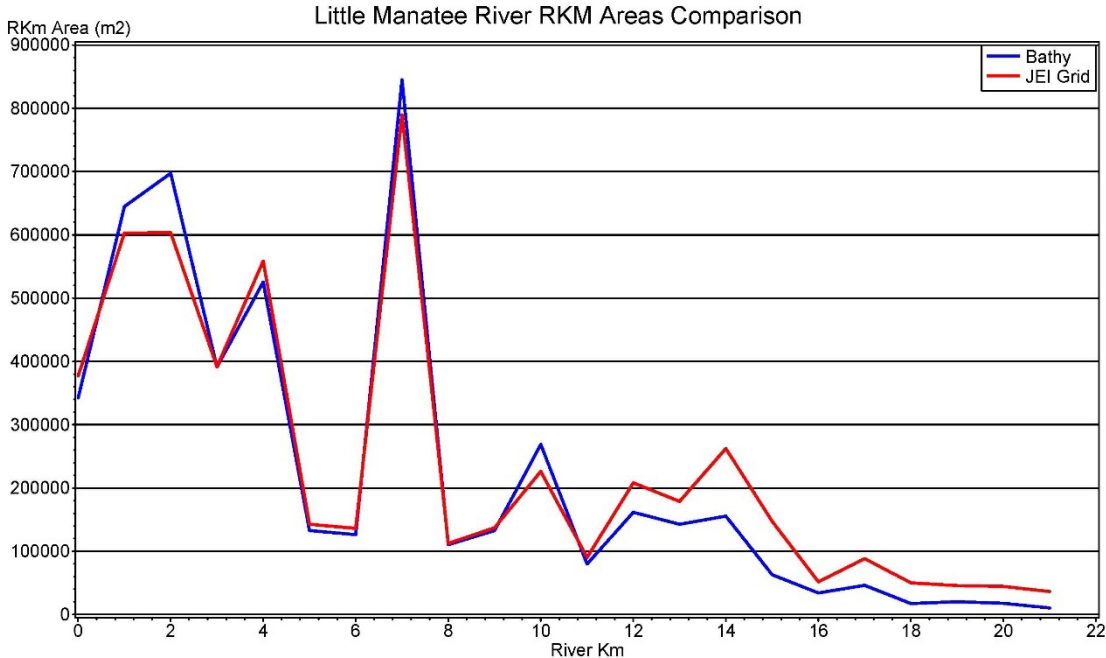


Figure 2-7. Comparison of bottom area for model grid system (JEI Grid) and that obtained from raster dataset (Bathy) by river km.

As seen in Figure 2-6, the grid system for the river section upstream of Rkm 12, where the river includes multiple branches with some relatively narrow interconnecting flow paths and narrows in the more upstream sections where there is a single channel, over-represents the bottom area as derived from the raster coverage developed from the bathymetry point coverage. It is important to note that during development of the river grid system, consideration of the model run time provides some constraints to the resolution of the grid system, with smaller cells and larger number of cells resulting in longer run times. Additionally, grid cell geometries are subject to constraints, such that grid cell horizontal dimensions may not be much greater in one direction than in another. These considerations sometimes result in grid cells over-estimating the horizontal extent of relatively narrow sections of a water body, or of relatively narrow channels when attempting to ensure appropriate movement of the salinity wedge during a tidal cycle. Evaluation of model results should include acknowledgment of these model constraints, with associated understanding that the model does still allow reasonable estimation of expected percentage changes in habitats within the areas of the river affected by these constraints.

Figure 2-8 provides the comparison of cumulative bottom area, with the upstream river sections on the right and the mouth of the river on the left at Rkm 0. Over the entire length of the river, the model overestimates the bottom area by 6%.

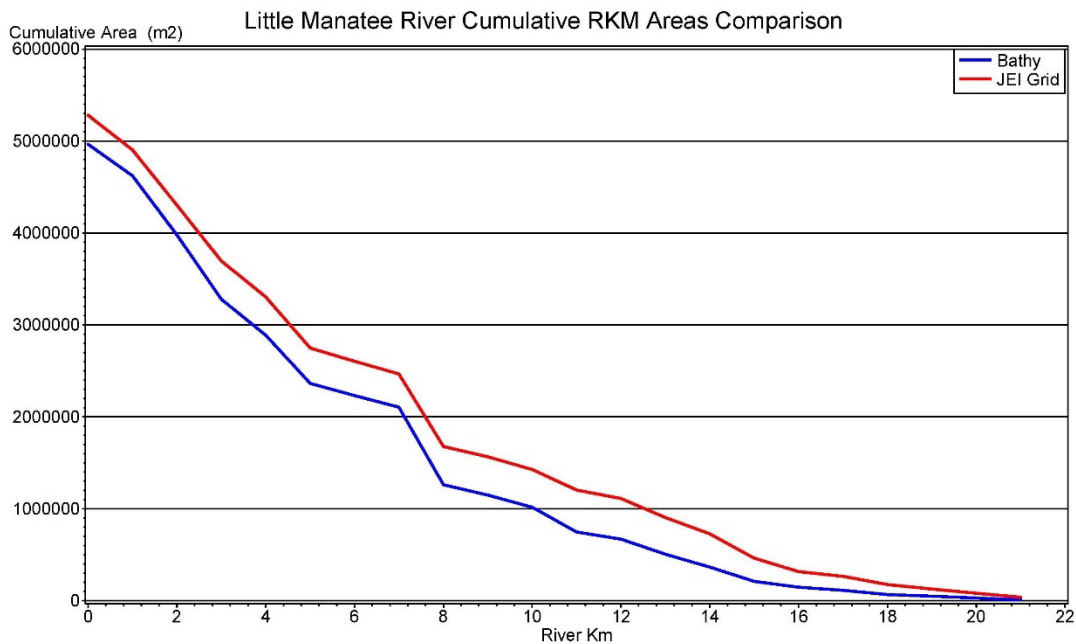


Figure 2-8. Comparison of cumulative bottom area (upstream on the right to downstream on the left) for model grid system (JEI Grid) and that obtained from raster dataset (Bathy) by river km.

Like the bottom area comparison, the river volumes for the grid system and that obtained from the raster developed from the bathymetry data are compared in Figures 2-9 (by river kilometer) and 2-10 (cumulative volumes comparison). These comparisons are similar to those for the bottom area, showing some over-estimation of volume in the river upstream of Rkm 12, related to the grid system

constraints as described above. Over the entire system, the cumulative river volume is over-estimated by 11%.

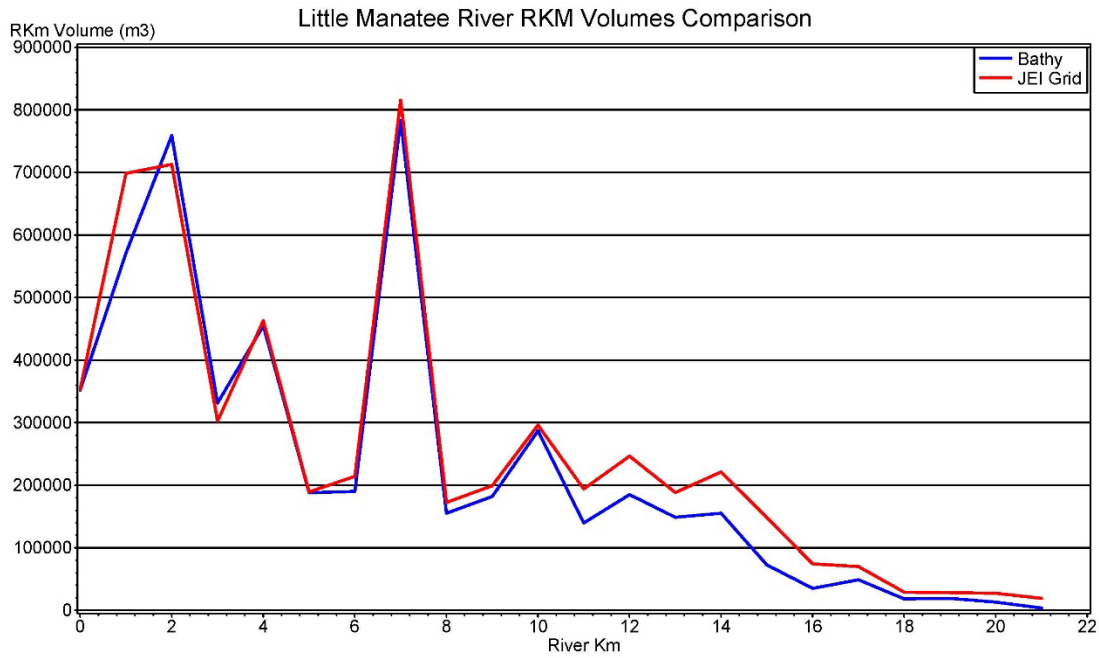


Figure 2-9. Comparison of volume for model grid system (JEI Grid) and that obtained from raster dataset (Bathy) by river km.

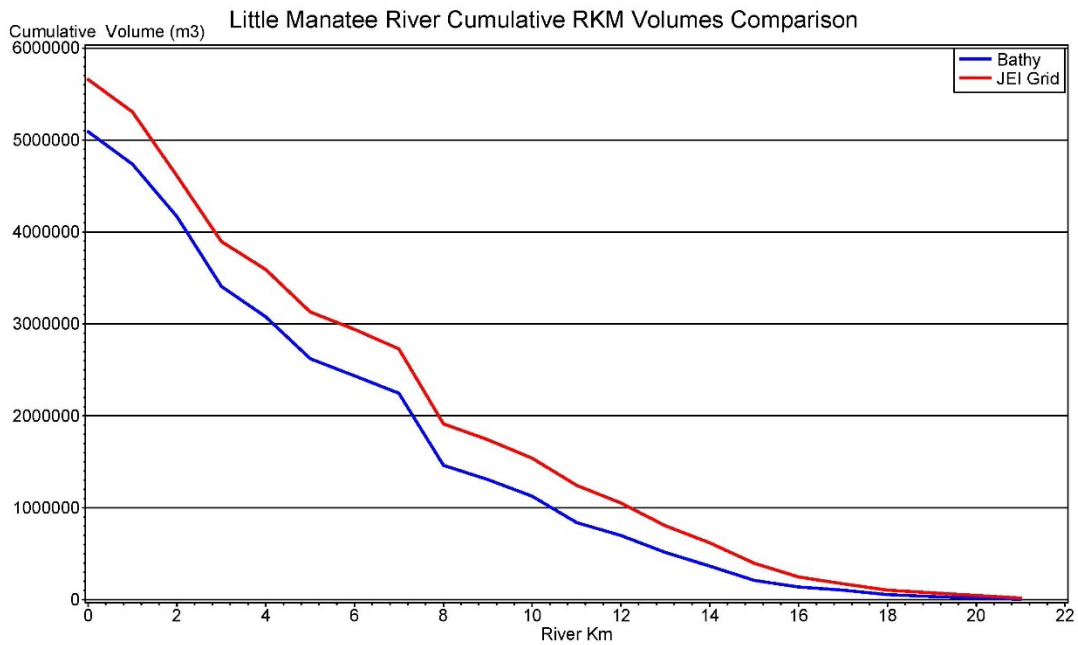


Figure 2-10. Comparison of cumulative volume (upstream on the right to downstream on the left) for model grid system (JEI Grid) and that obtained from raster dataset (Bathy) by river km.

2.3 AVAILABLE DATA AND MODEL CALIBRATION AND VERIFICATION PERIODS

The previous EFDC model developed for the Lower Little Manatee River (Huang and Liu 2007) utilized data collected specifically for use in model development. The USGS deployed continuous recorders and collected data at four stations in the lower river (Figure 2-11) beginning in March 2004 at the mouth of the river with, all four sites having simultaneous records starting in October 2004 and continuing through September 2005 at the three upstream sites, and to March 2006 at the site at the mouth of the river. The downstream-most site, near the river mouth, was the Little Manatee River at Shell Point near Ruskin, FL (No. 02300554), the next upstream site was the Little Manatee River at Ruskin, FL (No. 02300546), the next upstream site was the Little Manatee River at I-75 near Ruskin, FL (No. 02300542), and the upstream-most site was the Little Manatee River near Ruskin (No. 02300532). At all sites except the upstream-most site, 15-minute data were collected for water surface elevation, surface and bottom specific conductance, and surface and bottom temperature. For the upstream-most site, 02300532, only 15-minute water surface elevation data were collected.

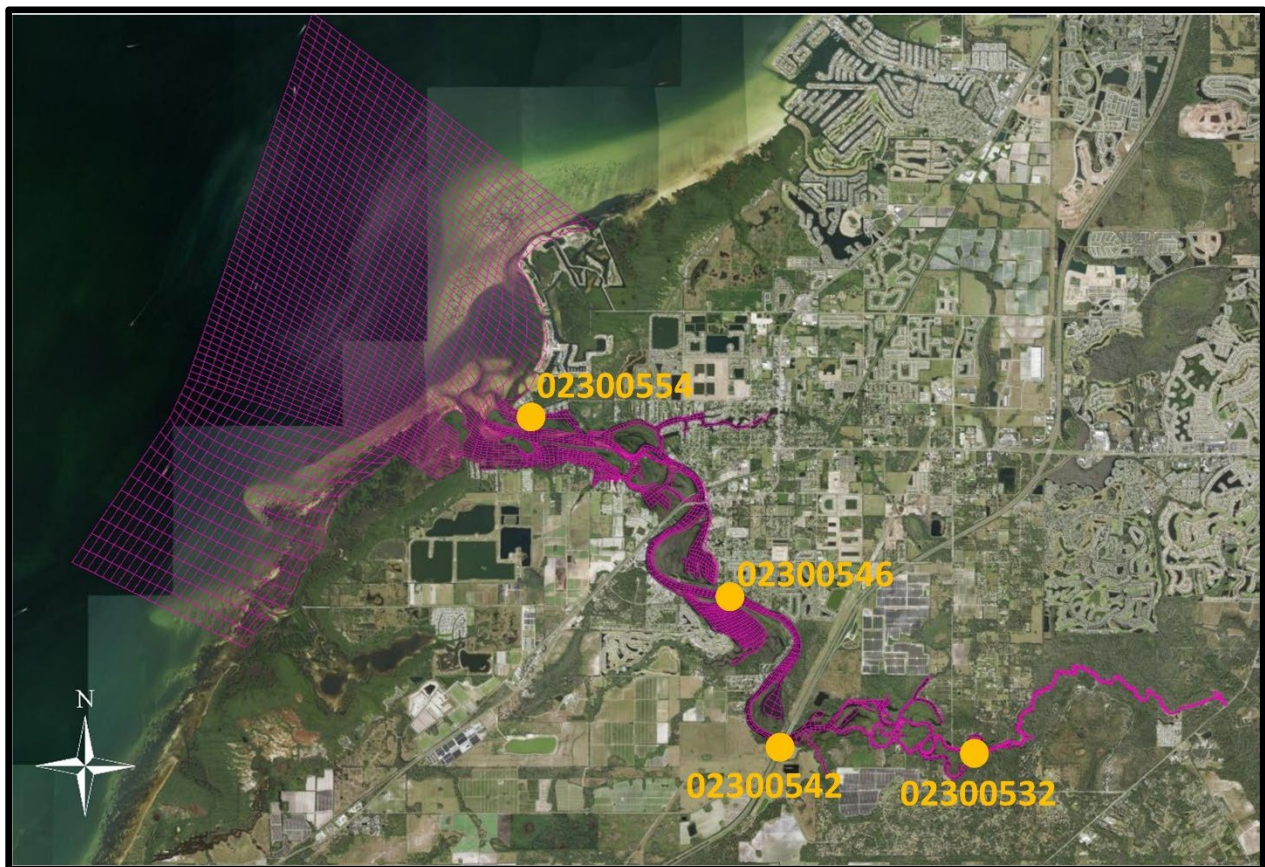


Figure 2-11. Locations of USGS sites for data collection from March 2004 through March 2006.

As part of this project, a search was completed for additional data for the system which could be used for model development, but the USGS March 2004 – March 2006 dataset was the most complete dataset available. The USGS dataset provides the necessary data for comparison of simulated water

surface elevation, salinity, and temperature at multiple locations within the lower river, and as such constrained the model development effort to this time period. Given the period of time when data were available simultaneously at all four sites (October 2004 – September 2005), and the desire to calibrate and verify the model for a relatively low-flow period, the time period January-February 2005 was selected for model calibration and the time period March-June 2005 was selected for model verification, with a model spin-up period of December 2004 to allow the model sufficient time to adjust to observed conditions based on model inputs. These are the same periods selected for model calibration and verification by Huang and Liu (2007).

Additional data needs include the hydrologic loadings to the upstream limit of the model domain and to the remainder of the ungaged downstream areas. The daily inflows at the upstream end of the model domain are from the USGS flow gage Little Manatee River at US 301 near Wimauma, FL (No. 02300500), located at the US Highway 301 bridge. The time series of daily flows for the USGS gage at US Highway 301 are provided in Figure 2-12 for the calibration period January-February 2005, and in Figure 2-13 for the verification period March-June 2005.

The estimated daily freshwater inflows to the ungaged areas downstream of this location are available from the Hydrologic Simulation Program – Fortran (HSPF) surface water model completed by Intera and Aqua Terra Consultants (2006). The objectives of their work effort was to provide ungaged inflows to the river in response to rainfall events to assist in the evaluation of salinity responses in aid of minimum flows determination. The authors noted that the ungaged portion of the watershed accounts for approximately one-third of the total watershed, with HSPF model calibration based on the responses in the gaged portion of the watershed to rainfall and associated runoff events. The ungaged flows enter the downstream portions of the river at the locations provided in Figure 2-14, with time series of the ungaged inflows for the calibration and verification periods provided in Attachment 1 for each of the 10 numbered locations.

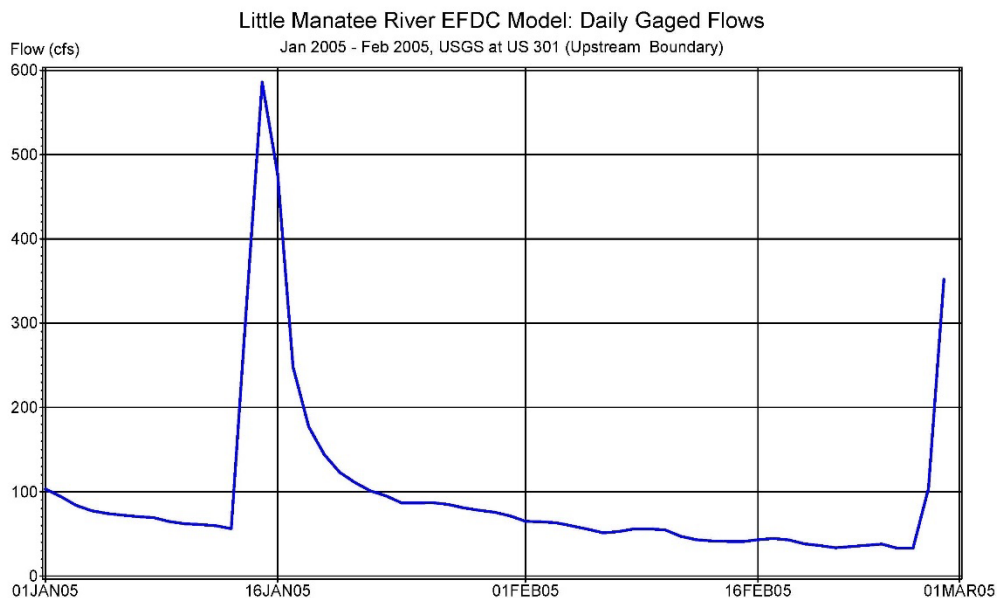


Figure 2-12. Upstream inflows from the USGS gage at US 301 for calibration period January-February 2005.

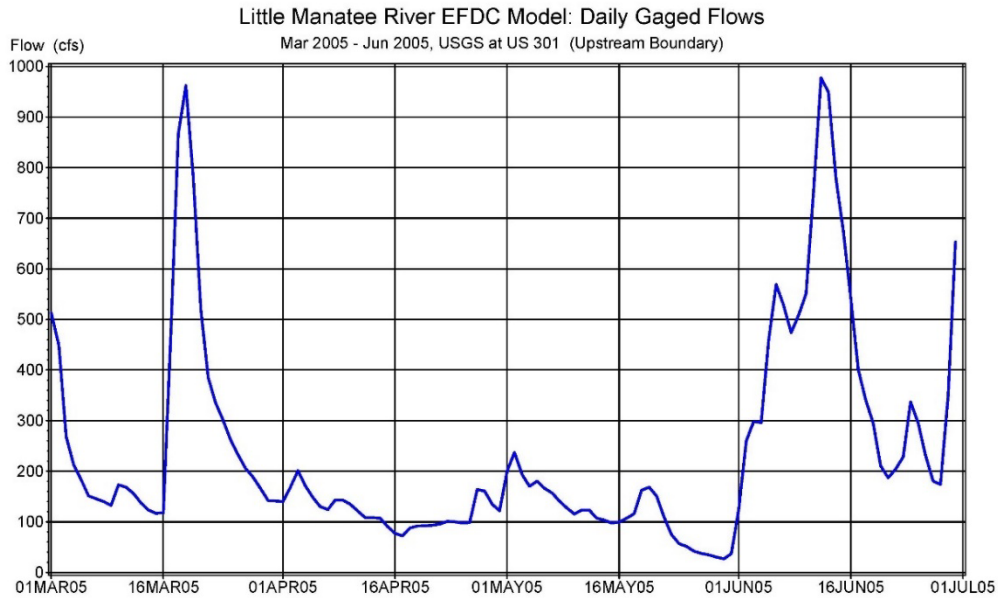


Figure 2-13. Upstream inflows from the USGS gage at US 301 for verification period March-June 2005.

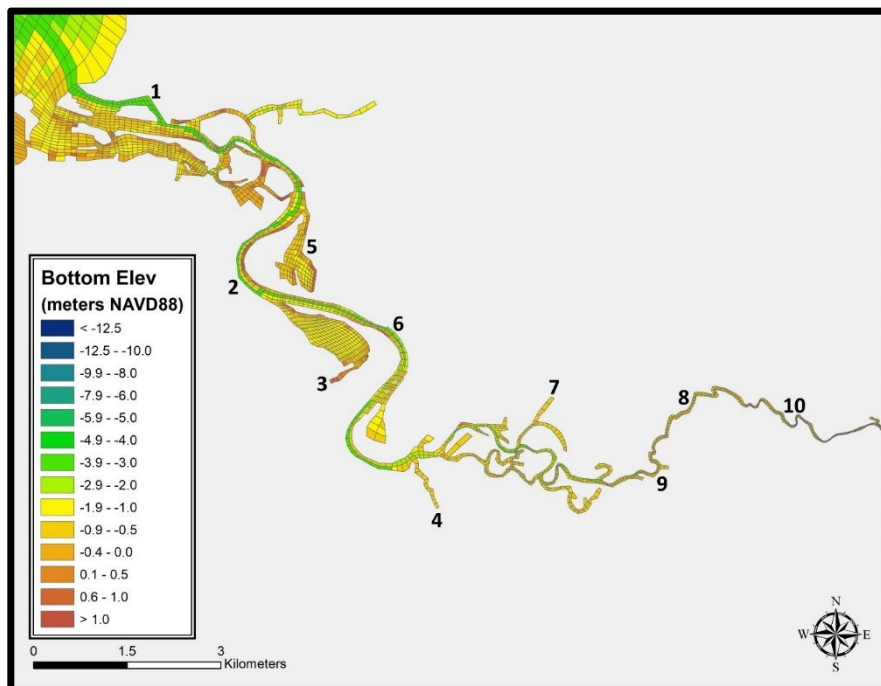


Figure 2-14. Locations of ungaged inflows to model domain. Gaged inflow from USGS site at US 301 enters at upstream boundary (right border of figure).

Additional data needed to drive the hydrodynamic model include meteorological inputs and boundary conditions at the downstream model limits for water surface elevation, salinity, and temperature, as well as temperature associated with all freshwater inflows. The freshwater inflow temperatures were set to a constant 22 C.

The meteorological inputs and data sources are provided below, with associated time series plots of the data for the calibration and verification periods.

- Atmospheric Pressure: National Oceanic and Atmospheric Administration (NOAA) National Weather Service site at Tampa International Airport, hourly (Figures 2-15 and 2-16 for calibration and verification periods, respectively).

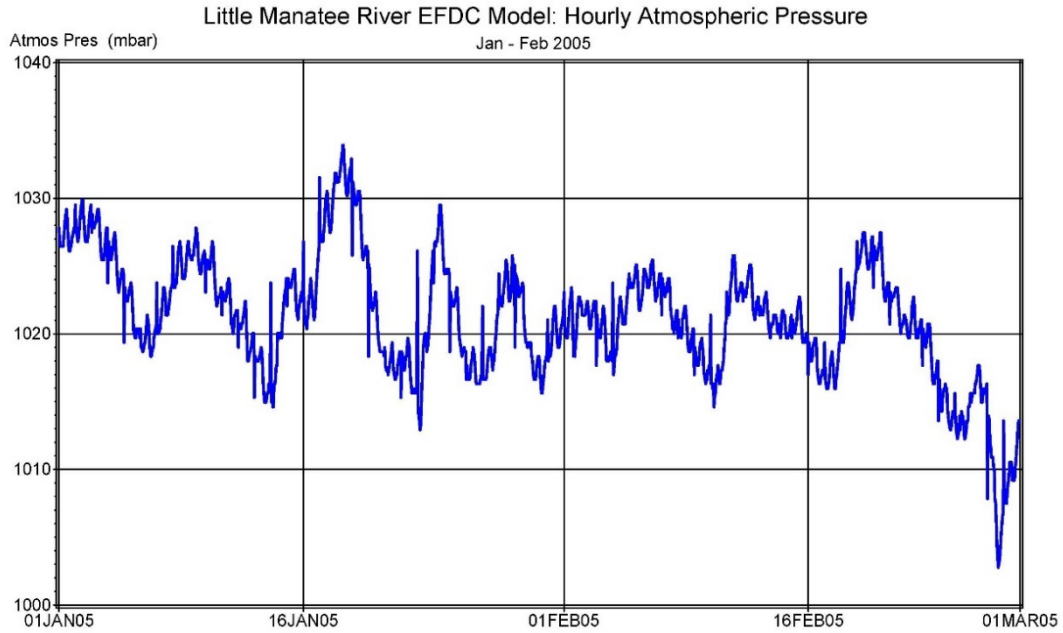


Figure 2-15. Time series of hourly atmospheric pressure from Tampa International Airport for calibration period January-February 2005.

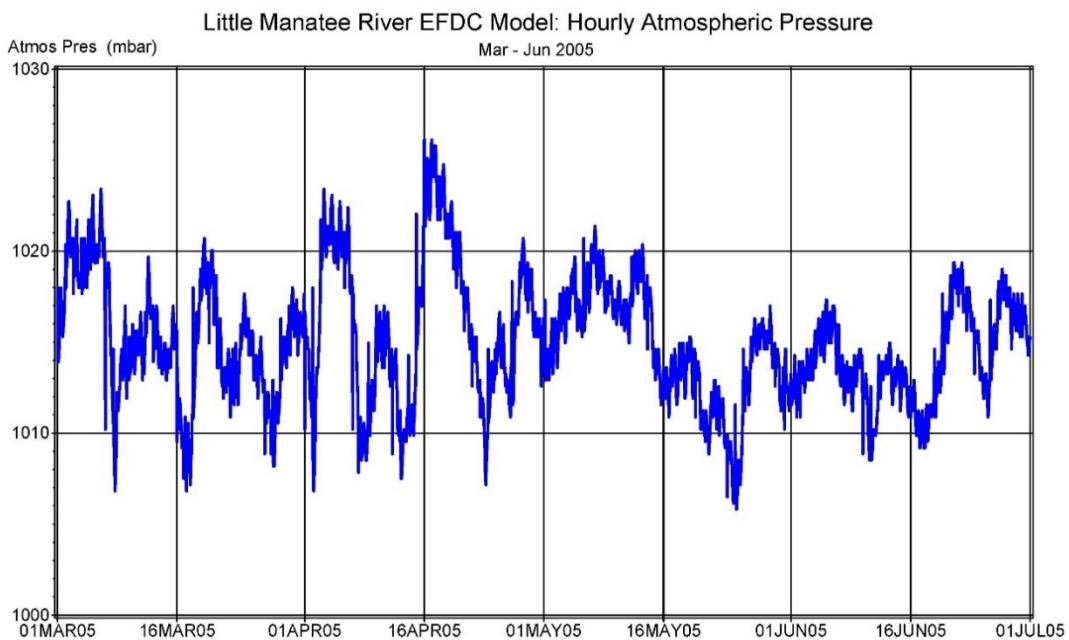


Figure 2-16. Time series of hourly atmospheric pressure from Tampa International Airport for verification period March-June 2005.

- Air Temperature: Dover site of University of Florida (UF) Institute of Food and Agricultural Sciences (IFAS) Florida Automated Weather Network (FAWN), hourly (Figures 2-17 and 2-18 for calibration and verification periods, respectively).

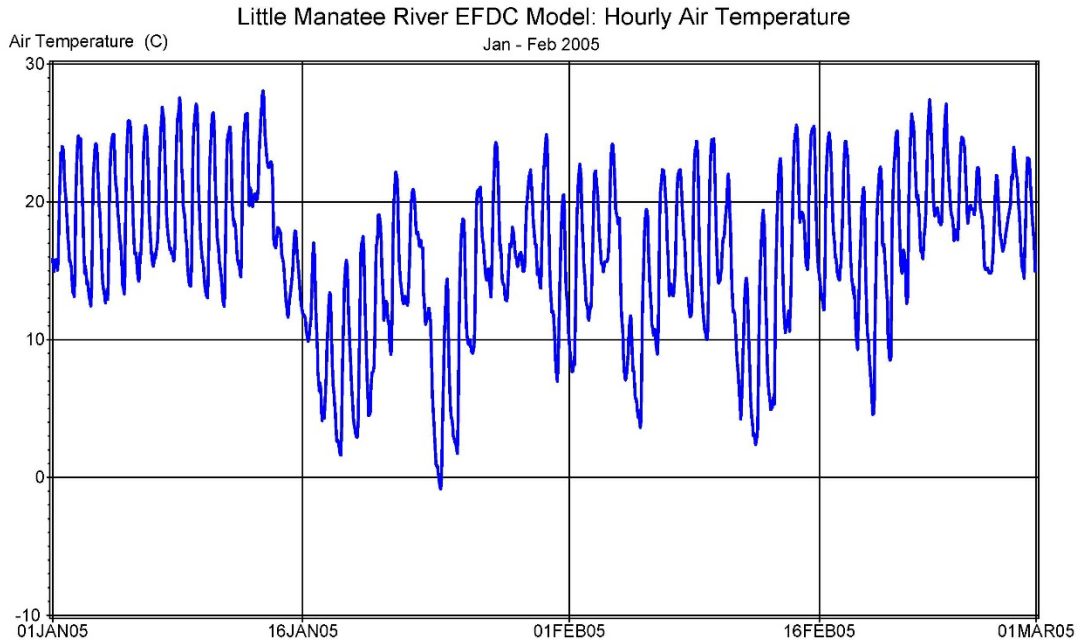


Figure 2-17. Time series of hourly air temperature data from UF IFAS FAWN Dover site for calibration period January-February 2005.

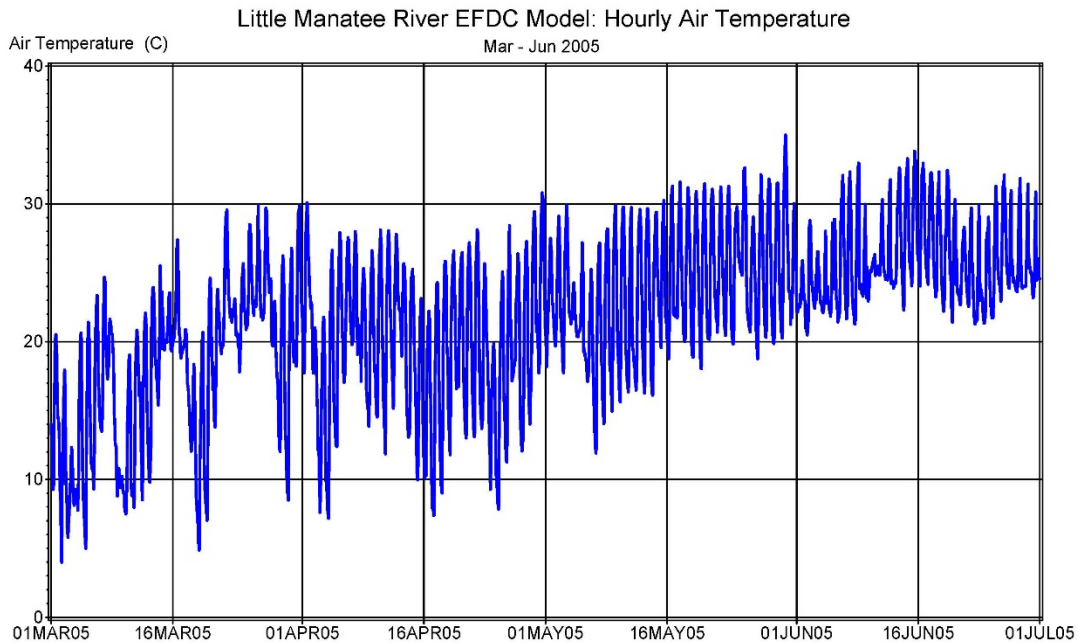


Figure 2-18. Time series of hourly air temperature from UF IFAS FAWN Dover site for verification period March-June 2005.

- Relative Humidity: Dover site of UF IFAS FAWN, hourly (Figures 2-19 and 2-20 for calibration and verification periods, respectively).

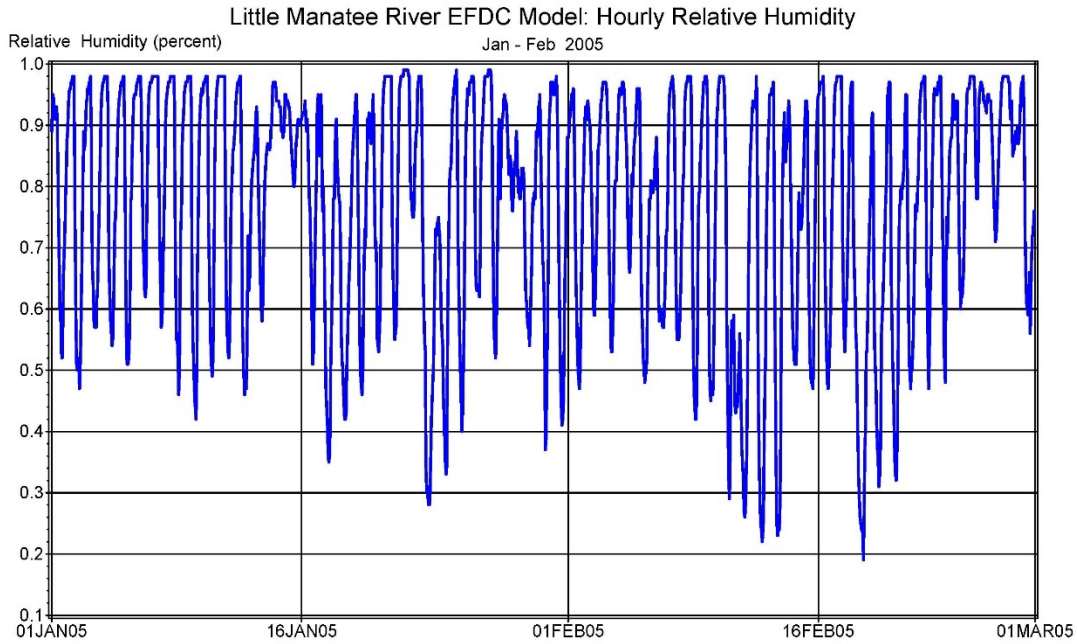


Figure 2-19. Time series of hourly relative humidity from UF IFAS FAWN Dover site for calibration period January-February 2005.

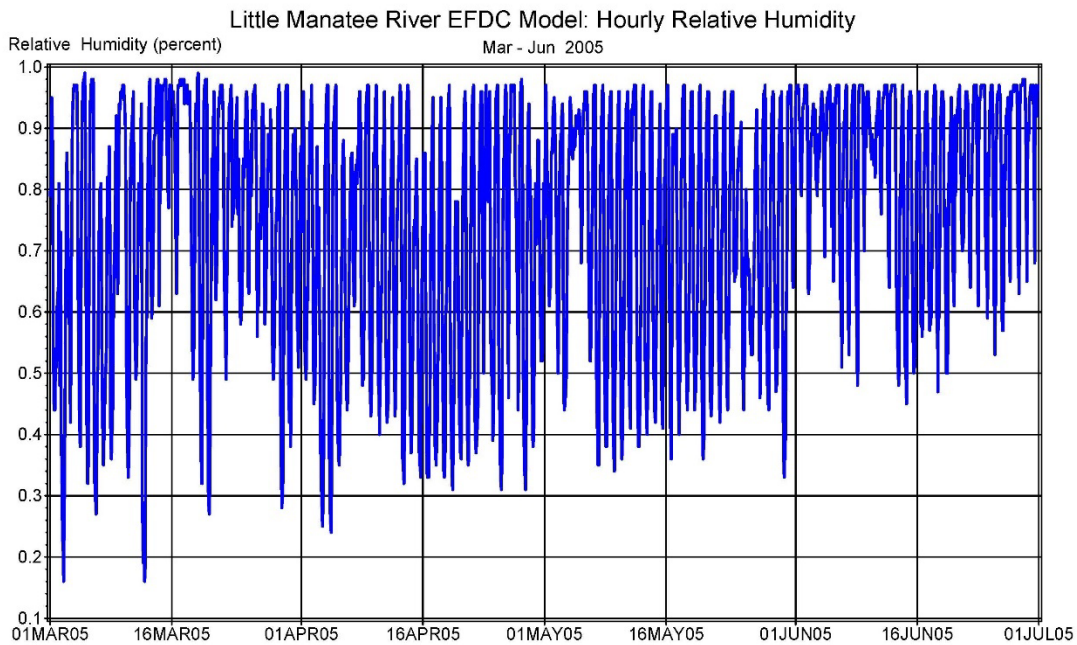


Figure 2-20. Time series of hourly relative humidity from UF IFAS FAWN Dover site for verification period March-June 2005.

- Rainfall: Tampa Bay Estuary Program (TBEP) estimates for rainfall to surface of Middle Tampa Bay, derived using inverse-distance squared algorithm from multiple National Weather Service rain gages (Zarbock et al. 1994, 1996), daily values distributed equally to hourly frequency for model input (Figures 2-21 and 2-22 for calibration and verification period daily rainfall, respectively).

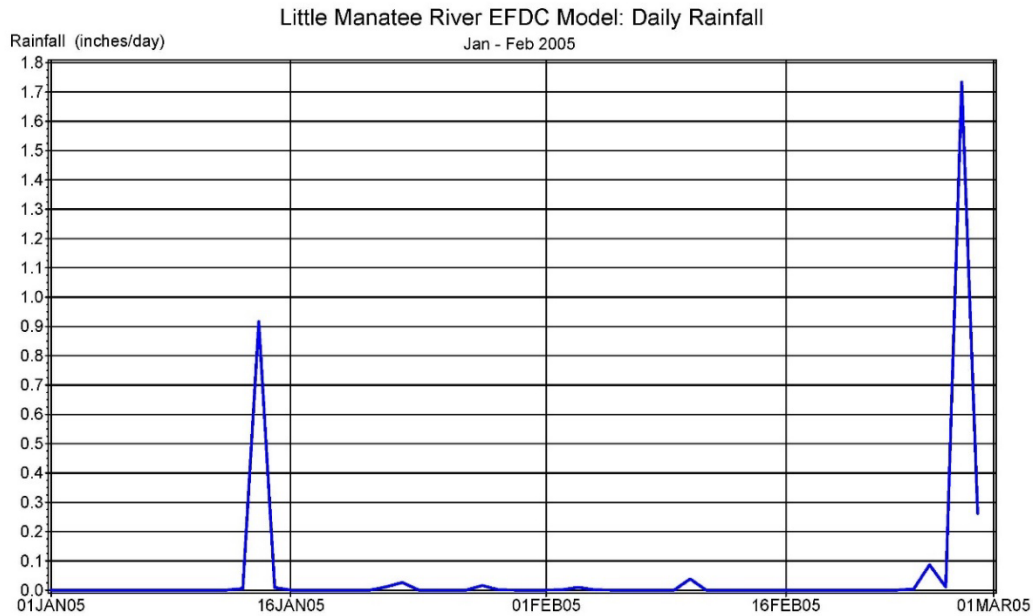


Figure 2-21. Time series of daily rainfall from TBEP estimates of rainfall to surface of Middle Tampa Bay for calibration period January-February 2005.

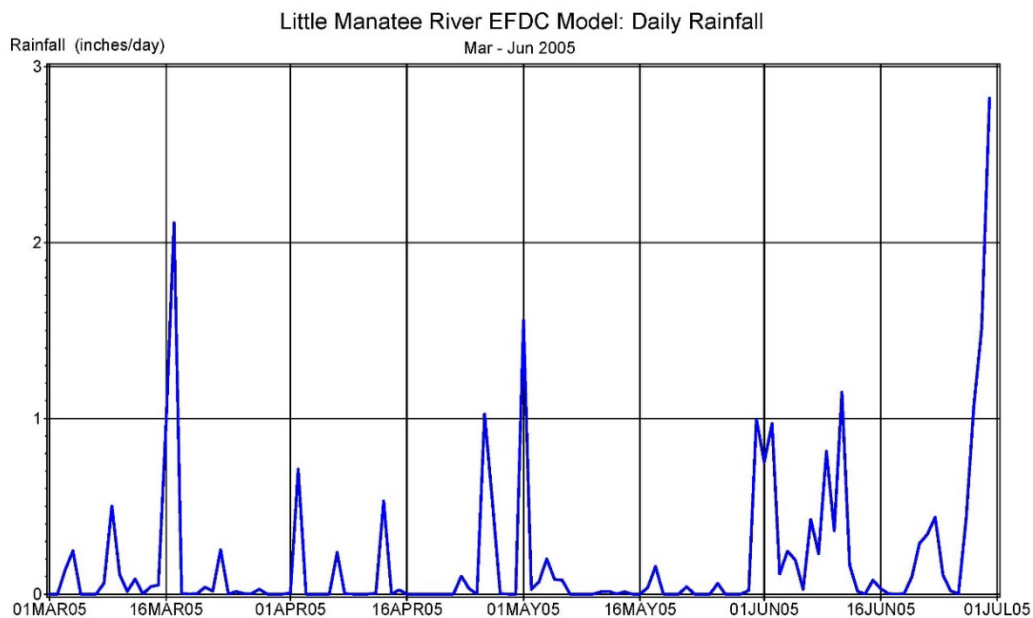


Figure 2-22. Time series of daily rainfall from TBEP estimates of rainfall to surface of Middle Tampa Bay for verification period March-June 2005.

- Cloud Cover: NOAA National Weather Service site at Tampa International Airport, hourly (Figures 2-23 and 2-24 for calibration and verification periods, respectively).

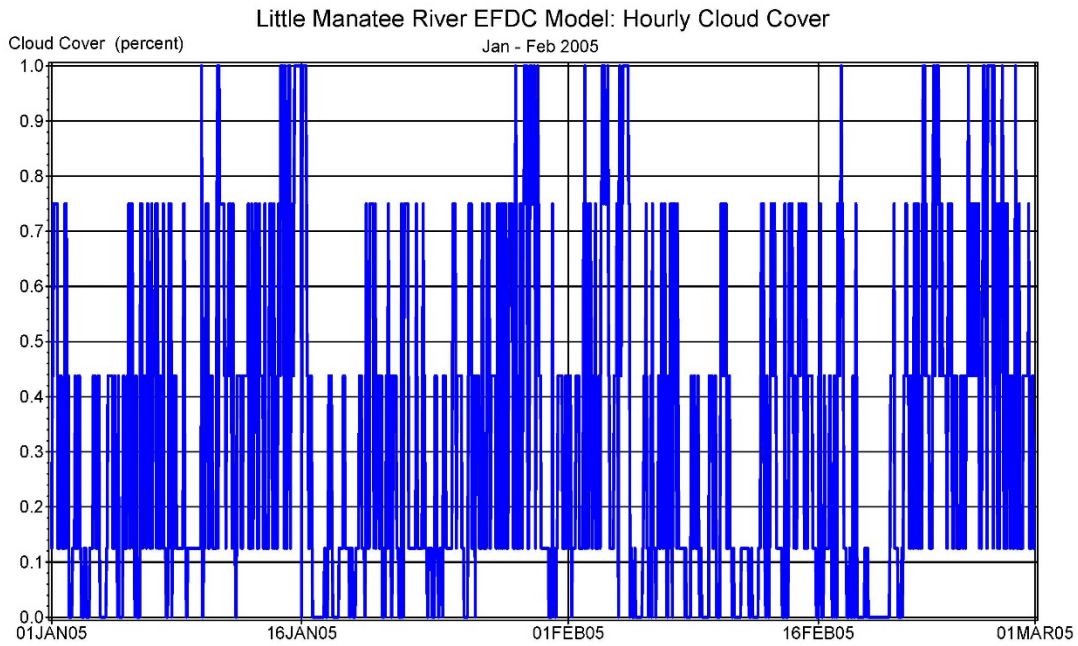


Figure 2-23. Time series of hourly cloud cover from Tampa International Airport for calibration period January-February 2005.

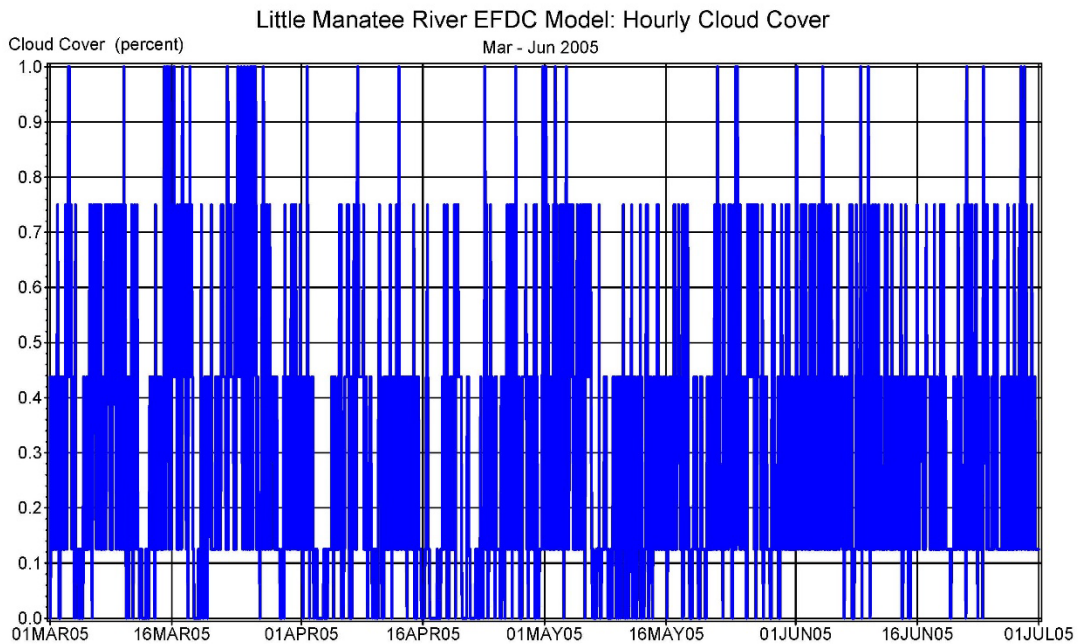


Figure 2-24. Time series of hourly cloud cover from Tampa International Airport for verification period March-June 2005.

- Evapotranspiration: Dover site of UF IFAS FAWN, daily values distributed equally to hourly frequency for model input (Figures 2-25 and 2-26 for calibration and verification period daily evapotranspiration, respectively). For the verification period, missing daily data for April 6-25, 2005 were interpolated between the values of April 5 and April 26, 2005.

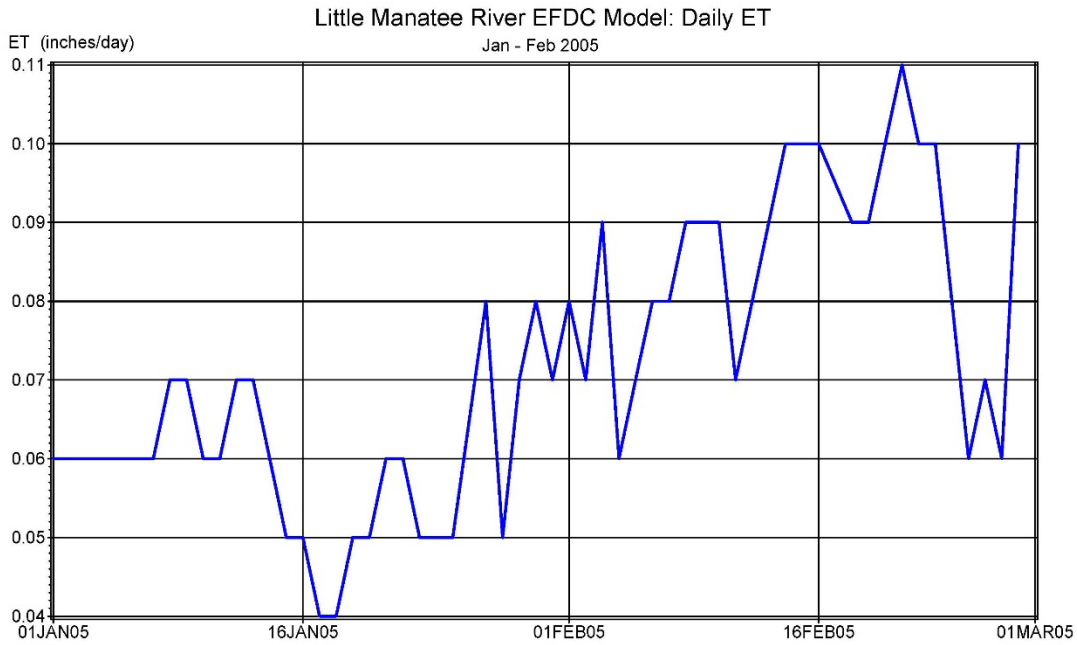


Figure 2-25. Time series of daily evapotranspiration from UF IFAS FAWN Dover site for calibration period January-February 2005.

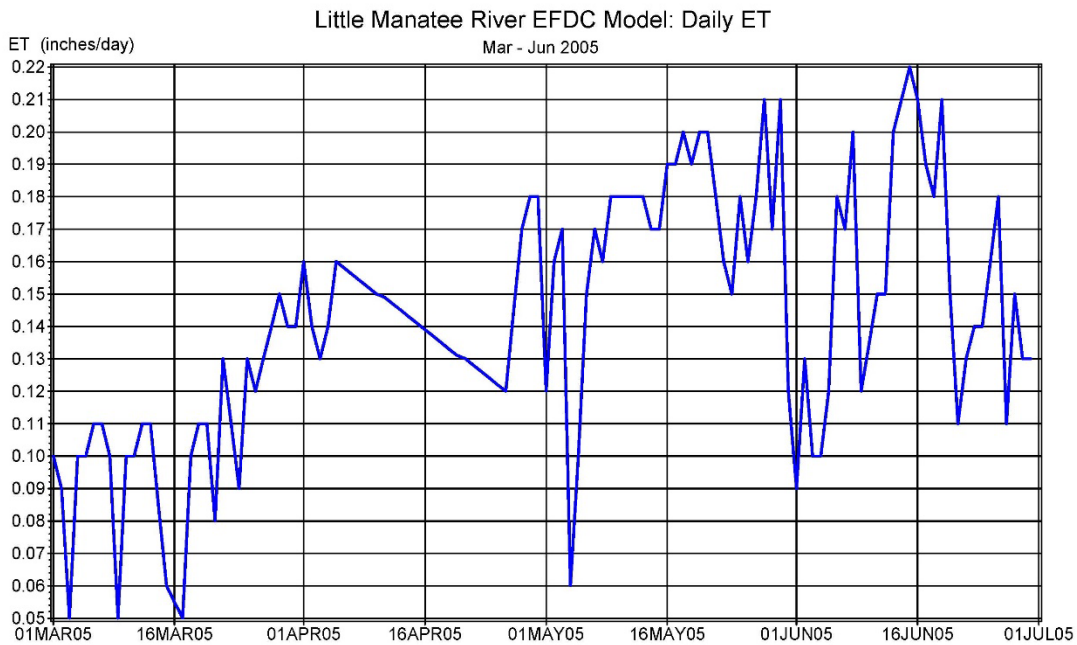


Figure 2-26. Time series of daily evapotranspiration from UF IFAS FAWN Dover site for verification period March-June 2005.

- Solar Radiation: Dover site of UF IFAS FAWN, hourly (Figures 2-27 and 2-28 for calibration and verification periods, respectively).

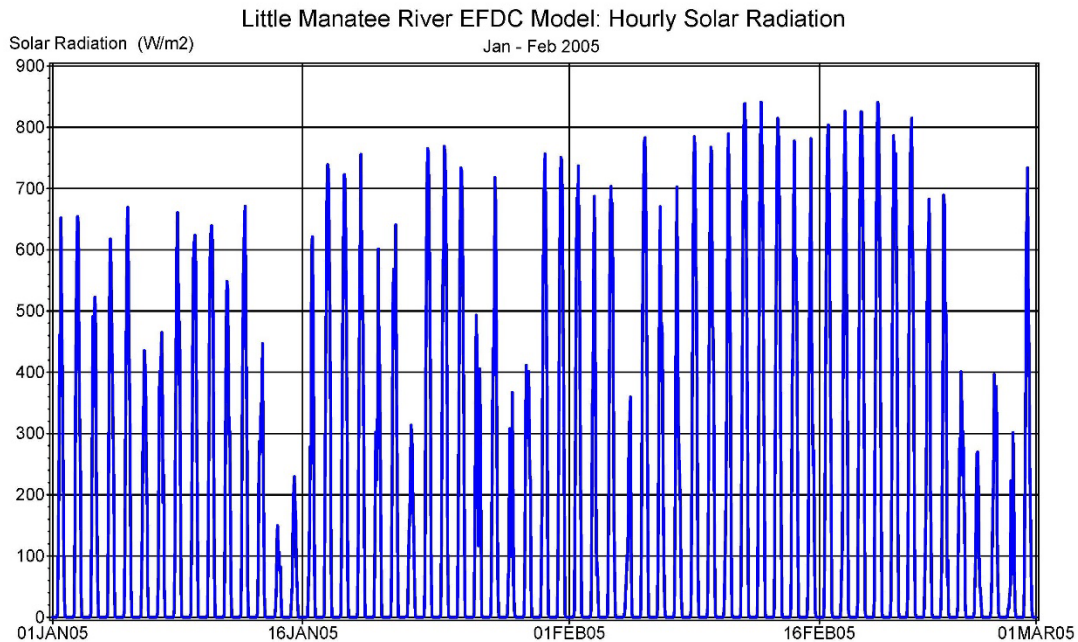


Figure 2-27. Time series of hourly solar radiation from UF IFAS FAWN Dover site for calibration period January-February 2005.

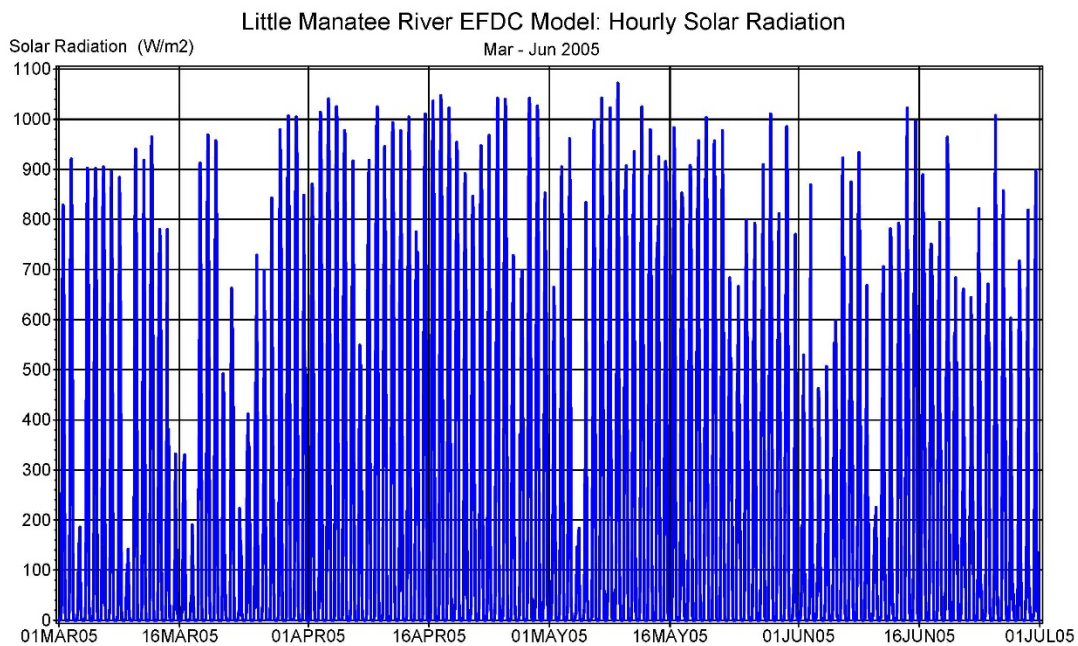


Figure 2-28. Time series of hourly solar radiation from UF IFAS FAWN Dover site for verification period March-June 2005.

- Wind Speed: Dover site of UF IFAS FAWN, hourly (Figures 2-29 and 2-30 for calibration and verification periods, respectively).

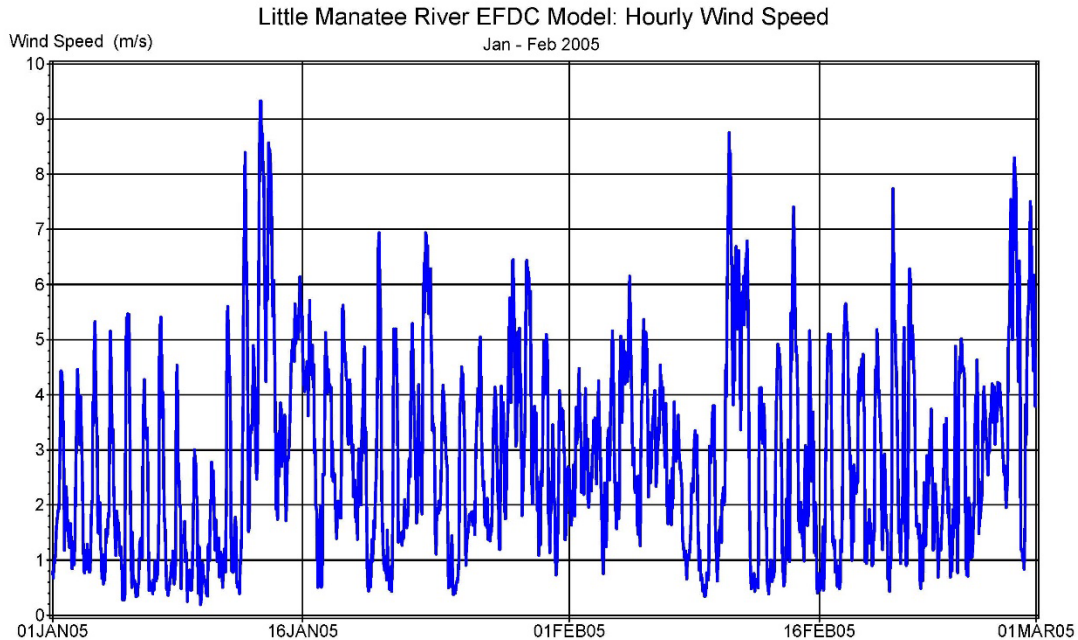


Figure 2-29. Time series of hourly wind speed from UF IFAS FAWN Dover site for calibration period January-February 2005.

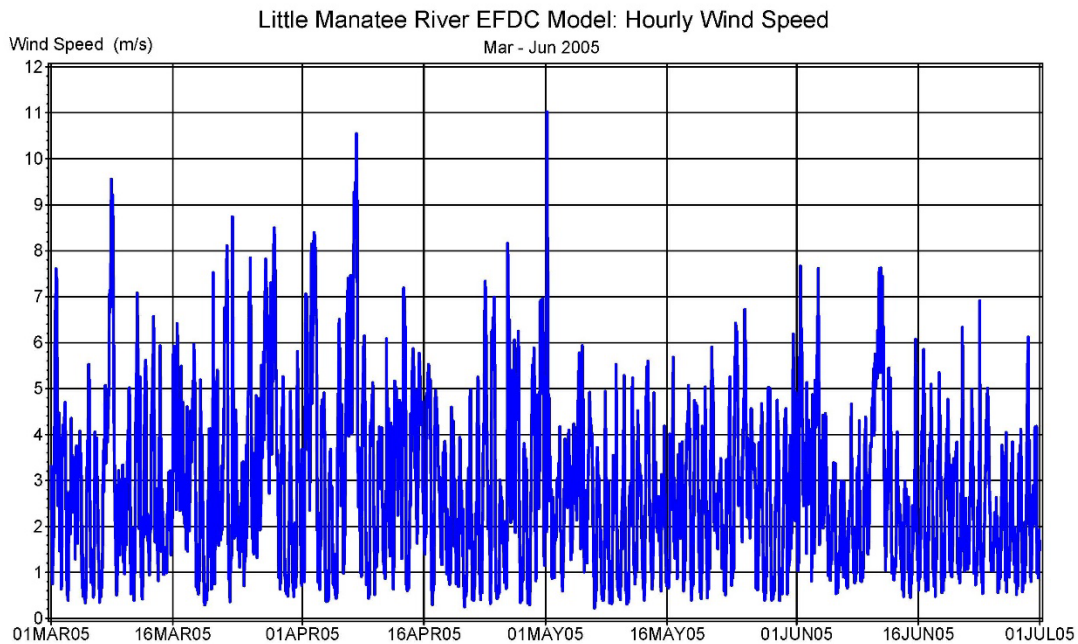


Figure 2-30. Time series of hourly wind speed from UF IFAS FAWN Dover site for verification period March-June 2005.

- Wind Direction: Dover site of UF IFAS FAWN, hourly (Figures 2-31 and 2-32 for calibration and verification periods, respectively);

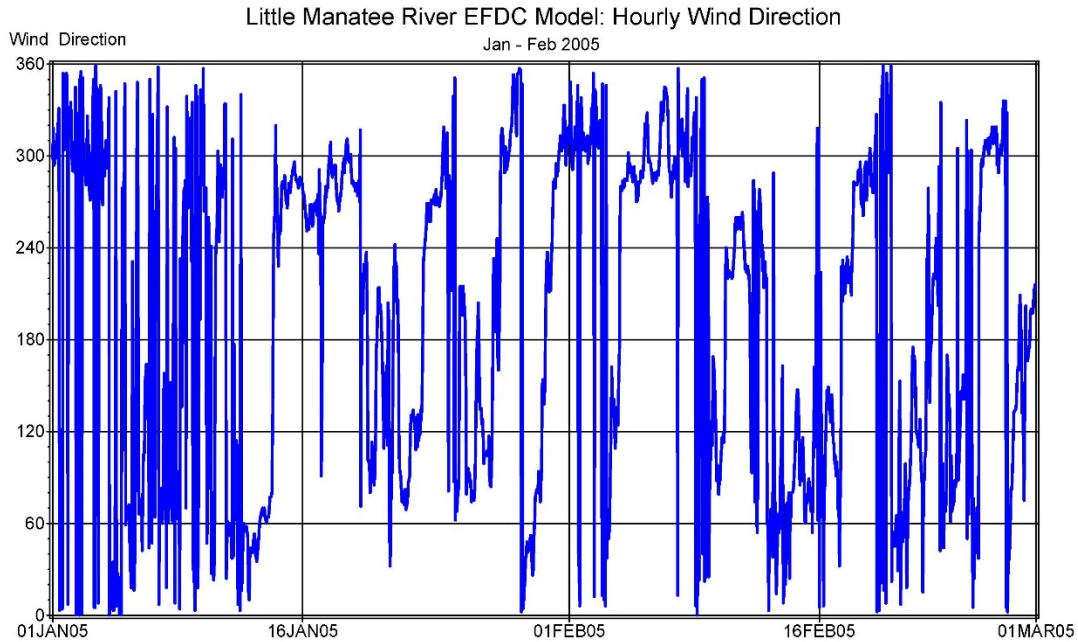


Figure 2-31. Time series of hourly wind direction (relative to 0 degrees as north, increasing in clockwise direction) from UF IFAS FAWN Dover site for calibration period January-February 2005.

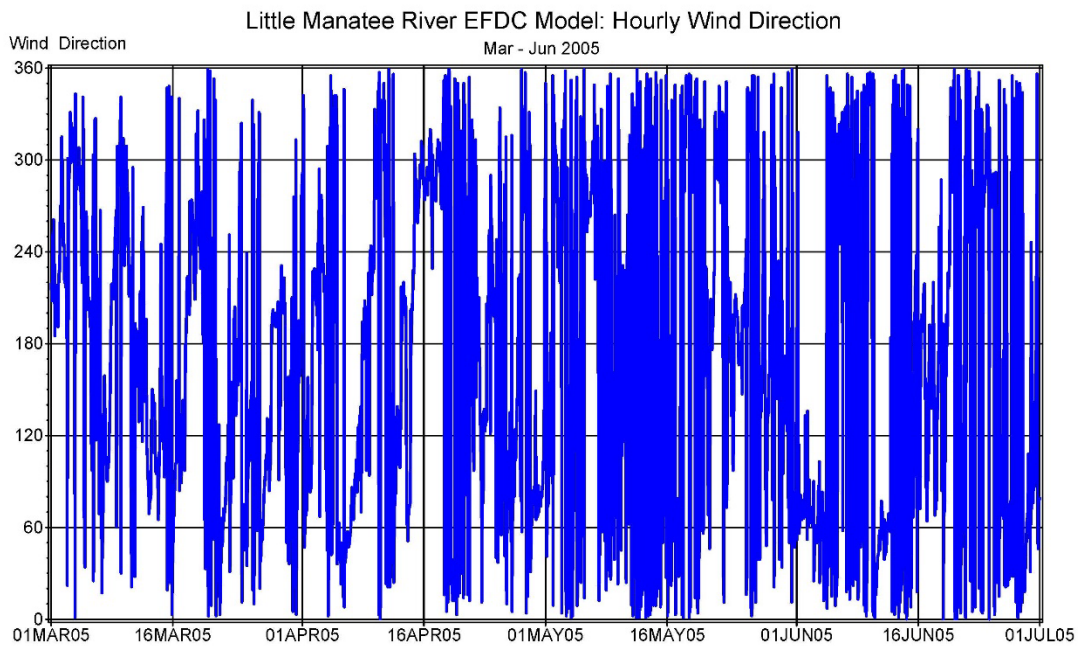


Figure 2-32. Time series of hourly wind direction (relative to 0 degrees as north, increasing in clockwise direction) from UF IFAS FAWN Dover site for verification period March-June 2005.

Boundary conditions are needed at the downstream model limits for water surface elevation, salinity, and temperature. The downstream boundary conditions are applied to the northern and southern borders of the model grid within Tampa Bay. The Old Tampa Bay (OTB) hydrodynamic model (ATM 2014), developed as part of the Old Tampa Bay Integrated Model Development project for the TBEP (Sherwood et al. 2016), has previously been run for the 2000-2009 period, inclusive of the Lower Little Manatee River calibration and verification periods. Since model output of sufficient frequency was not available specifically for the OTB model grid cells coinciding with the northern and southern boundary cells of the Lower Little Manatee River model grid, the OTB hydrodynamic model was re-run for the 2000-2009 period with output specified for the needed locations. The OTB hydrodynamic output was then used to develop time series of salinity, temperature, and water surface elevation at the northern and southern boundaries of the Lower Little Manatee River model grid system. One time series of salinity was applied to all grid cells along the northern boundary, with a second time series of salinity applied to all grid cells along the southern boundary, with similar application of two time series each for temperature and water surface elevation to the northern and southern boundary grid cells. The western boundary of the Lower Little Manatee River model grid was treated as a closed boundary, as the primary movement of water is along the north-south axis of the bay.

The time series of 10-minute frequency salinity for the calibration and verification periods are provided in Figures 2-33 and 2-34, respectively, for the northern boundary, and in Figures 2-35 and 2-36, respectively, for the southern boundary. The boundary conditions include salinity for each of the four vertical layers of the model, although often the vertical salinity gradient is very small, as seen in Figures 2-33 through 2-36.

The time series of 10-minute frequency temperature for the calibration and verification periods are provided in Figures 2-37 and 2-38, respectively, for the northern boundary, and in Figures 2-39 and 2-40, respectively, for the southern boundary. The boundary conditions include temperature for each of the four vertical layers of the model, with vertical temperature differences seldom visible on the time series plots.

The time series of 10-minute frequency water surface elevation for the calibration and verification periods are provided in Figures 2-41 and 2-42, respectively, for the northern boundary, and in Figures 2-43 and 2-44, respectively, for the southern boundary.

As noted above, the downstream boundary conditions for the Little Manatee River model are derived from OTB hydrodynamic output for the calibration and verification periods. Since the boundary conditions result from a hydrodynamic model, and not from observed data, this can introduce error in the boundary condition associated with the OTB model, which is then translated into the Little Manatee River proper. This consideration should be recalled when evaluating the statistical measures of the calibration and verification efforts.

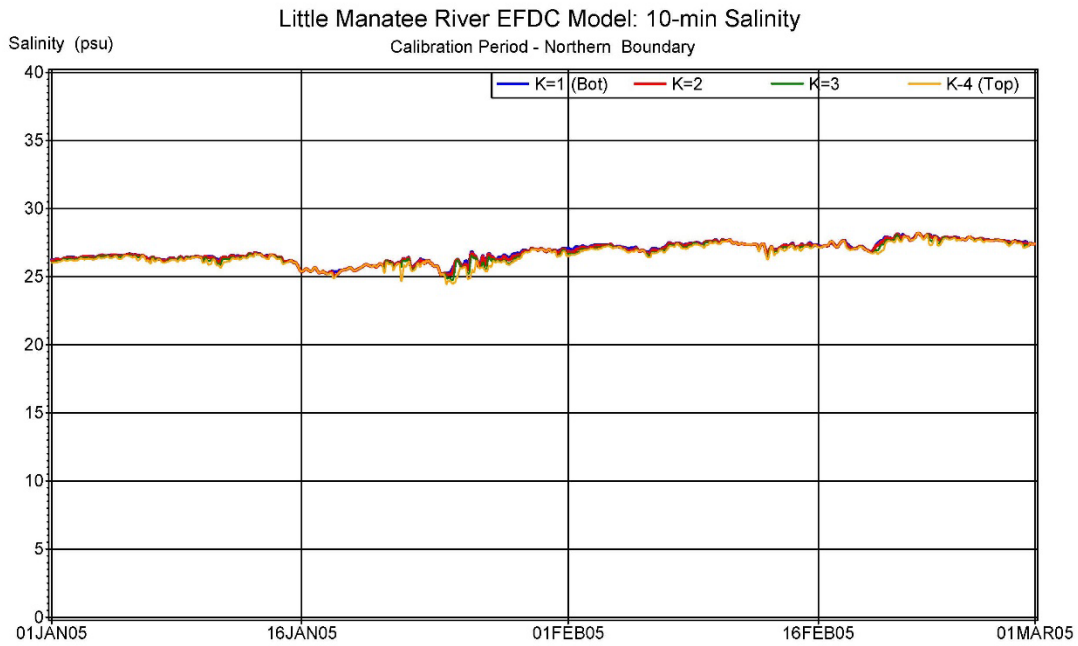


Figure 2-33. Time series of 10-minute frequency salinity at four vertical levels for the northern boundary in Tampa Bay, derived from output from the Old Tampa Bay hydrodynamic model, for the calibration period January-February 2005.

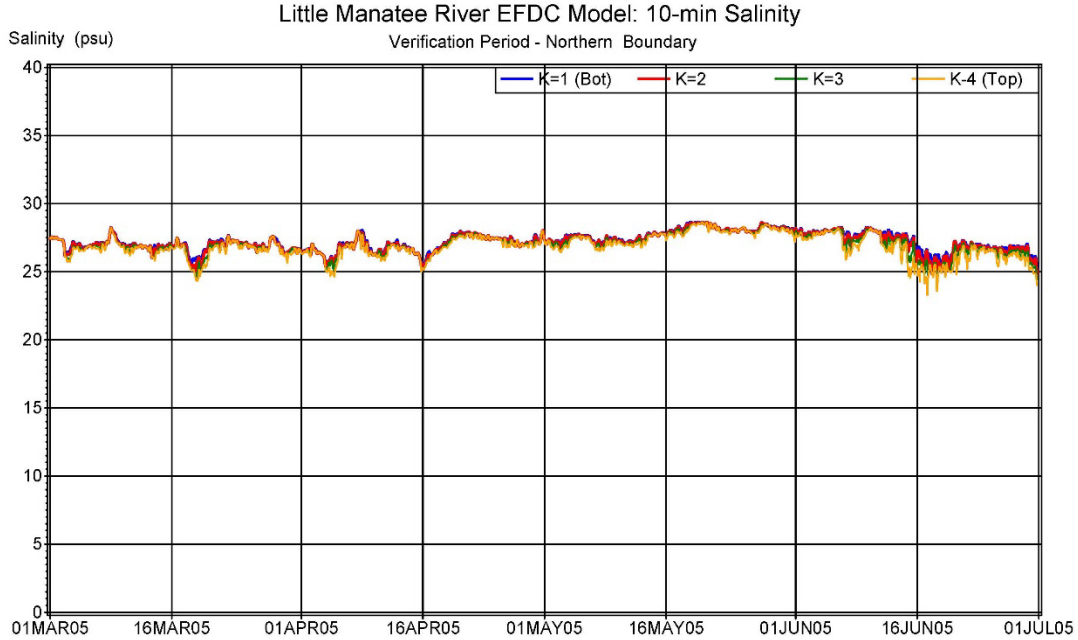


Figure 2-34. Time series of 10-minute frequency salinity at four vertical levels for the northern boundary in Tampa Bay, derived from output from the Old Tampa Bay hydrodynamic model, for the verification period March-June 2005.

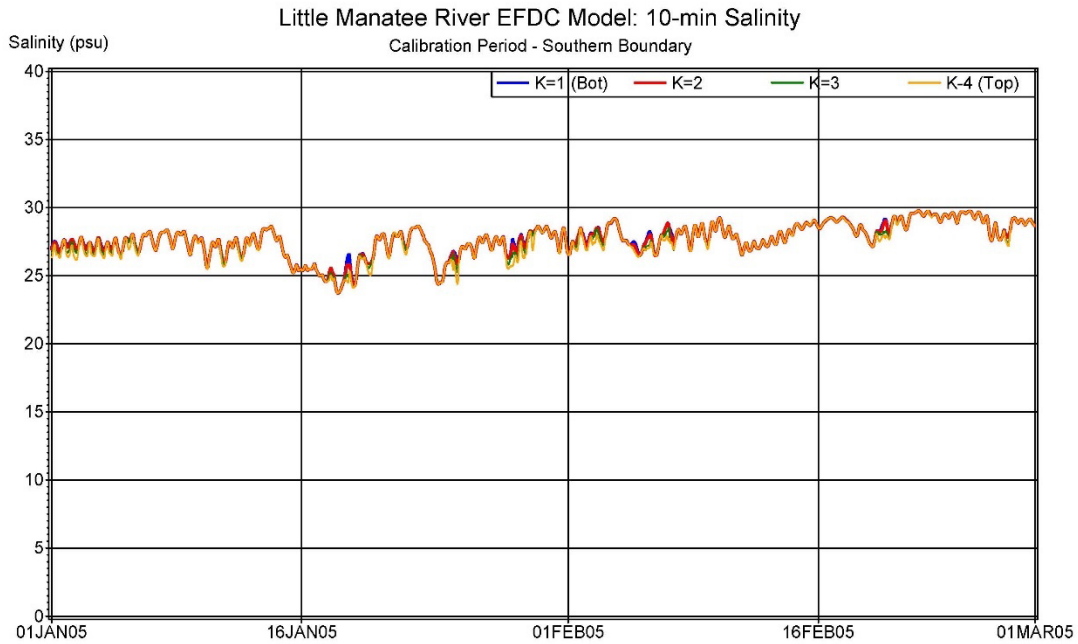


Figure 2-35. Time series of 10-minute frequency salinity at four vertical levels for the southern boundary in Tampa Bay, derived from output from the Old Tampa Bay hydrodynamic model, for the calibration period January-February 2005.

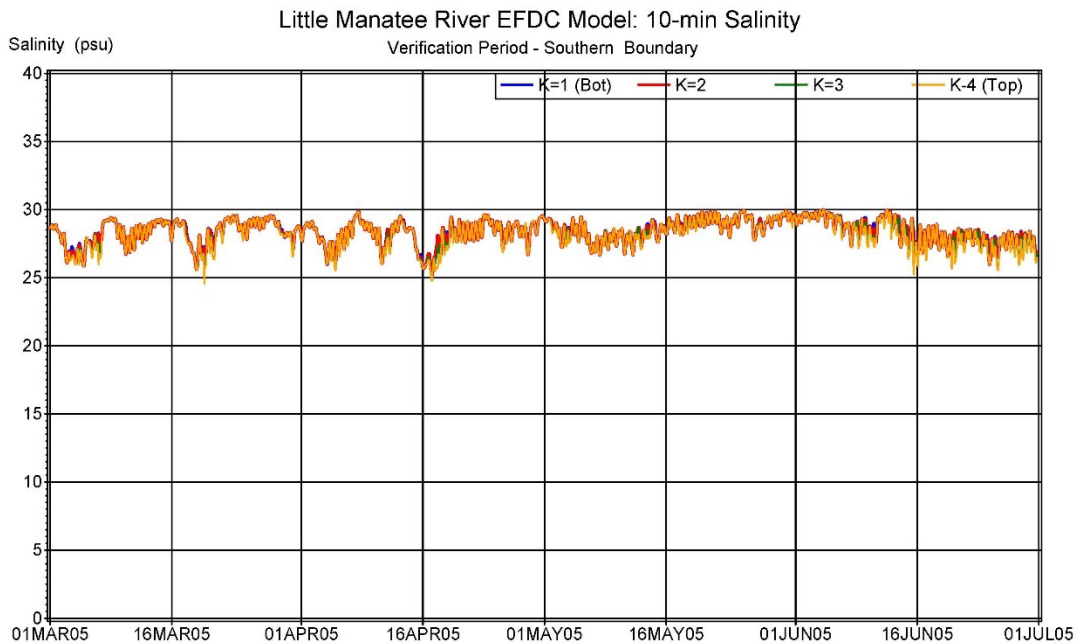


Figure 2-36. Time series of 10-minute frequency salinity at four vertical levels for the southern boundary in Tampa Bay, derived from output from the Old Tampa Bay hydrodynamic model, for the verification period March-June 2005.

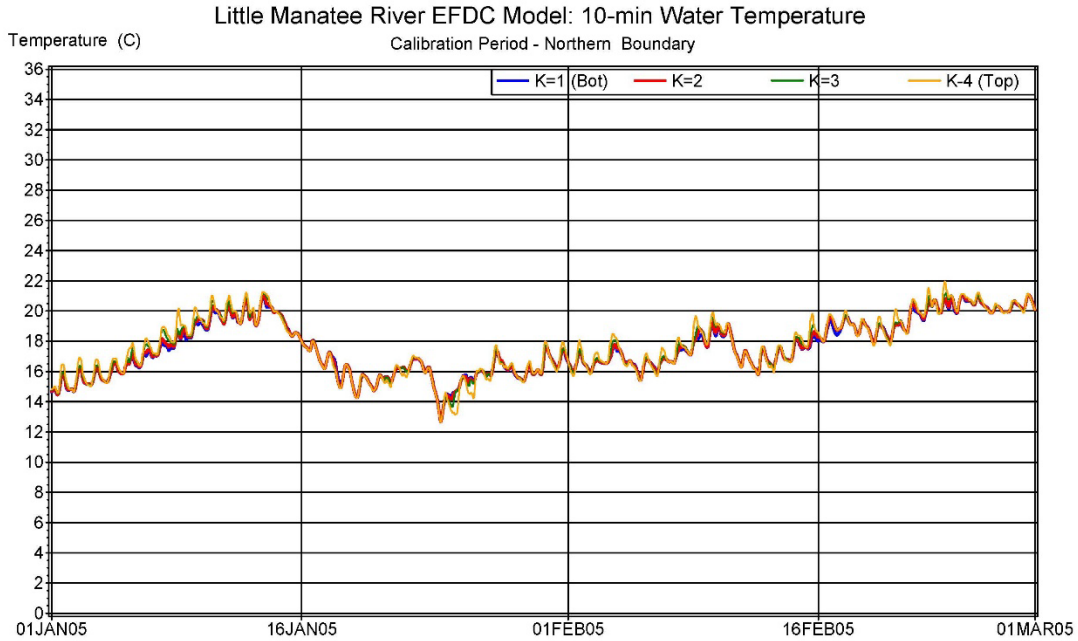


Figure 2-37. Time series of 10-minute frequency temperature at four vertical levels for the northern boundary in Tampa Bay, derived from output from the Old Tampa Bay hydrodynamic model, for the calibration period January-February 2005.

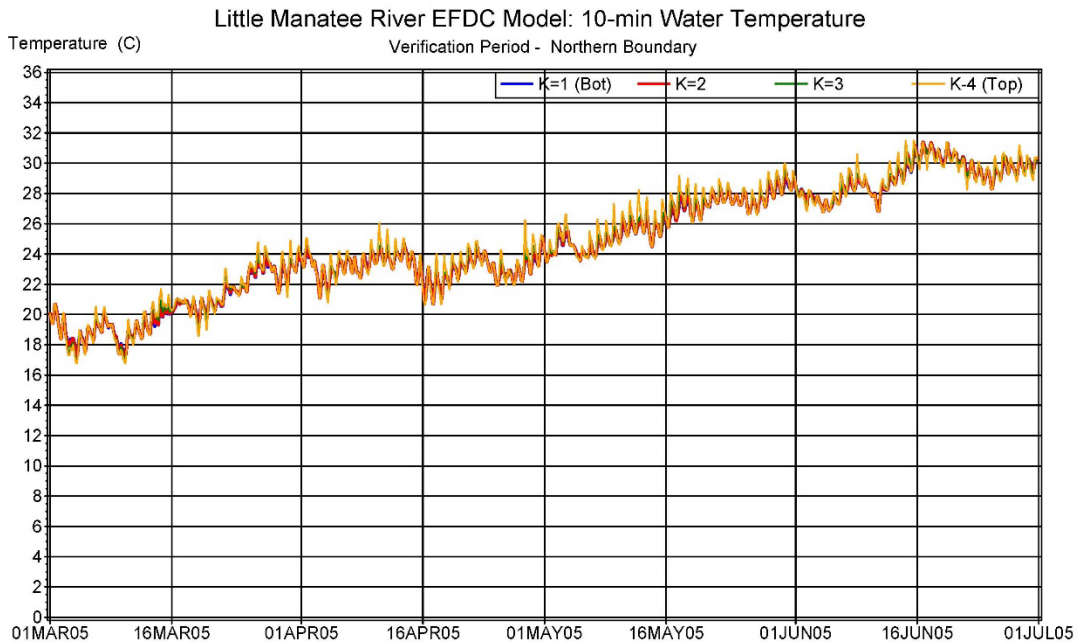


Figure 2-38. Time series of 10-minute frequency temperature at four vertical levels for the northern boundary in Tampa Bay, derived from output from the Old Tampa Bay hydrodynamic model, for the verification period March-June 2005.

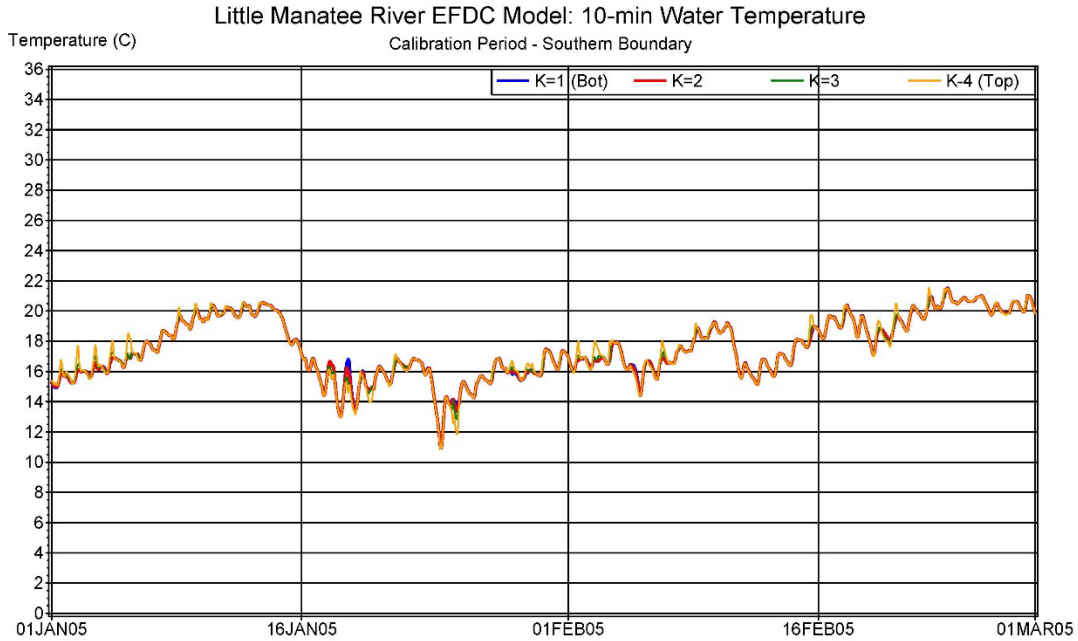


Figure 2-39. Time series of 10-minute frequency temperature at four vertical levels for the southern boundary in Tampa Bay, derived from output from the Old Tampa Bay hydrodynamic model, for the calibration period January-February 2005.

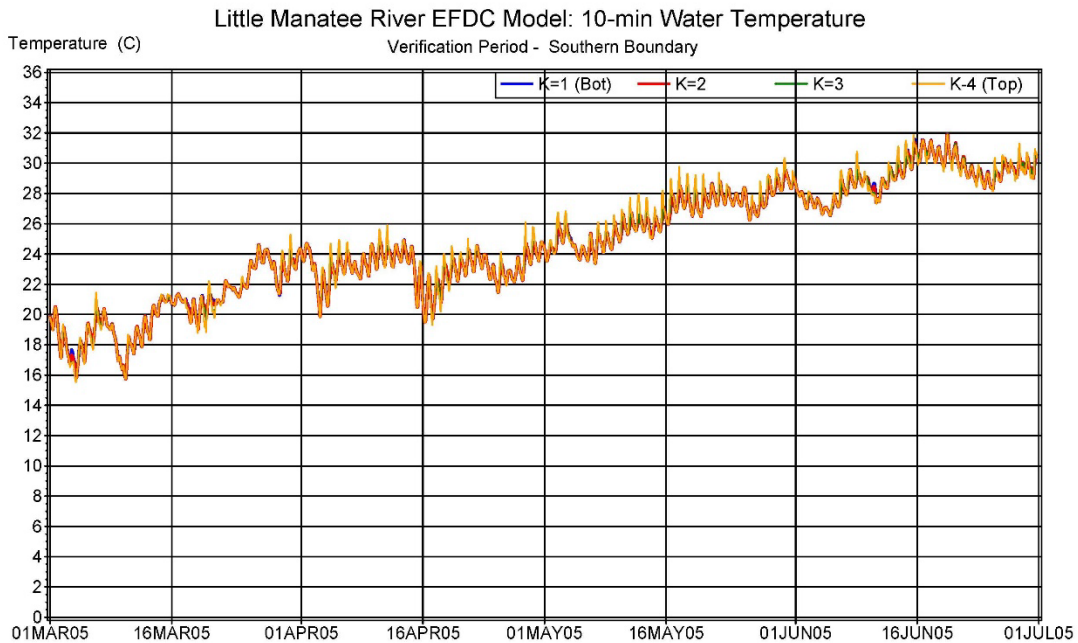


Figure 2-40. Time series of 10-minute frequency temperature at four vertical levels for the southern boundary in Tampa Bay, derived from output from the Old Tampa Bay hydrodynamic model, for the verification period March-June 2005.

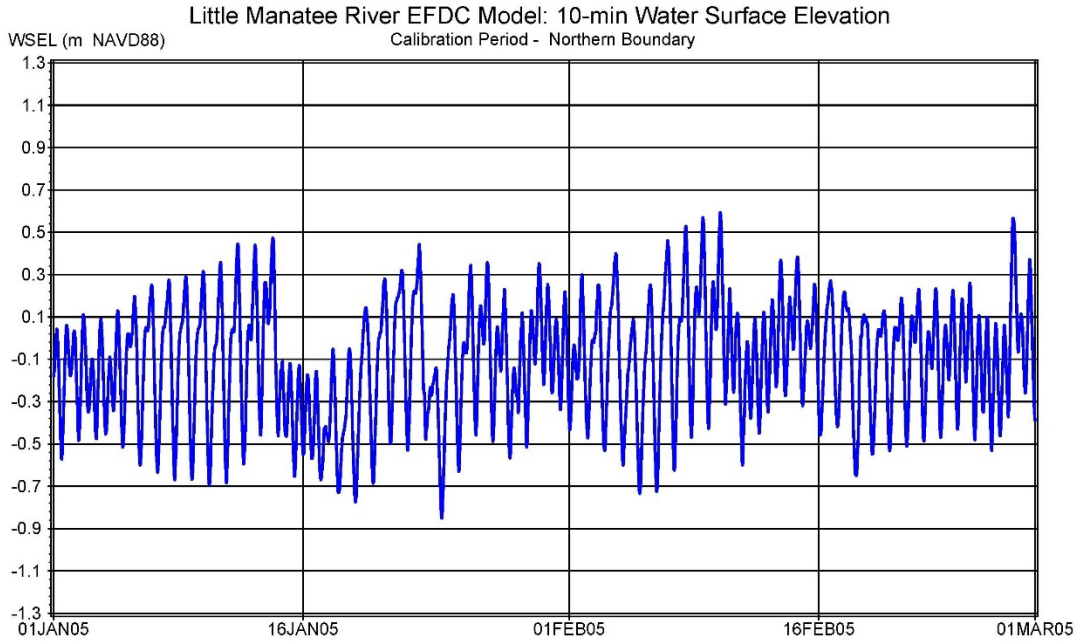


Figure 2-41. Time series of 10-minute frequency water surface elevation for the northern boundary in Tampa Bay, derived from output from the Old Tampa Bay hydrodynamic model, for the calibration period January-February 2005.

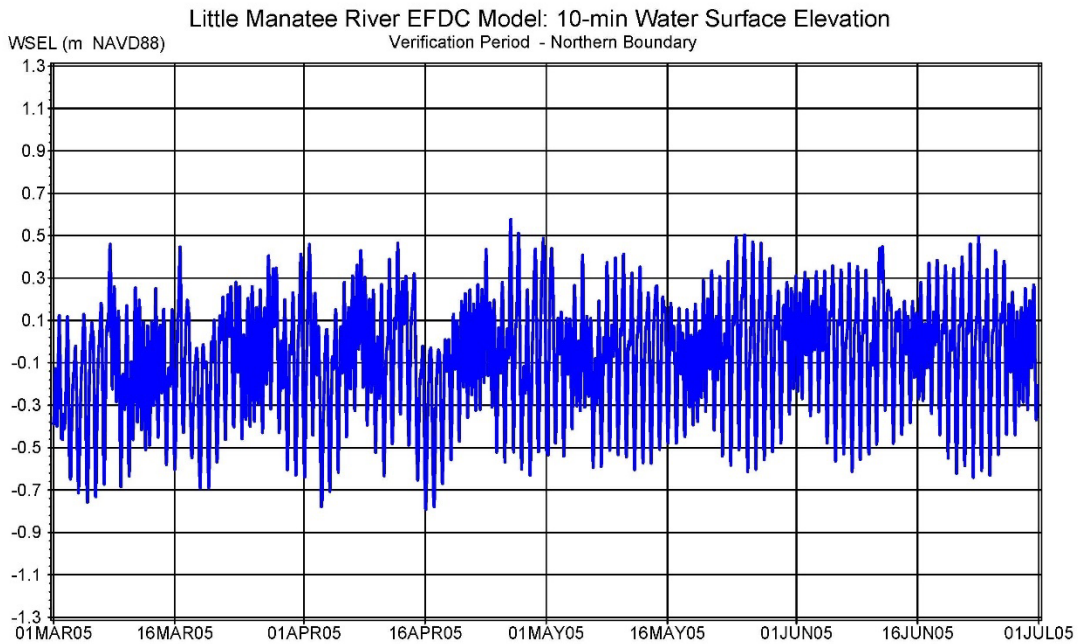


Figure 2-42. Time series of 10-minute frequency water surface elevation for the northern boundary in Tampa Bay, derived from output from the Old Tampa Bay hydrodynamic model, for the verification period March-June 2005.

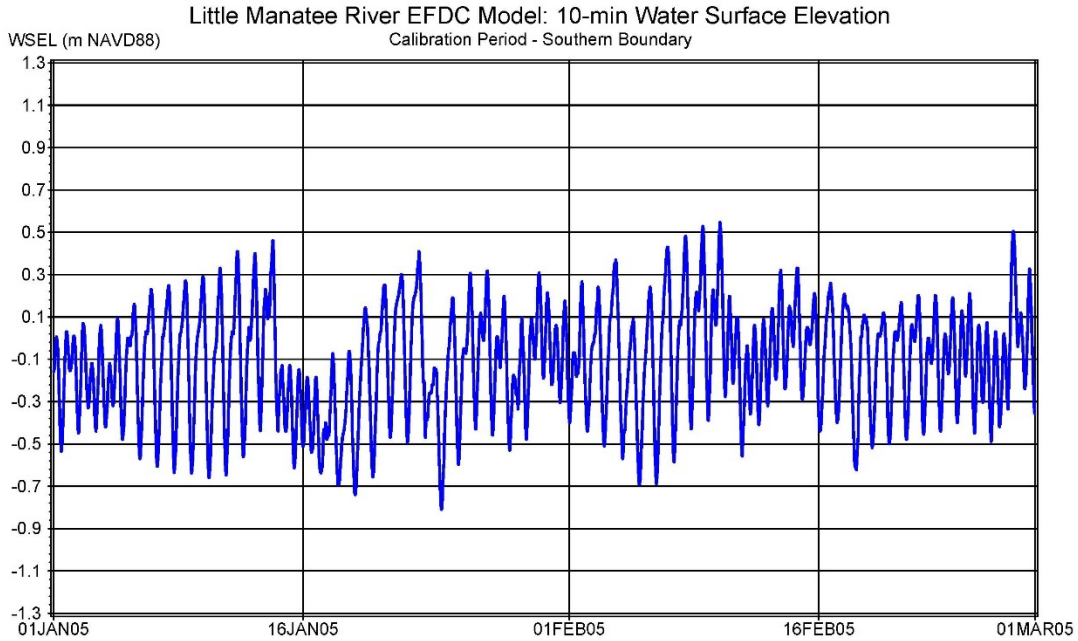


Figure 2-43. Time series of 10-minute frequency water surface elevation for the southern boundary in Tampa Bay, derived from output from the Old Tampa Bay hydrodynamic model for the calibration period January-February 2005.

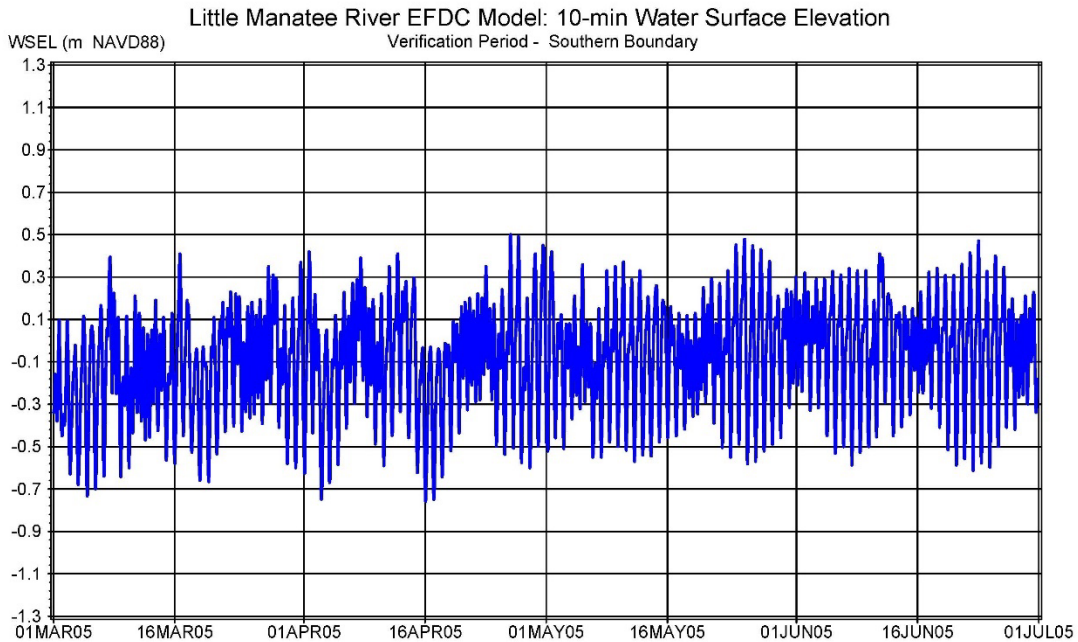


Figure 2-44. Time series of 10-minute frequency water surface elevation for the southern boundary in Tampa Bay, derived from output from the Old Tampa Bay hydrodynamic model for the verification period March-June 2005.

3.0 HYDRODYNAMIC MODEL CALIBRATION AND VERIFICATION

This section provides a description of the calibration and verification of the hydrodynamic model, including presentation of comparisons of model simulations to the observed data for water surface elevation, salinity, and temperature. First, the statistical measures of goodness of fit are provided, with the statistical evaluations then provided for both the calibration and verification periods.

3.1 STATISTICAL MEASURES OF GOODNESS OF FIT

Statistical comparisons include the mean error (ME), absolute mean error (AME), root mean square error (RMSE), coefficient of determination (R^2), and the Skill statistic. The statistical comparisons are defined as follows:

MEAN ERROR

$$ME = \frac{1}{n} \sum_{i=1}^n (P_i - O_i)$$

ABSOLUTE MEAN ERROR

$$AME = \frac{1}{n} \sum_{i=1}^n |P_i - O_i|$$

ROOT MEAN SQUARE ERROR

$$RMSE = \sqrt{\frac{\sum_{i=1}^n (P_i - O_i)^2}{n}}$$

COEFFICIENT OF DETERMINATION

$$R^2 = \frac{[n \sum_{i=1}^n O_i P_i - (\sum_{i=1}^n O_i)(\sum_{i=1}^n P_i)]^2}{[n \sum_{i=1}^n (O_i)^2 - (\sum_{i=1}^n O_i)^2][n \sum_{i=1}^n (P_i)^2 - (\sum_{i=1}^n P_i)^2]}$$

$$\text{Skill} = 1 - \frac{\sum (P_i - O_i)^2}{\sum (|P_i - \bar{O}_i| + |O_i - \bar{O}_i|)^2}$$

Here,

- P_i is simulated value for variable (water surface elevation, salinity, temperature),
- O_i is measured value for variable,
- \bar{O}_i is the mean of the measured values of the variable over the time period, and
- n is the number of matched pairs of simulated and observed values.

For mean error (ME), absolute mean error (AME), and root mean square error (RMSE), the closer the value to 0 the better the fit. For R^2 and Skill, the closer the value to 1 the better the fit.

Model outputs were extracted to match the times of the observed data for the statistical analyses, with the statistics calculated over the relevant period (calibration or verification).

The ME provides information related to a bias in the results, with units of measure of the variable being evaluated. For example, if the ME for salinity at a site is less than zero, it means that the model is under-predicting salinity at that site over the selected period. The AME provides a measure of how great the absolute difference is between paired measurements over the period, with a value near zero indicative of very good fit. The AME is expressed in units of measure of the variable being evaluated. The RMSE represents the deviation of each of the individual simulated and observed data pairs, providing a measure of overall differences with units of the variable being evaluated. The coefficient of determination (R^2) provides a measure of how the model and data line up both in time and magnitude, with a perfect fit resulting in a value of 1. The Skill statistic ranges in value from 1 (perfect agreement) to 0 (complete disagreement).

The locations of the continuous recorders which provided the observed data used in the calibration effort were provided above in Figure 2-9 and are shown again here in Figure 3-1 for easy reference.



Figure 3-1. Locations of four USGS sites with data used in calibration and verification.

3.2 CALIBRATION RESULTS

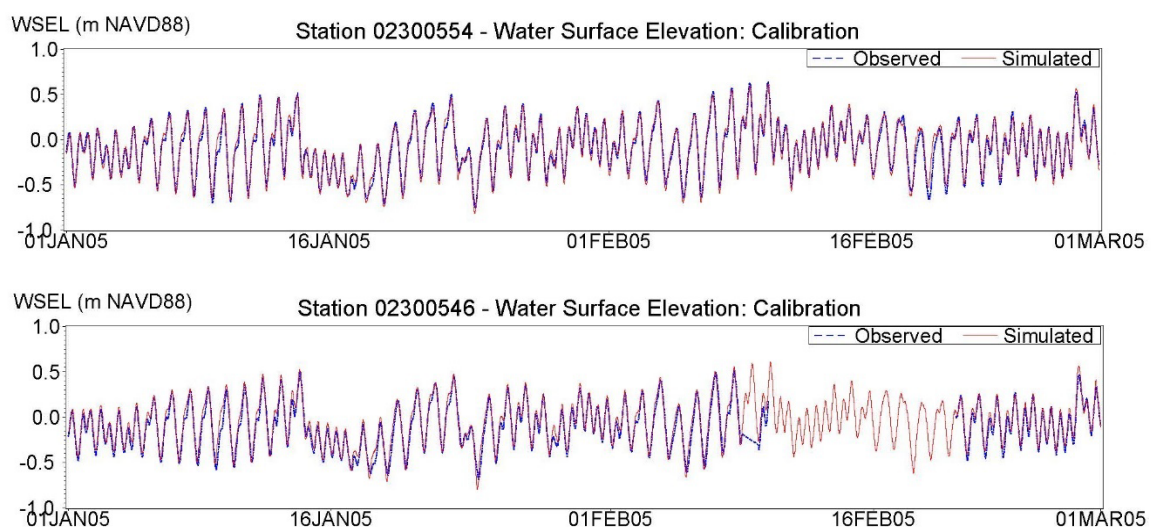
Evaluation of model calibration appropriateness is based on the combination of time series comparisons of modeled and observed data and statistical analysis of paired simulated and observed data. Simulation of temporally varying signals in tidal environments are often subject to slight shifts in timing when comparing simulated and observed variables, which may, for example, result in lower than expected R^2 values compared to signals that temporally line up exactly. However, viewing the time series plots of simulated and observed values may show that the magnitude and periodicity of the simulated and observed data are very similar, and indicative of appropriate simulation. Utilizing both time series comparisons and statistical comparisons allows for decisions on appropriateness of calibration based on a robust information set. Thus, both time series presentations and statistical comparisons are provided in the following for calibration evaluation.

When evaluating the ability of the model to simulate observed conditions, an important consideration is the primary purpose of the modeling effort. The model is to be used to evaluate changes in salinity as a function of changes in inflows, so that a key qualitative metric is how the model responds to changes in flows with respect to simulation of salinity. An additional consideration is that the downstream boundary conditions for the model are derived from a model of Tampa Bay, so that there is some error associated with the Tampa Bay model output that may impact comparisons to observed data within the Little Manatee River. Hence, in addition to the statistical measures of fit, visual

evaluation of the time series comparisons between simulated and observed data can provide necessary input to determination of the model's calibration status.

Time series comparisons of the simulated and observed water surface elevation, salinity, and temperature are provided for the locations where observed data were collected in the lower river. These locations were provided above in Figure 3-1. The calibration period was January 1, 2005 – February 28, 2005. Only water surface elevation was measured at the upstream-most location, USGS Station 02300532. At this location, no reliable vertical reference datum was established, and use of a vertical reference datum conversion suggested in comments from the USGS website resulted in water surface elevations at this location being considerably lower, by approximately 0.15 m, than those downstream. Therefore, the reported water surface elevations were adjusted upward by 0.15 m prior to performing graphical and statistical comparisons with model output.

Figure 3-2 presents time series comparisons of the simulated and observed water surface elevations at all four sites for the calibration period. Table 3-1 provides the comparative statistical measures for the water surface elevation simulation. The statistics for Station 02300554, at the mouth of the river, are very good, indicating that the downstream boundary water surface elevations developed from the OTB hydrodynamic model are appropriately driving water surface elevations at the mouth of the Little Manatee River. The overall ME is less than 2 cm (0.02 m), and the Skill statistic values are all greater than 0.95, with an overall value of 0.975. The calibration metrics for water surface elevation indicate the model is appropriately simulating observed water surface elevation conditions at the four sites. Given the locations of the fixed sites from the mouth of the river upstream to approximately Rkm 17, these results indicate that the water surface elevations throughout the lower river are being accurately simulated.



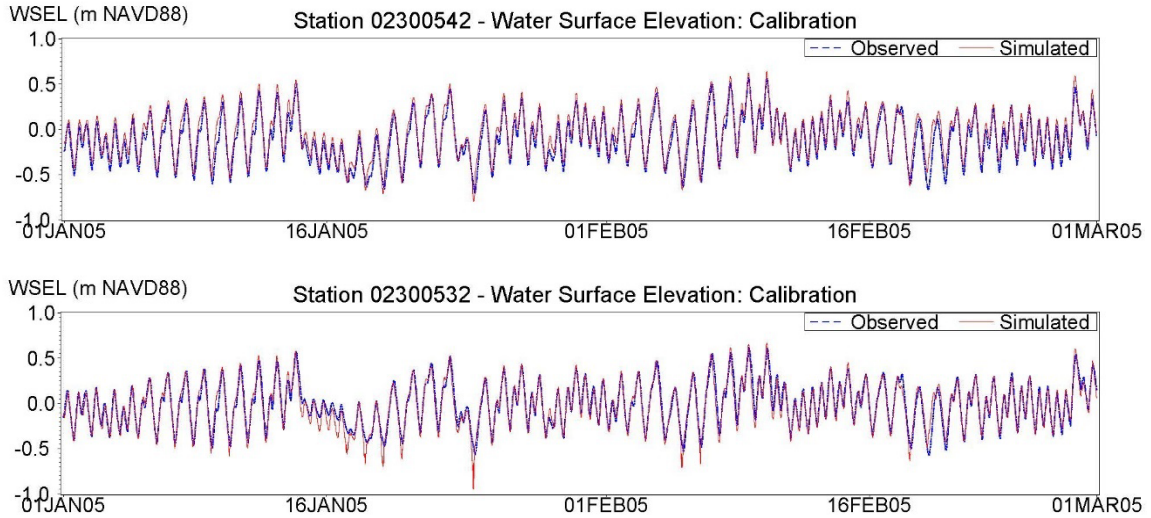


Figure 3-2. Time series comparisons of observed (blue dashed line) and simulated (red line) water surface elevations at the four continuous recorders during the calibration period, January – February 2005.

Table 3-1. Calibration statistics for water surface elevation. Units of ME, AME, and RMSE are meters.					
Station	ME	AME	RMSE	R ²	Skill
02300554	0.00	0.04	0.05	0.9611	0.990
02300546	0.03	0.05	0.09	0.8705	0.959
02300542	0.06	0.07	0.08	0.9380	0.971
02300532	-0.02	0.06	0.08	0.9061	0.974
Overall	0.02	0.05	0.08	0.9094	0.975

Figure 3-3 presents time series comparisons of the simulated and observed surface and bottom salinity at the three downstream sites (recall only water surface elevations were collected at the upstream site, Station 02300532). It is important to note that the variability in salinity is high, as expected in a tidal river, with tidally driven periodicity as well as inflow-induced variability. The simulated surface and bottom salinity values show the same tidally driven variability as do the observed data, and the salinity ranges at each site are well simulated. Differences between simulated and observed salinity values do exist, but the time series presentation of the simulated and observed data indicate that the model is generating similar salinity regimes as those observed at all sites. The statistical measures evaluated to ensure appropriate calibration, provided in Table 3-2, also indicate that the model is appropriately simulating salinity, with an overall ME of less than 1 psu less than observed, an overall R^2 value of 0.89, and an overall Skill statistic value of 0.96.

The simulated responses of salinity to changes in inflows is the most important aspect of the calibration, as these salinity responses are then used to evaluate expected responses to reductions in flow as part of the minimum flow development process. The simulated variations in salinity due to changes in flows ranging from less than 50 cfs to almost 600 cfs during the calibration period (Figure 2-12) are very similar to those of the observed salinity at the continuous recorder sites, as shown in Figure 3-3. These results provide confidence that the model is providing appropriate salinity responses to flow changes.

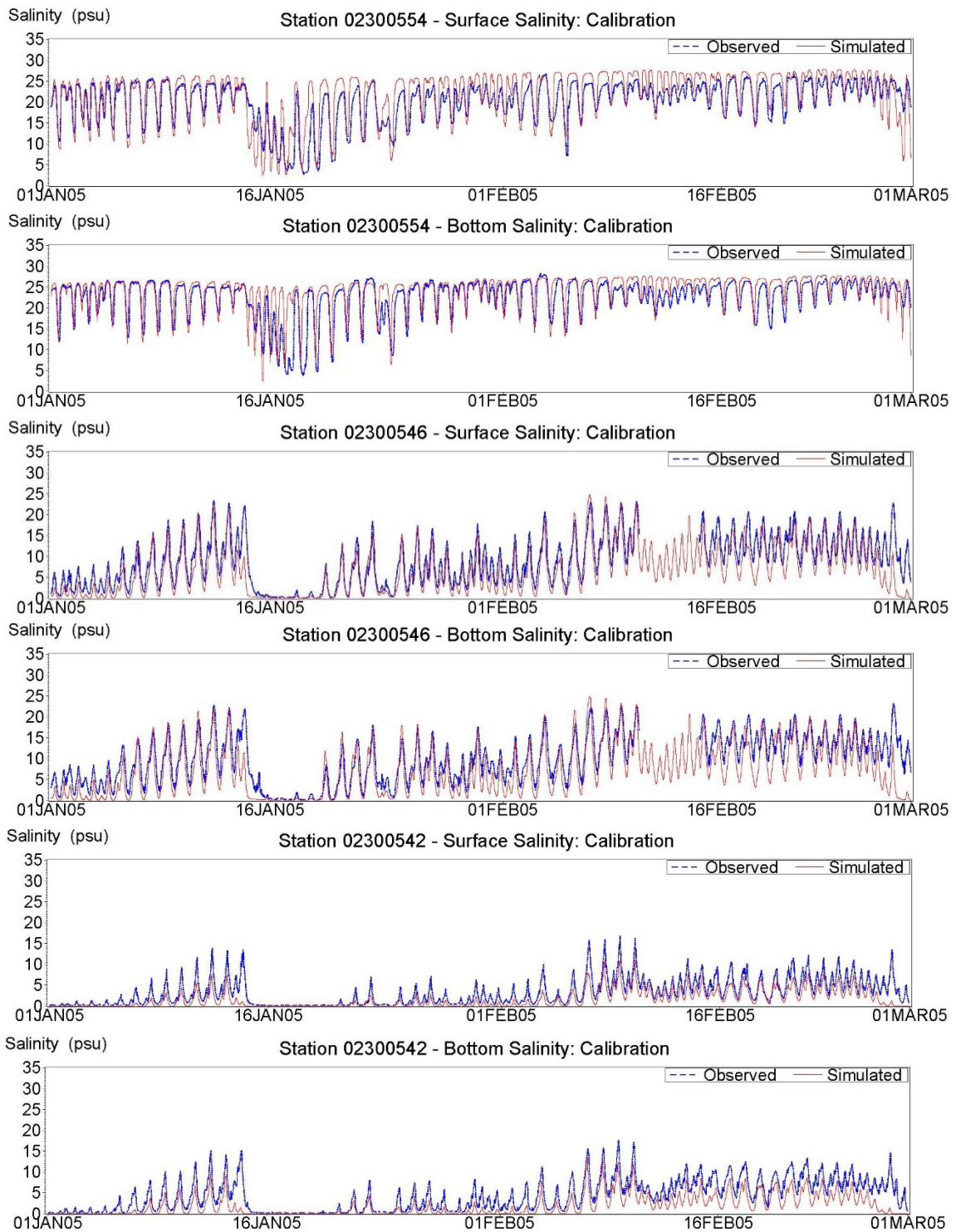


Figure 3-3. Time series comparisons of observed (blue dashed line) and simulated (red line) surface and bottom salinity at the three continuous recorders during the calibration period, January – February 2005.

Table 3-2. Calibration statistics for surface and bottom salinity. Units of ME, AME, and RMSE are psu.					
Station	ME	AME	RMSE	R²	Skill
02300554 Surface	1.79	2.95	4.03	0.6148	0.857
02300554 Bottom	1.86	2.38	3.92	0.4620	0.769
02300546 Surface	-2.29	2.54	3.49	0.7988	0.903
02300546 Bottom	-2.69	3.16	4.13	0.7327	0.873
02300542 Surface	-1.68	1.69	2.36	0.7844	0.813
02300542 Bottom	-2.38	2.38	3.11	0.7738	0.789
Overall	-0.90	2.52	3.56	0.8944	0.964

Figure 3-4 provides time series of the simulated and observed surface and bottom temperatures for the three downstream-most sites, with the daily pattern of temperature variability as well as the absolute temperatures being well simulated by the model. From examination of the time series, it appears that the simulated temperatures are slightly lower than the observed temperatures. Based on the statistical measures reported in Table 3-3, the ME is -1.1 C, indicating that, overall, the model does under-predict the water temperature by that amount. The overall statistical measures, including the Skill statistic value of 0.88 and the R² value of 0.77, along with the time series comparisons, indicate sufficient agreement between the simulated and observed temperatures, as these relatively small differences in simulated and observed temperatures are not expected to play an important role in simulation of salinity or variations in salinity.

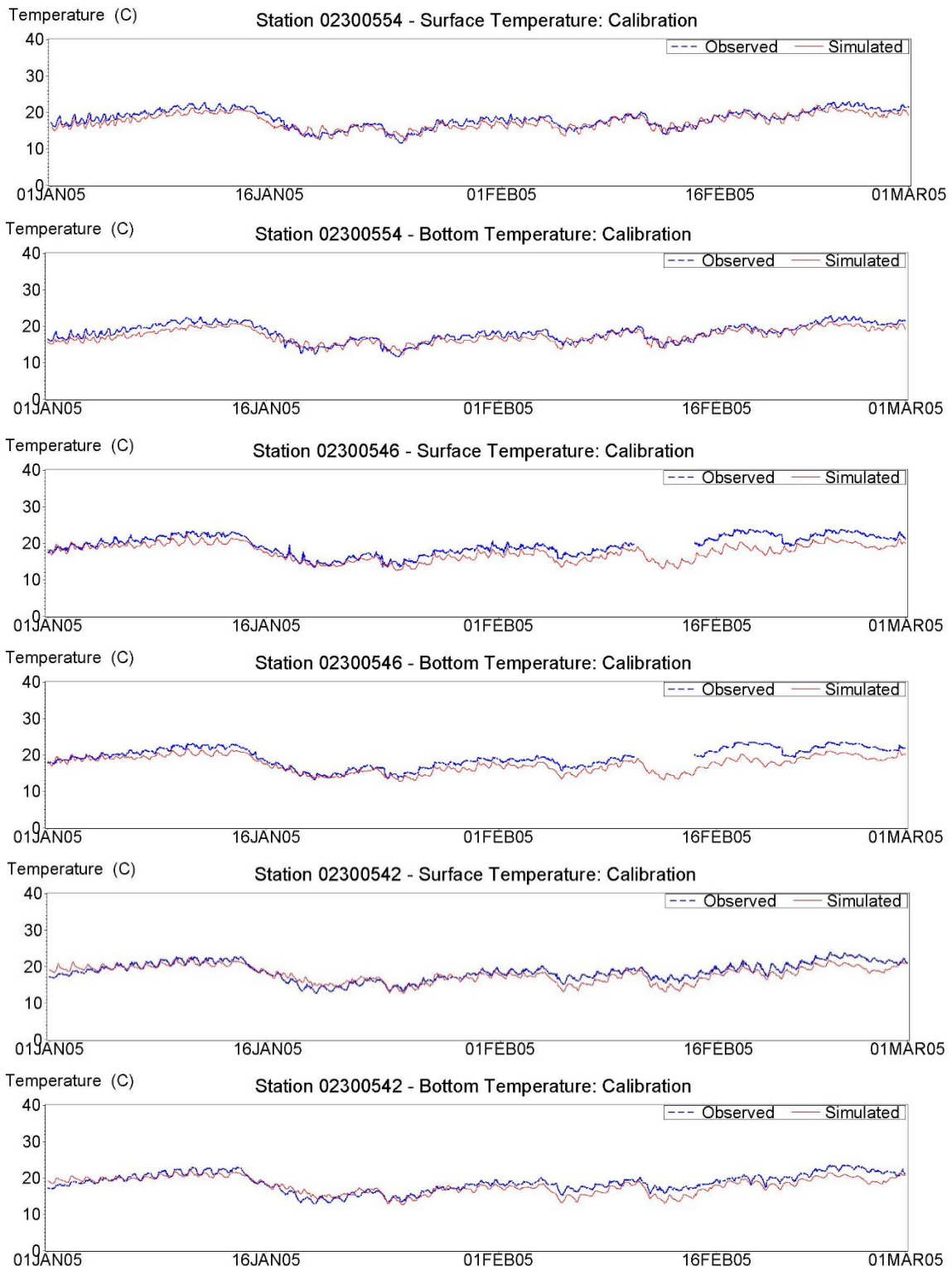


Figure 3-4. Time series comparisons of observed (blue dashed line) and simulated (red line) surface and bottom temperature at the three continuous recorders during the calibration period, January – February 2005.

Table 3-3. Calibration statistics for surface and bottom temperature. Units of ME, AME, and RMSE are degree C.					
Station	ME	AME	RMSE	R ²	Skill
02300554 Surface	-0.76	1.06	1.22	0.8538	0.925
02300554 Bottom	-0.81	1.10	1.27	0.8501	0.915
02300546 Surface	-1.72	1.75	2.13	0.7998	0.824
02300546 Bottom	-1.64	1.68	2.07	0.7987	0.830
02300542 Surface	-0.75	1.24	1.48	0.8910	0.896
02300542 Bottom	-0.89	1.29	1.53	0.7450	0.890
Overall	-1.10	1.36	1.66	0.7668	0.876

It is worthy of note that a previous model of the Lower Little Manatee River (Huang and Liu 2007), utilizing the observed data at the mouth of the river as provided by Station 02300554 to establish the downstream boundary conditions, resulted in calibration statistics very similar to those provided here, where the downstream boundary conditions are established in Tampa Bay, well removed from the mouth of the river. For the sites upstream of the river mouth, Stations 02300546, 0230542, and 02300532, the previous model calibration for water surface elevation had RMSE values ranging from 0.05 m to 0.08 m (Huang and Liu 2007), similar to those for this effort of 0.05 m to 0.09 m for all four stations (Table 3-1). Similarly, the R² values for the previous model water surface elevation calibration for the three stations upstream of the mouth ranged from 0.89 to 0.95, similar to the range of R² values for the current model, 0.87 to 0.96 for all four river stations, as provided in Table 3-1.

The salinity calibration metric values presented in Table 3-2 also compare favorably to those from the previous model which used the downstream boundary conditions established using data from Station 02300554. The R² values for the previous model salinity calibration for the two stations upstream of the mouth with salinity data, Stations 02300546 and 02300542, ranged from 0.82 to 0.92, similar to the overall R² value for the current model, 0.89 for all three river stations with salinity data, as provided in Table 3-2. The overall RMSE for the current model, 3.56 psu (Table 3-2), was somewhat elevated compared to the range of values from the previous model 1.07 ppt – 1.95 ppt (Huang and Liu 2007), but it is evident from the time series comparisons that the current model simulated salinity does respond appropriately to changes in freshwater inflows.

A comparison is also provided here to calibration criteria utilized in the Old Tampa Bay Integrated Model Development Project for the hydrodynamic model developed for the study (ATM 2014). The OTB study was funded by the Tampa Bay Estuary Program and the District, with peer review of all model components. It is important to keep in mind that the calibration criteria for water surface elevation and salinity were developed for assessing calibration in OTB, an open estuary system rather than an estuarine river like the Lower Little Manatee River.

For water surface elevation, the OTB criteria, the OTB hydrodynamic overall calibration results, and the corresponding Little Manatee River overall calibration results as provided in Table 3-1 are as follows:

Metric	OTB Criterion	OTB Model Overall	Little Manatee River Overall
RMSE	0.05 m	0.07 m	0.08 m
ME	±0.03 m	0.02 m	0.02 m
AME	0.05 m	0.05 m	0.05 m
R ²	0.90	0.96	0.91

The calibration metric values for this Little Manatee River EFDC model compare very favorably with both the OTB criteria and the OTB model calibration results for water surface elevation, even though the Little Manatee River model represents a tidal river system instead of a more open estuarine bay systems.

Similar comparison of the Little Manatee River salinity calibration results (provided in Table 3-2) to the OTB model criteria and OTB salinity calibration results are more indicative of the greater salinity variability expected in the estuarine river as compared to the more open OTB system, as seen in the following (where two values are given for the OTB model overall, these are for bottom and surface, respectively):

<u>Metric</u>	<u>OTB Criterion</u>	<u>OTB Model Overall</u>	<u>Little Manatee River Overall</u>
RMSE	2.5 psu	1.2 psu	3.56 psu
ME	±0.5 psu	-0.1, -0.2 psu	-0.90 psu
AME	2.0 psu	1.0 psu	2.52 psu
R ²	0.70	0.93, 0.92	0.89

This comparison of salinity calibration results indicates that the Little Manatee River model, although representing a tidal river and not a more open bay system, results in calibration metric values that come very close to satisfying the calibration criteria selected for the more open bay system. These comparisons provide additional assurance that the Little Manatee River model is well calibrated.

3.3 VERIFICATION RESULTS

Like the calibration period, evaluation of model verification over the March – June 2005 period is based on the combination of time series comparisons of modeled and observed data and statistical analysis of paired simulated and observed data. Time series comparisons of the simulated and observed water surface elevation, salinity, and temperature are provided for the locations where observed data were collected in the lower river. As mentioned above, only water surface elevation was measured at the upstream-most location, USGS Station 02300532, where observed water surface elevation data were adjusted upward by 0.15 m prior to performing graphical and statistical comparisons with model output.

Figure 3-5 presents time series comparisons of the simulated and observed water surface elevations at all four sites for the verification period, with the comparative statistical measures for the water surface elevation simulation provided in Table 3-4. The overall ME for water surface elevations during the verification period is 1 cm (0.01 m), and the Skill statistic values are all greater than 0.97, with an overall value of 0.980. The statistical comparisons for water surface elevation verification support the conclusion that the model is appropriately simulating observed water surface elevation conditions at the four sites.

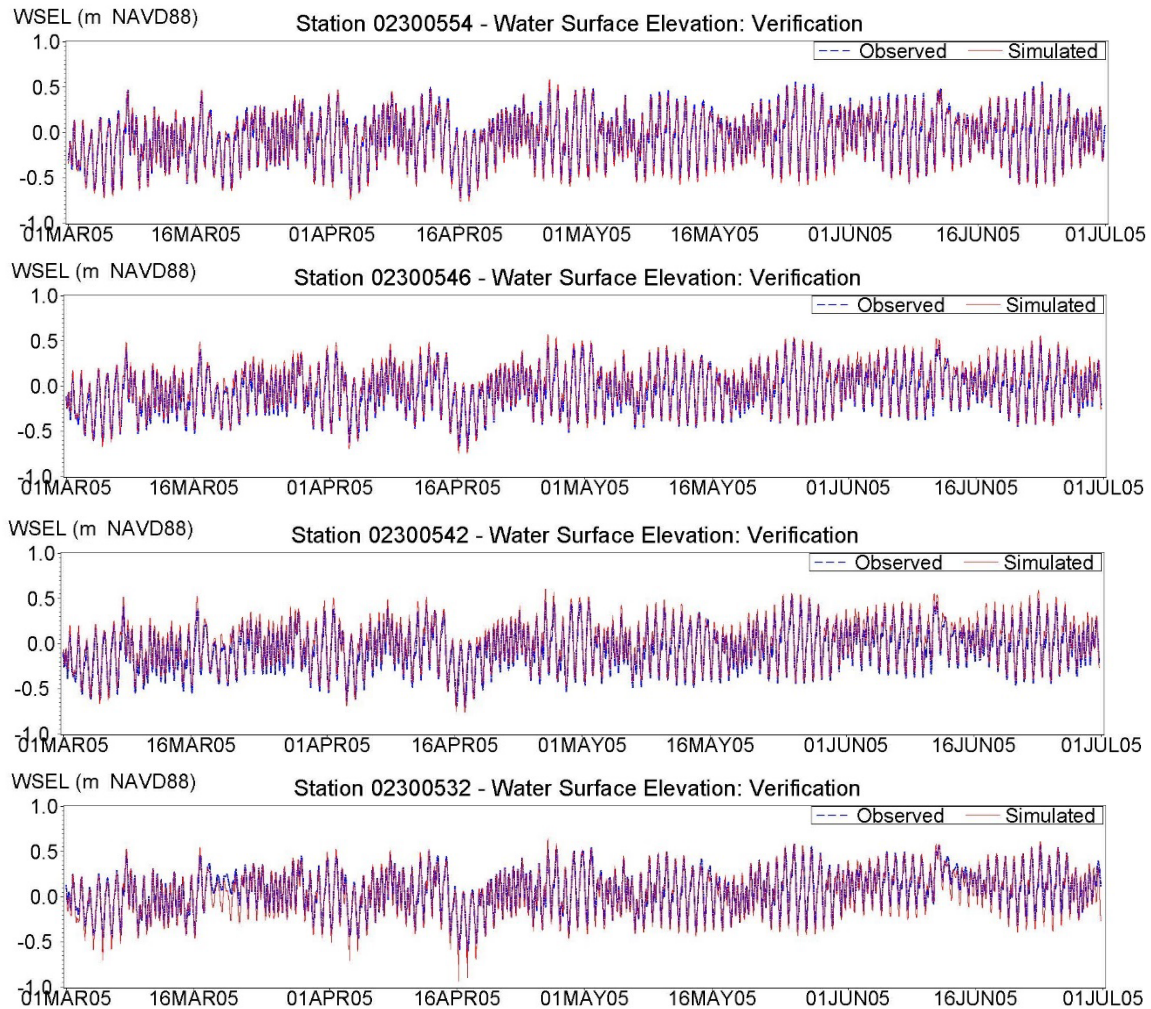


Figure 3-5. Time series comparisons of observed (blue dashed line) and simulated (red line) water surface elevations at the four continuous recorders during the verification period, March – June 2005.

Table 3-4. Verification statistics for water surface elevation. Units of ME, AME, and RMSE are meters.					
Station	ME	AME	RMSE	R ²	Skill
02300554	-0.01	0.03	0.04	0.9740	0.993
02300546	0.03	0.05	0.06	0.9433	0.981
02300542	0.05	0.06	0.08	0.9483	0.973
02300532	-0.04	0.06	0.08	0.9001	0.967
Overall	0.01	0.05	0.07	0.9248	0.980

Figure 3-6 presents time series comparisons of the simulated and observed surface and bottom salinity at the three downstream sites. As with the calibration period, variability in salinity is high, especially at the more downstream sites. The simulated surface and bottom salinity reflect the effects of tidally driven variability similar to the observed values, and the salinity ranges at each site are well simulated. The time series presentations indicate that the model is generating similar salinity regimes as those observed at all sites. The statistical measures provided in Table 3-5 indicate that the model is

appropriately simulating salinity, with an overall ME of 1.1 psu less than observed, an overall R² value of 0.89, and an overall Skill statistic value of 0.96.

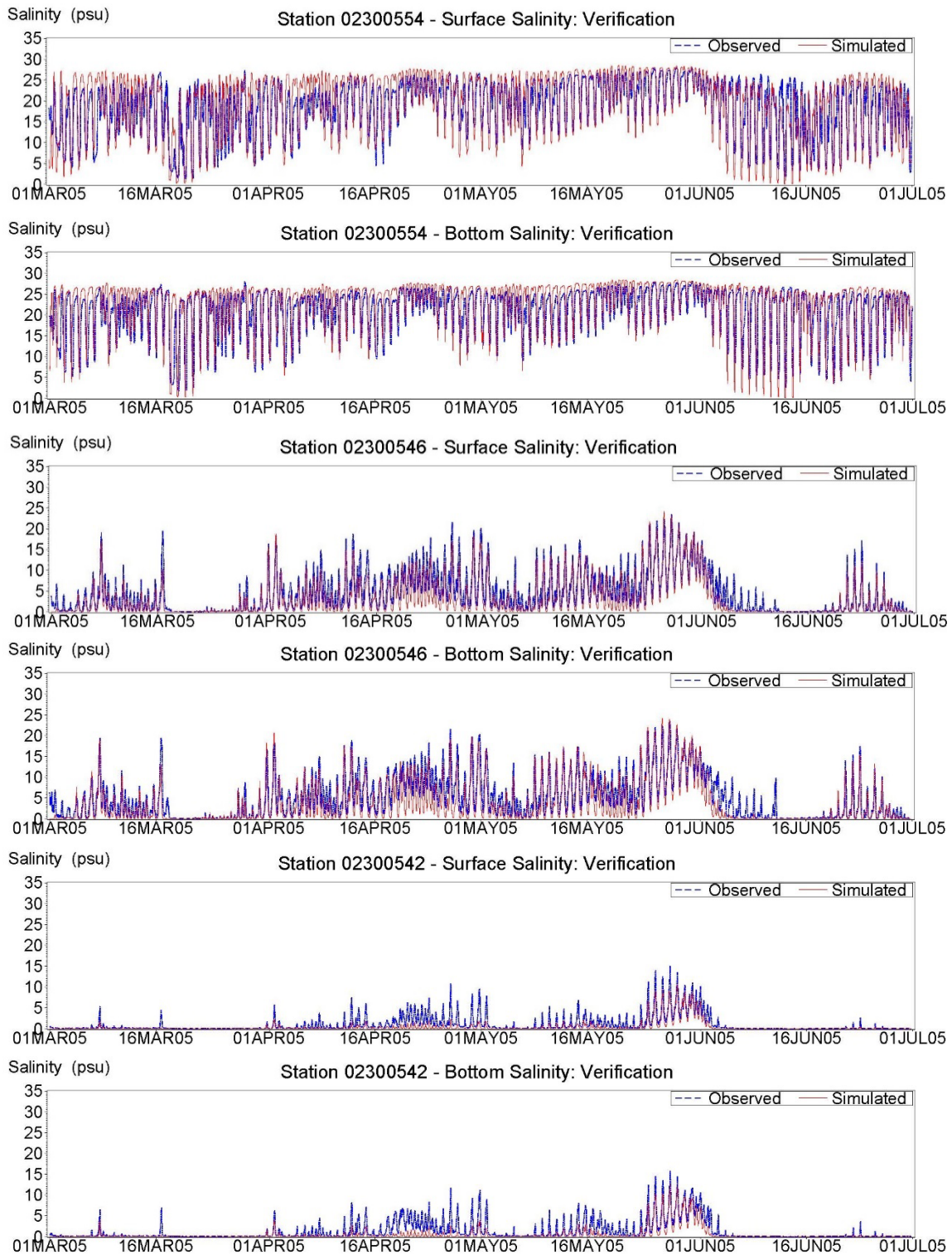


Figure 3-6. Time series comparisons of observed (blue dashed line) and simulated (red line) surface and bottom salinity at the three continuous recorders during the verification period, March – June 2005.

Table 3-5. Verification statistics for surface and bottom salinity. Units of ME, AME, and RMSE are psu.					
Station	ME	AME	RMSE	R²	Skill
02300554 Surface	1.30	3.09	4.23	0.6954	0.900
02300554 Bottom	2.54	3.31	5.01	0.4750	0.789
02300546 Surface	-1.51	1.65	2.37	0.8538	0.930
02300546 Bottom	-1.85	2.17	3.05	0.7725	0.903
02300542 Surface	-0.68	0.68	1.27	0.7119	0.835
02300542 Bottom	-0.86	0.87	1.62	0.6845	0.820
Overall	-0.18	1.96	3.22	0.9121	0.973

Figure 3-7 shows the time series of the simulated and observed surface and bottom temperatures for the three downstream-most sites, with the daily pattern of temperature variability as well as the observed temperature ranges and magnitudes being well simulated by the model. Late in the verification period, most notably in June, the model underpredicts the observed temperature at Station 02300546 and Station 02300542, but the daily variability is still captured well at all sites. The statistical measures reported in Table 3-6 show that the overall ME is -1.1 C, indicating that, overall, the model does under-predict the water temperature by that amount. The overall statistical measures, including the Skill statistic value of 0.94 and the R² value of 0.90, along with the time series comparisons, indicate that the verification period temperature simulation agreement to observed data is very similar to that of the calibration period.

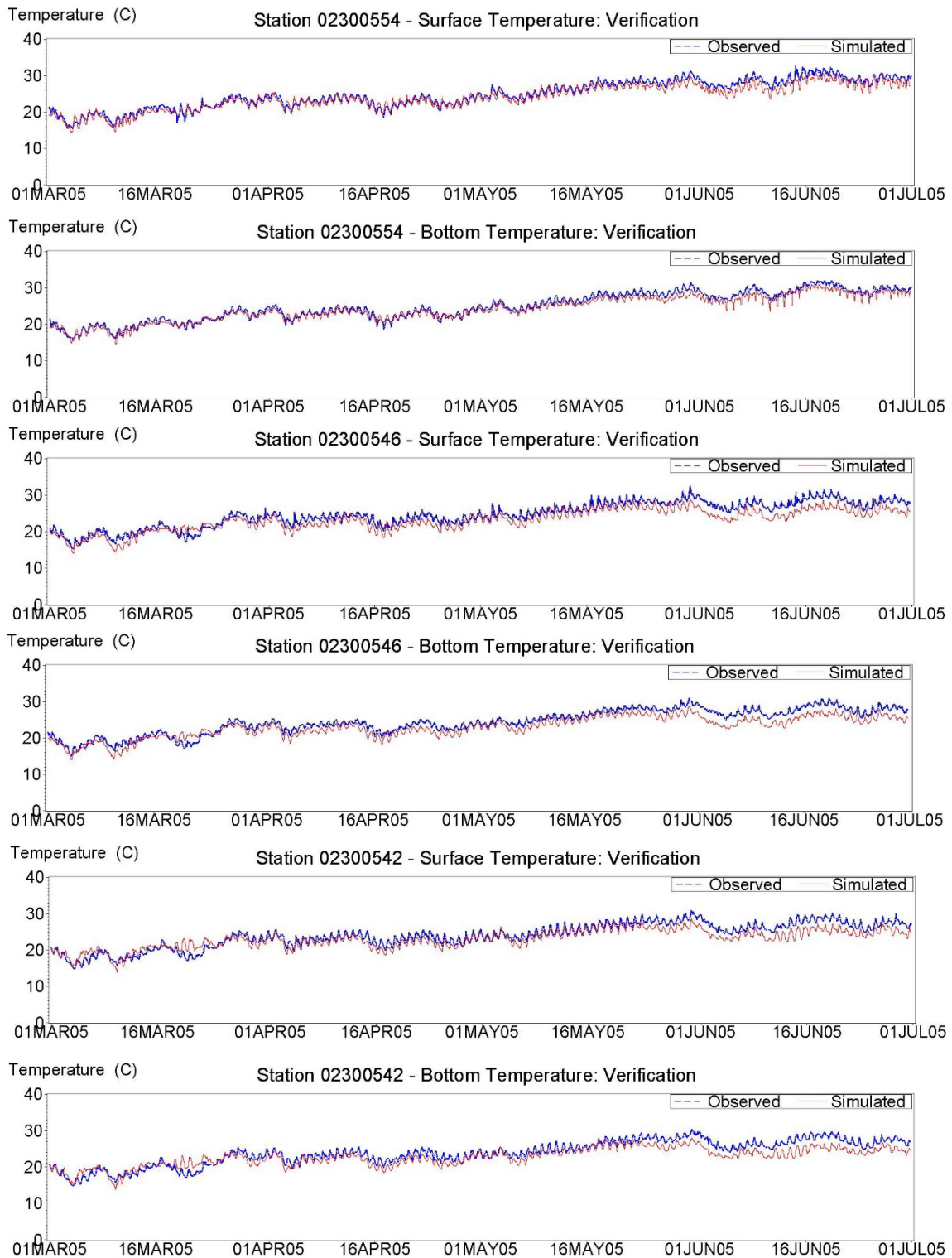


Figure 3-7. Time series comparisons of observed (blue dashed line) and simulated (red line) surface and bottom temperature at the three continuous recorders during the verification period, March – June 2005.

Table 3-6. Verification statistics for surface and bottom temperature. Units of ME, AME, and RMSE are degree C.					
Station	ME	AME	RMSE	R²	Skill
02300554 Surface	-0.83	1.02	1.24	0.9475	0.971
02300554 Bottom	-0.71	0.85	1.05	0.9653	0.979
02300546 Surface	-1.55	1.72	1.93	0.8925	0.911
02300546 Bottom	-1.46	1.64	1.83	0.9020	0.917
02300542 Surface	-1.04	1.48	1.75	0.8910	0.914
02300542 Bottom	-1.18	1.59	1.85	0.8545	0.902
Overall	-1.13	1.38	1.64	0.8960	0.938

Given the results of the calibration period comparisons to observed data, and supported by the very similar findings of the verification period comparisons, the hydrodynamic model is appropriate for use in the assessment of expected changes in salinity due to changes in inflows.

4.0 BASELINE AND FLOW REDUCTION SCENARIOS

The development of baseline flows for the Little Manatee River are described previously in JEI (2018), and account for upstream withdrawals and the impacts of agricultural operations on the observed flow record. For evaluation of scenarios, a relatively long time period was needed for evaluating potential flow reductions over a range of hydrologic conditions. This hydrodynamic modeling effort used the same 5-year period (2000-2004) as in JEI (2018) as the simulation period for the baseline and flow reduction scenario runs and utilized the baseline flow as developed previously (JEI 2018).

4.1 DESCRIPTION OF SCENARIOS

Eight flow reduction scenarios at 5 percent increments between 5 percent and 40 percent were applied to the upstream baseline inflow. All un-gaged inflows were left unchanged in these scenarios. The only modification to the baseline flow scenario was the reduction of the baseline inflows at the upstream end of the model domain at the US 301 location. As in the model calibration and verification effort, the water surface elevation, salinity, and temperature boundary conditions in Tampa Bay were derived from the Old Tampa Bay model output for the 2000-2004 period.

The flows at US 301 (USGS gage 02300500) during the 2000-2004 period were similar to those of the long-term flow record (1940-2020), with the time series of mean annual flows for the entire 1940-2020 period provided in Figure 4-1, where the 2000-2004 period is marked by the black vertical lines.

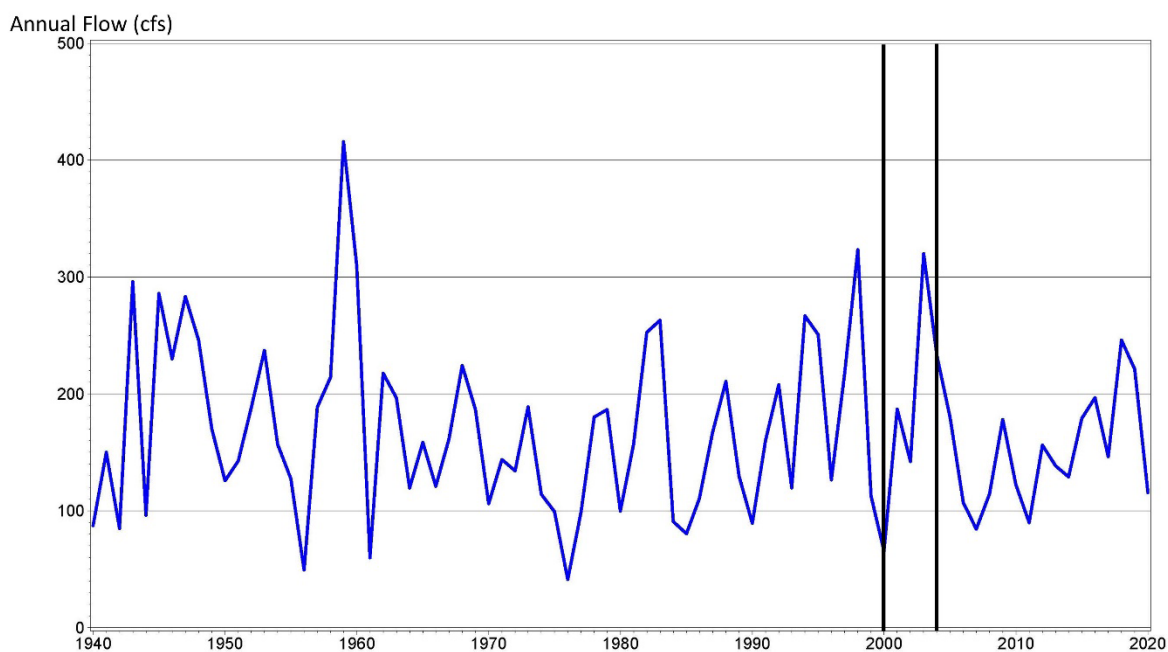


Figure 4-1. Long-term flow record, 1940-2020, showing mean annual flow at USGS Little Manatee River at US 301 near Wimauma, FL (No. 02300500), with the 2000-2004 period demarcated with black vertical lines.

Mean annual flows during 2000-2004 were 190 cfs, somewhat higher than the mean annual flows for the complete 1940-2020 record at 168 cfs. The maximum annual flow during the 2000-2004 period was 320 cfs, lower than the 1940-2020 maximum annual flow of 416 cfs. The minimum annual flow during

the 2000-2004 period was 66 cfs, higher than the 1940-2020 minimum annual flow of 41 cfs. The 2000-2004 period did not provide the extreme annual flows seen over the complete 1940-2020 period, but did provide sufficient similarity to the long-term record to be considered appropriate for this effort.

4.2 COMPARISON OF RESULTS

The simulated salinity was output over the entire river for each grid cell and for each of the four vertical levels at hourly intervals for the 5-year period for the baseline flow condition and for each of the eight flow reduction scenarios. Daily mean simulated salinity values were then calculated for each horizontal grid cell and used in the comparison of salinity habitats. Salinity habitats assessed included water volumes, bottom areas, and shoreline lengths for each integer increment of salinity from 0 to 30 psu. The analysis of expected changes compared to baseline conditions was completed for the three flow blocks, where Block 1 was defined by flows ≤ 29 cfs, Block 2 was for flows from >29 cfs to ≤ 96 cfs, and Block 3 flows were >96 cfs.

As part of the development of the hydrodynamic model, considerations of model run time required limitations on the resolution of the river as it narrows upstream of the highly braided area, as discussed in Section 2.2. For that section upstream of the braided area which is typically in the freshwater zone, developing the grid system to solely represent the much more narrow meandering river while resolving the deeper channel distinct from shallower areas within this river section would result in grid cells so finely resolved that numerical considerations would lead to excessive run times due to the greater number of cells and reduced simulation time step. This portion of the river was therefore discretized so that the cross-stream sizes of the grid cells representing the deeper channel were sometimes similar to the river width, but with additional adjacent rows of cells that may overlay and extend beyond the river shorelines. As noted in Section 2.2, these considerations sometimes result in the set of cross-river grid cells over-estimating the horizontal extent of relatively narrow sections of the river. The inclusion of these additional cells provided for acceptable run times and did not seriously compromise the simulation of salinity distributions along the river axis. However, when post-processing model output for comparison of volumes and bottom areas, inclusion of the metrics associated with these additional cells would result in inaccurate representation of the true river physiography. Therefore, a set of grid cells extending from that point in the river where a single channel begins upstream of the braided areas, from Rkm 17 and upstream, were identified and excluded from the comparison calculations, so that inaccuracies due to over-representation of the river volume and bottom area in this region were minimized.

Figures 4-2 through 4-4 present the relative changes in water volume, bottom area, and shoreline length for each flow reduction scenario when compared to the baseline scenario, associated with each of the salinity isohalines for Blocks 1, 2, and 3. For each habitat metric, the oligohaline habitats were more sensitive to reductions in freshwater inflows than were the mesohaline and polyhaline habitats. It is also notable that the responses of all salinity habitats were much more pronounced in Block 1 than in Blocks 2 and 3.

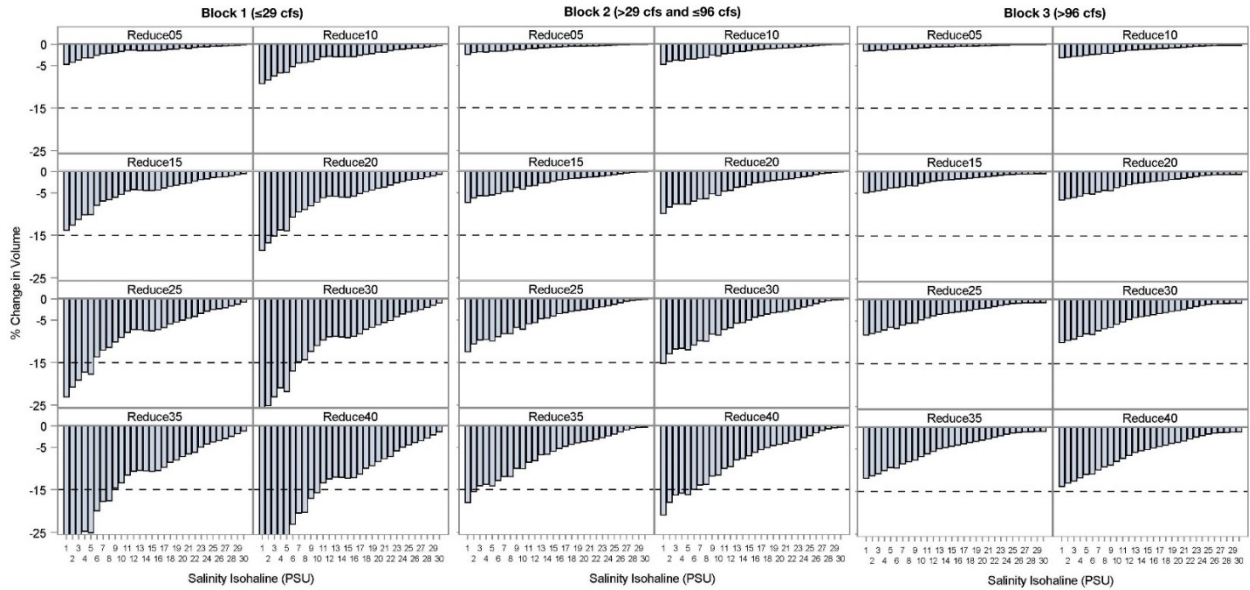


Figure 4-2. Relative changes of water volumes (relative to those of the baseline flow condition) for every integer psu of the isohaline for 5 through 40 percent flow reduction scenarios (in 5 percent increments) for Blocks 1 (left panel), 2 (center panel), and 3 (right panel) during the model period from 2000 through 2004.

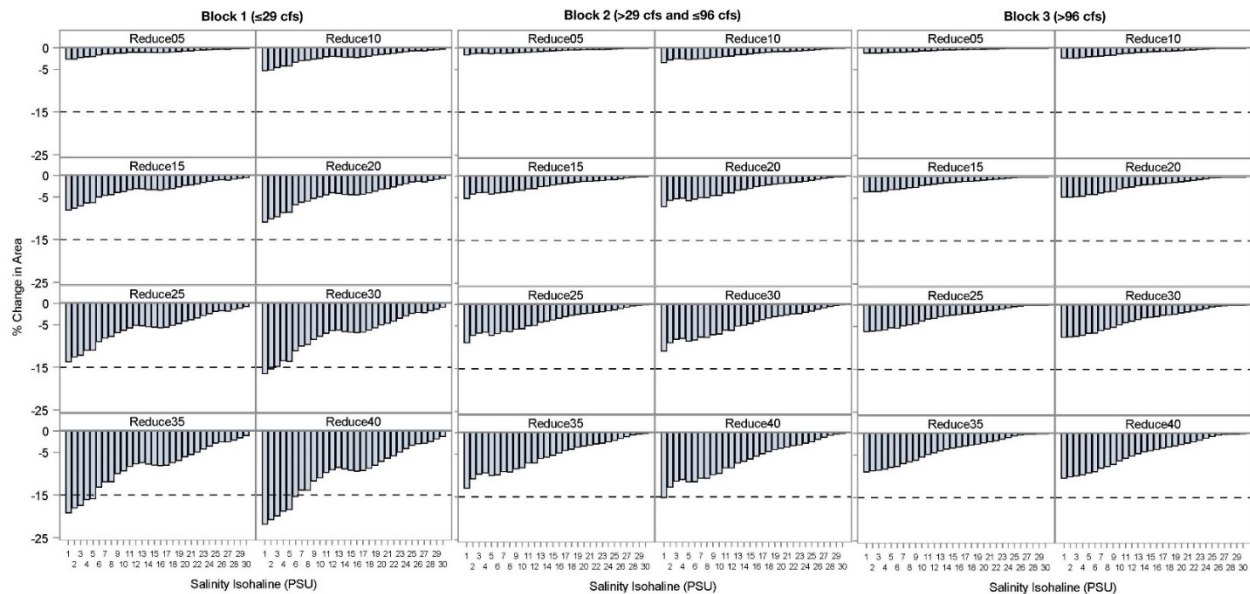


Figure 4-3. Relative changes of bottom areas (relative to those of the baseline flow condition) for every integer psu of the isohaline for 5 through 40 percent flow reduction scenarios (in 5 percent increments) for Blocks 1 (left panel), 2 (center panel), and 3 (right panel) during the model period from 2000 through 2004.

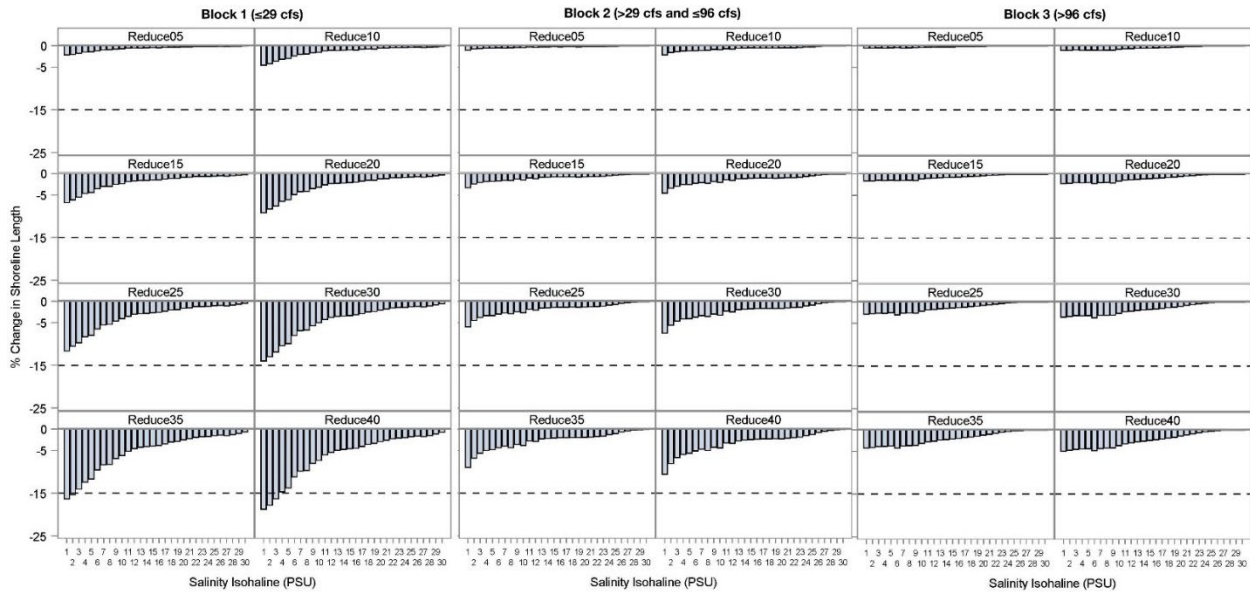


Figure 4-4. Relative changes of shoreline lengths (relative to those of the baseline flow condition) for every integer psu of the isohaline for 5 through 40 percent flow reduction scenarios (in 5 percent increments) for Blocks 1 (left panel), 2 (center panel), and 3 (right panel) during the model period from 2000 through 2004.

In keeping with previous recent estuarine minimum flow evaluations (Herrick et al. 2019a, 2019b; Ghile et al. 2021), habitat metrics for the ≤ 2 psu isohaline were considered as critical for the estuarine system. As this low salinity habitat is most sensitive to flow reductions (as seen in Figure 4-2 through 4-4), ensuring protection of the ≤ 2 psu metrics also protects higher salinity habitats.

Figure 4-2 indicates that the ≤ 2 psu volume would be reduced by more than 15 percent in Block 1 with a 20 percent flow reduction, with the less sensitive ≤ 2 psu bottom area showing a 15 percent reduction in Block 1 at nearly 30 percent flow reduction (Figure 4-2). The least sensitive habitat type was shoreline (Figure 4-4), with a 15 percent reduction of ≤ 2 psu shoreline found at a nearly 35 percent flow reduction in Block 1.

During Block 2 flow periods, the ≤ 2 psu volume would be reduced by more than 15 percent with a 35 percent flow reduction, but even the 40 percent flow reduction did not result in a 15 percent reduction in either bottom area or shoreline length. As for Block 1, the low salinity volume is the most sensitive of the habitat types to flow reductions.

During Block 3 flow periods, no habitat types showed reductions of 15 percent or more for any of the flow reductions. As in Blocks 1 and 2, the ≤ 2 psu volume was the most sensitive of the low salinity habitat types, with shoreline length the least sensitive to flow reductions.

Interpolation of the model results provided in Figures 4-2 through 4-4 provide estimates of the exact flow reduction percentages corresponding to 15 percent reductions in salinity habitats for the ≤ 2 psu isohaline. A 17.9 percent flow reduction at the USGS Little Manatee River at US Highway 301 near Wimauma, FL (No. 02300500) gage corresponds to a 15 percent reduction in ≤ 2 psu volume in Block 1, when flows are 29 cfs or less at the gage. For Block 2, with flows at the USGS gage between 29 cfs and 96 cfs, a 15 percent reduction in ≤ 2 psu volume corresponds to a 34.2 percent flow reduction. At any flow reduction evaluated, up to 40 percent at the gage, a 15 percent reduction in the ≤ 2 psu volume

would not occur. For the ≤ 2 psu bottom area, a 15 percent reduction in Block 1 corresponds to a gaged flow reduction of 29.4 percent, with none of the flow reductions evaluated up to 40 percent at the gage resulting in ≤ 2 psu bottom area reductions of 15 percent or more in Blocks 2 and 3. For ≤ 2 psu shoreline length, a 15 percent reduction in the ≤ 2 psu habitat in Block 1 corresponds to a 34.3 percent flow reduction at the gage, with none of the flow reductions evaluated up to 40 percent at the gage resulting in ≤ 2 psu bottom area reductions of 15 percent or more in Blocks 2 and 3.

A low-flow threshold of 29 cfs is proposed for the US 301 gage, aimed at maintenance of a minimum water depth at an upstream cross section. This low-flow threshold is expected to aid in protecting low salinity estuarine habitats. Given the simulated impact on the ≤ 2 psu volume of a 17.9 percent flow reduction during Block 1, implementation of the proposed low-flow threshold was evaluated to more fully understand the potential impact on low salinity habitats.

Figure 4-5 provides the expected percentage changes in bottom area and volume from baseline conditions for flow reductions of 10 percent (10% Reduct), 15 percent (15% Reduct), 20 percent (20% Reduct), 20 percent with the low-flow threshold (20L Reduct), 25 percent (25% Reduct), and 30 percent (30% Reduct) flow reductions during Block 1. Expected changes in bottom areas are provided in the left panel and those for volumes in the right panel. Comparisons of the shaded middle two graphics, labeled “20% Reduct” and “20L Reduct”, indicate the differences expected from implementing the low-flow threshold of 29 cfs (“20L Reduct”) for the 20 percent flow reduction scenario.

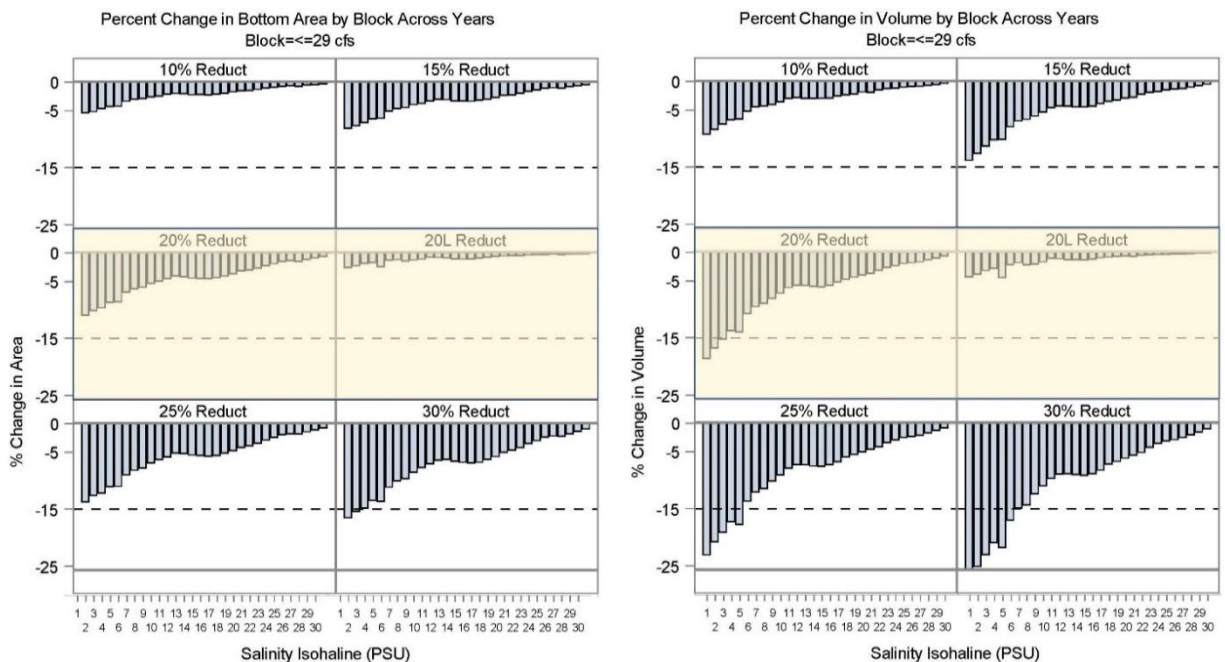


Figure 4-5. Percentage reductions in bottom area (left panel) and volume (right panel) associated with the salinity isohalines of 1, 2, ... 30 psu relative to those under the baseline flow condition during Block 1, with difference in low salinity habitat changes for the 20 percent (20% Reduct) and 20 percent with proposed low-flow threshold (20L Reduct) reductions scenarios highlighted to emphasize effects of the low-flow threshold.

Since the Block 1 flow cutoff is at ≤ 29 cfs, implementation of the low-flow threshold allows no flow reduction during this block, with flow reductions of 20 percent only occurring during days falling into Blocks 2 and 3. Given that during Block 1 there are no flow reductions when flows are ≤ 29 cfs, at first thought it would seem that there should be no differences in salinity habitat availability between the

20 percent flow reduction scenario and baseline during this Block. However, days falling into Blocks 2 and 3 are interspersed with those in Block 1, so that any flow reductions occurring during Blocks 2 and 3 days which precede Block 1 days impact the resultant salinities during the Block 1 days, hence resulting in some reduction in salinity habitat even on Block 1 days. These changes expected to occur with the low-flow threshold in place are much reduced from those expected without the 29 cfs low-flow threshold in place, however.

Table 4-1 provides the percentage flow reductions at the USGS gage at US 301 derived from the findings of the flow reduction scenarios. Allowable flow reductions have been rounded to the nearest integer. Implementing the proposed 29 cfs low-flow threshold increases the level of protection associated with these potential minimum flows as formulated based on the EFDC modeling results.

Table 4-1. Percent-of-flow reductions that result in a 15 percent decrease in the amount of low-salinity habitat (volume, bottom area, and shoreline length) at the USGS Little Manatee River at US 301 near Wimauma, FL (No. 02300500) gage based on results of the EFDC model.			
	Block 1 (≤ 29 cfs)	Block 2 (> 29 and ≤ 96 cfs)	Block 3 (> 96 cfs)
Volume	18	34	>40
Bottom Area	29	>40	>40
Shoreline Length	34	>40	>40

4.3 SENSITIVITY ANALYSIS

The percent-of-flow reductions that result in a 15 percent decrease in the amount of low-salinity habitat derived from the EFDC model scenarios utilizing the flow blocks described in Section 4.2 are provided in Table 4-1 above. The sensitivity of these percent-of-flow reductions was evaluated by applying different flow limits for the flow blocks, namely ≤ 35 cfs for Block 1, > 35 and ≤ 72 cfs for Block 2, and > 72 cfs for Block 3. When these definitions are applied, the resultant set of percentage reduction graphics, similar to Figures 4-2 through 4-4, are provided in Figures 4-6 through 4-8.

As for the values provided in Table 6-5, the results of the sensitivity analysis using the revised flow blocks definitions were interpolated to arrive at percent-of-flow reductions resulting from this analysis. The values for ≤ 2 psu salinity habitats are provided in Table 4-2. The results indicate that the definitions of the flow block boundaries, with the Block 1 boundary increased from ≤ 29 cfs to ≤ 35 cfs and the Block 2 boundary modified from > 29 and ≤ 96 cfs to > 35 and ≤ 72 cfs, result in relatively small changes to the percent-of-flow reductions. Comparing the sensitivity analysis block definitions to those used to establish the proposed minimum flows, the Block 1 percent-of-flow reductions increased from 18% to 20% for volume, 29% to 31% for bottom area, and 34% to 37% for shoreline length. The Block 2 percent-of-flow reduction for volume increased from 34% to 35%.

Table 4-2. Sensitivity analysis results: Percent-of-flow reductions that result in a 15 percent decrease in the amount of low-salinity habitat (volume, bottom area, and shoreline length) at the USGS Little Manatee River at US 301 near Wimauma, FL (No. 02300500) gage based on results of the EFDC model.			
	Block 1 (≤ 35 cfs)	Block 2 (> 35 and ≤ 72 cfs)	Block 3 (> 72 cfs)
Volume	20	35	>40
Bottom Area	31	>40	>40
Shoreline Length	37	>40	>40

Based on the results of this sensitivity analysis of the flow block definition, it can be stated that although there are some changes to the percent-of-flow reductions resulting from the tested modified flow block definitions, the effects of changing the flow block definitions appear to be relatively small.

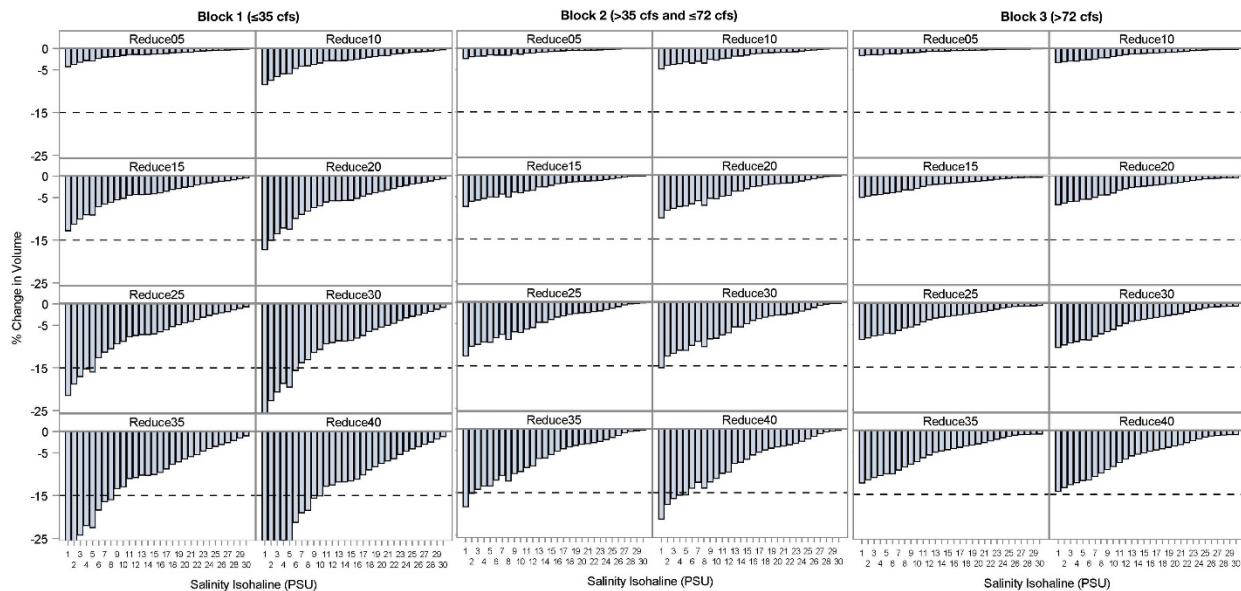


Figure 4-6. Relative changes of water volumes (relative to those of the baseline flow condition) for every psu of the isohaline for 5 through 40 percent flow reduction scenarios (in 5 percent increments) for sensitivity analysis Blocks 1 (left panel), 2 (center panel), and 3 (right panel) during the EFDC model period from 2000 through 2004.

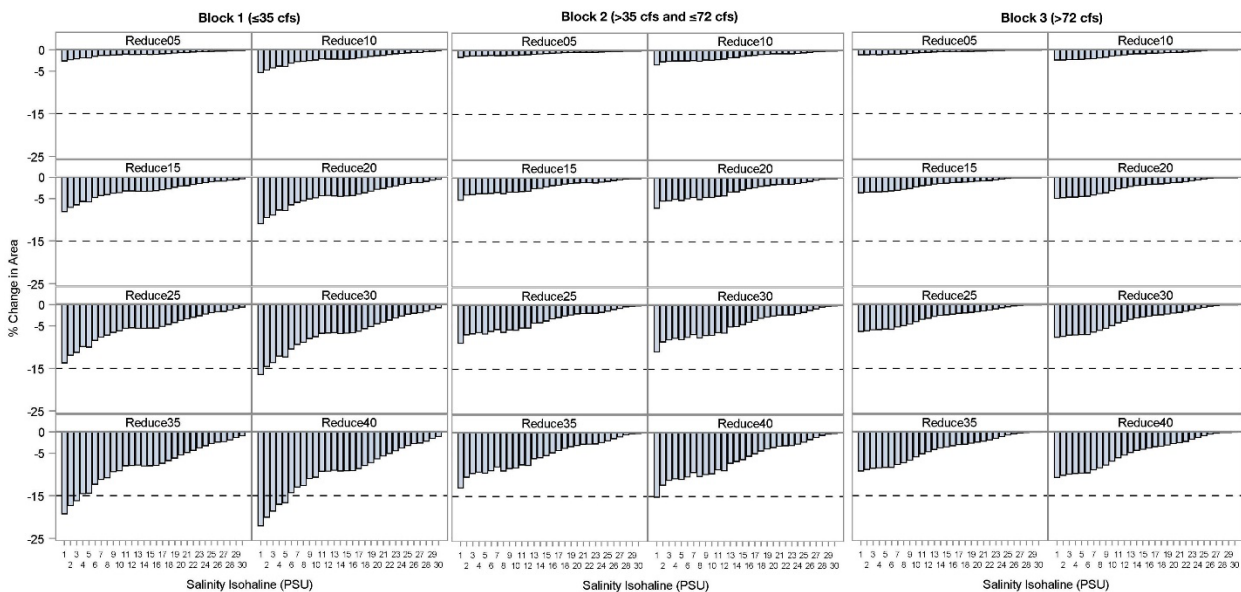


Figure 4-7. Relative changes of bottom areas (relative to those of the baseline flow condition) for every psu of the isohaline for 5 through 40 percent flow reduction scenarios (in 5 percent increments) for sensitivity analysis Blocks 1 (left panel), 2 (center panel), and 3 (right panel) during the EFDC model period from 2000 through 2004.

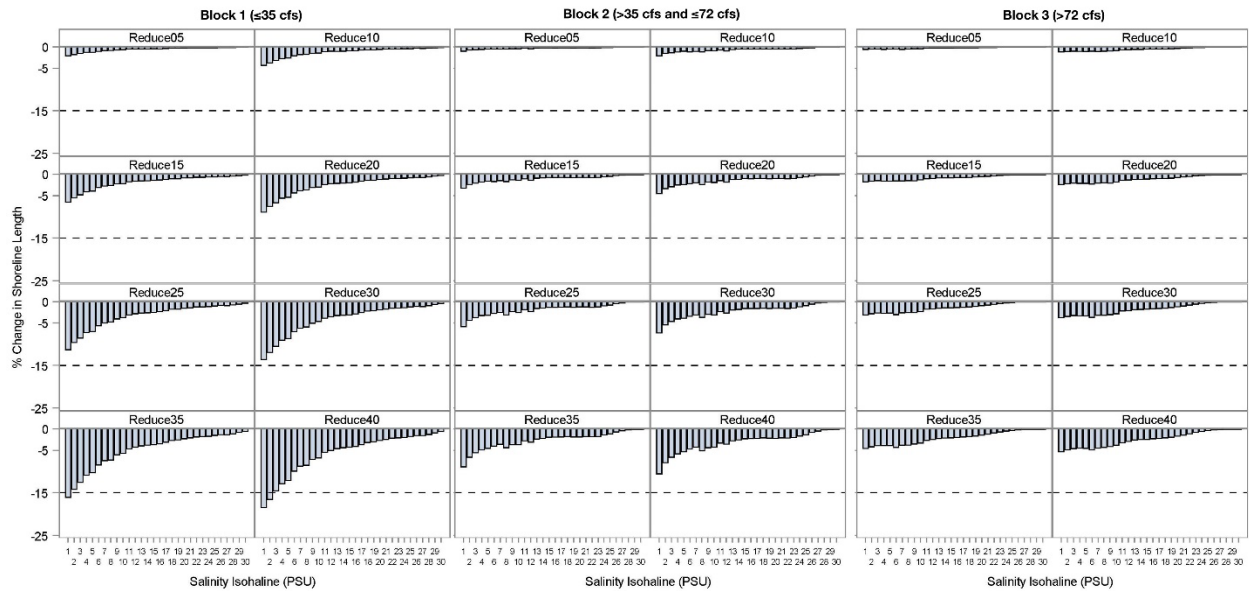


Figure 4-8. Relative changes of shoreline lengths (relative to those of the baseline flow condition) for every psu of the isohaline for 5 through 40 percent flow reduction scenarios (in 5 percent increments) for sensitivity analysis Blocks 1 (left panel), 2 (center panel), and 3 (right panel) during the EFDC model period from 2000 through 2004.

5.0 SEA LEVEL RISE SCENARIOS

The NOAA US Global Change Research Program 2017 project (Sweet et al. 2017) provided estimates of intermediate-low, intermediate, and high sea level rise (SLR) conditions from 2000 on. The estimates for the St. Petersburg station are assumed to be applicable for the nearby Lower Little Manatee River. The estimated increases in sea level over the 40-year period, from 2002 to 2041, for the intermediate-low, intermediate, and high SLR cases evaluated were 0.71' (0.22 m), 1.07' (0.33 m), and 1.78' (0.54 m), respectively, with these three SLR conditions selected based on DeWitt et al. (2020).

The potential effects of the proposed minimum flows for the three SLR conditions were evaluated as done previously for the minimum flows re-evaluation of the Lower Peace River (Ghile et al. 2021). The baseline flow record was applied for the three SLR scenarios, and the three scenarios were also run with the proposed minimum flows in place. This allowed for evaluation of whether the proposed minimum flows, under the three SLR conditions, would result in more than a 15 percent reduction of critical salinity habitats.

The proposed minimum flows for the Lower Little Manatee River were determined based on the results of the EFDC modeling exercise and the results of the Environmental Favorability Function (EFF) approach. As described in the main document for which this modeling report is an appendix, the EFF approach was used to predict relative favorability of habitats under different flow regimes for fish species that use the mid- and low-salinity habitats of the lower river and show a negative response to increasing salinity levels. The EFF approach resulted in more restrictive allowable flow reductions than did the EFDC modeling effort, with the proposed minimum flows provided in Table 5-1.

Flow-Based Block	If Previous Day's Flow, Adjusted for Upstream Withdrawals, is:	Minimum Flow is:	Potential Allowable Flow Reduction is:
1	≤29 cfs	Flow on Previous Day	0 cfs
2	>29 cfs and ≤34 cfs	29 cfs	Flow on Previous Day Minus 29 cfs
	>34 cfs and ≤96 cfs	87 percent of Flow on Previous Day	13 Percent of Flow on Previous Day
3	>96 cfs and ≤121 cfs	83 cfs	Flow on Previous Day Minus 83 cfs
	>121 cfs	68 percent of Flow on Previous Day	32 Percent of Flow on Previous Day

The implementation of the three SLR conditions was completed by adding the additional elevation for each to the time series of boundary condition water surface elevations along both the north and south boundaries within Tampa Bay. No other potential effects of SLR were incorporated in these scenarios, so that the only effect at the boundaries was to deepen the water column by the increased amount, with the boundary condition salinity and temperature remaining distributed through the four vertical layers of the water column in the same manner as for the non-SLR scenarios.

Comparisons of the simulated percentage reductions in salinity habitat volumes due to implementation of the recommended minimum flow, for the isohalines 1, 2, ... 30 psu under the three SLR scenarios and for the three flow blocks are provided in Figure 5-1. There are no incidents of 15 percent reduction in volume for any of the SLR conditions in any of the flow blocks.

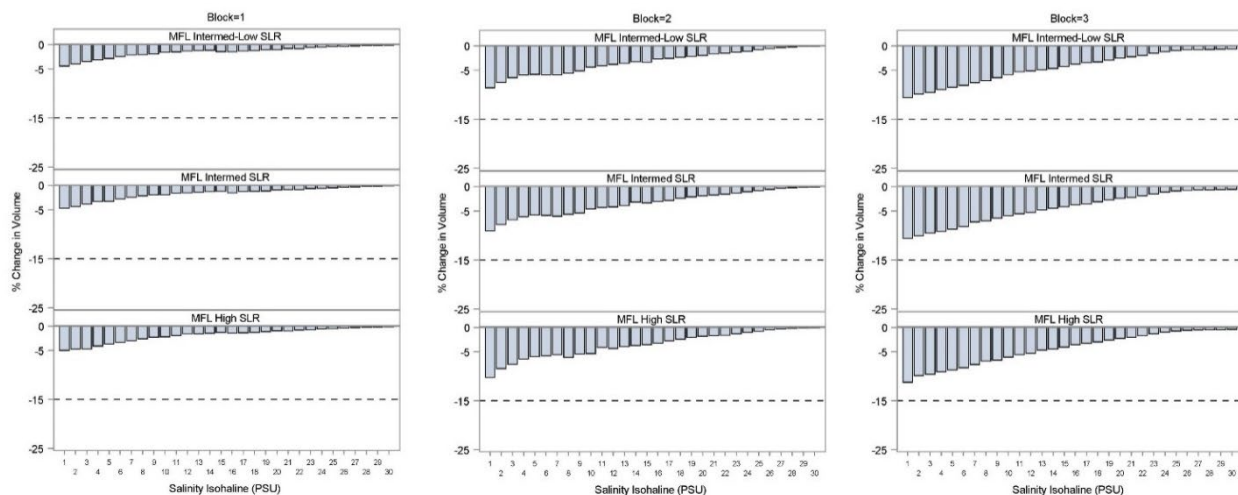


Figure 5-1. Percentage (PSU) changes of simulated water volumes of isohalines 1, 2, ... 30 psu under the minimum flow condition with the intermediate-low, intermediate, and high SLR projections relative to those under the baseline flow condition with the three SLR projections.

Figures 5-2 and 5-3 provide the results of the similar analyses for bottom area and shoreline length, respectively, for the three SLR conditions, with the recommended minimum flow applied to the SLR scenarios resulting in reductions in these metrics of less than 15 percent for the habitats in each of the flow blocks.

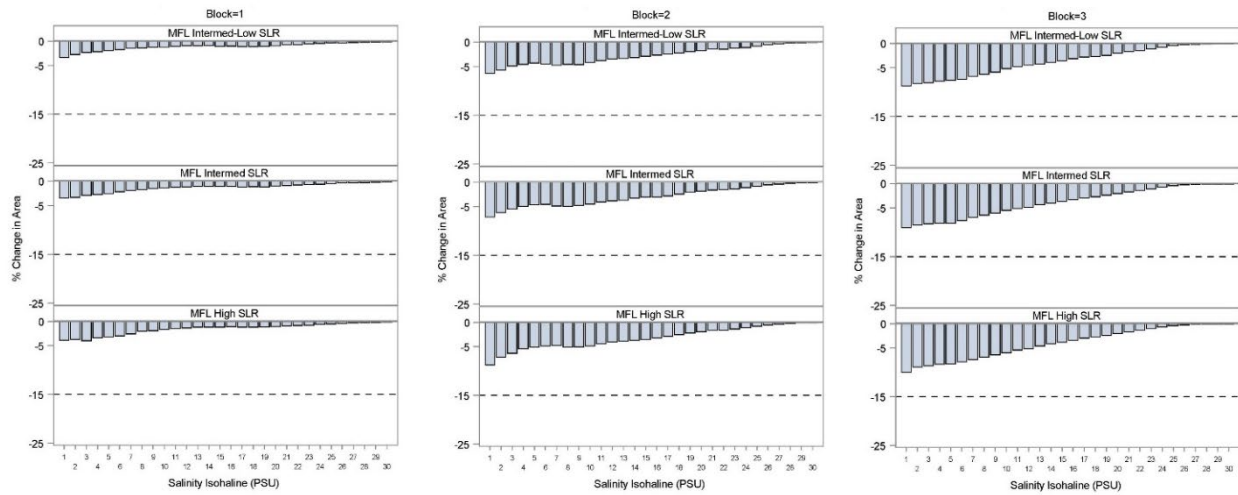


Figure 5-2. Percentage changes of simulated bottom areas of isohalines 1, 2, ... 30 psu under the minimum flow condition with the intermediate-low, intermediate, and high SLR projections relative to those under the baseline flow condition with the three SLR projections.

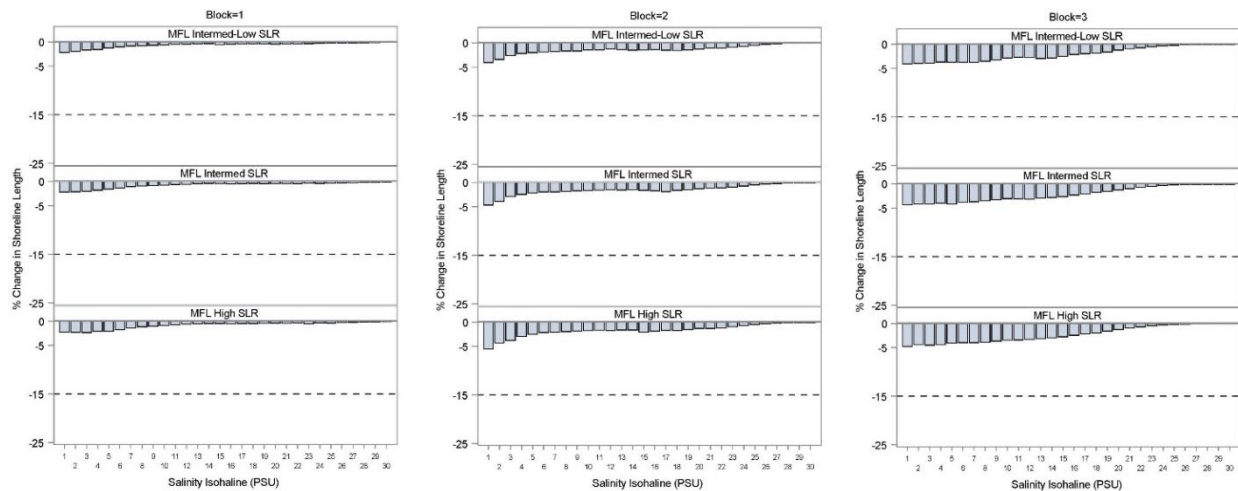


Figure 5-3. Percentage changes of simulated shoreline length of isohalines 1, 2, ... 30 psu under the minimum flow condition with the intermediate-low, intermediate, and high SLR projections relative to those under the baseline flow condition with the three SLR projections.

These results indicate that for the low salinity habitats, where the greatest reductions in habitat are expected due to potential flow reductions, the recommended minimum flow as provided in Table 5-1 does not result in 15 percent habitat reductions under any of the SLR scenarios during any of the flow blocks. It is notable that the results indicate the low salinity habitats are more impacted during the higher flow blocks than during the low flow block, most evident in the Intermediate and High SLR scenarios, as shown in Figures 5-1 through 5-3.

6.0 SUMMARY AND CONCLUSIONS

This document provides a summary of the development, calibration, verification, and application of a hydrodynamic model of the Lower Little Manatee River. The model construct, including the grid system, data availability, calibration and verification, and use of the model in evaluation of flow reduction scenarios and sea level rise scenarios was provided. The model was calibrated for the period January – February 2005, and verified using the period March – June 2005, with the calibration and verification efforts indicating that the model is appropriate for use in evaluating the likely effects of flow reductions on salinity distributions in the river.

Minimum flows were derived using the hydrodynamic model for three flow Blocks based on model runs covering 2000-2004 with baseline flow conditions. Block 1 is for flows ≤ 29 cfs, Block 2 for flows > 29 cfs and ≤ 96 cfs, and Block 3 for flows > 96 cfs. The effects of flow reductions of 5 percent through 40 percent, in 5 percent increments, were evaluated for the effects on salinity habitats as defined by isohalines, with evaluations of the expected effects on isohalines from 0 psu to 30 psu in integer increments. The habitats evaluated include volumes, bottom area, and shoreline length. Similar evaluations were completed to evaluate the expected effects of sea level rise, with scenarios driven by increased water surface elevations at the downstream boundaries of the model domain to account for Intermediate-Low, Intermediate, and High sea level rise scenarios as defined by expectations for 2041. Sea level rise scenarios were evaluated by implementing the three sea level rise scenarios with the baseline flow inputs at the upstream boundary of the model domain, at USGS gage 02300500 at US 301, and comparing the results of these three scenarios with the same flows modified for the proposed minimum flows for each of the three Blocks.

The results of this hydrodynamic model are used along with other evaluation efforts described in the main document, for which this is an appendix, to derive the proposed minimum flows for the Lower Little Manatee River.

7.0 REFERENCES

- Applied Technology and Management (ATM). 2014. Hydrodynamic Model Development and Calibration. Appendix B2 of Old Tampa Bay Integrated Model Development Project, Task 4 Development of Calibrated Models for the Old Tampa Bay Integrated Model System. Presented to Tampa Bay Estuary Program, St. Petersburg, FL. Presented by Janicki Environmental, Inc.
- Blumberg, A.F., and G.L. Mellor. 1987. A Description of a Three-Dimensional Coastal Ocean Circulation Model. In: Three-Dimensional Coastal Ocean Models, Coastal and Estuarine Science, Vol. 4, (Heaps, N.S., ed.) American Geophysical Union, pp. 1-19.
- Dewitt, D., L. LeMond, M. Ritter, M. Fulkerson, R. Basson, and C. Anastasiou. 2020. Sea Level Rise – How is SWFWMD Addressing the Issue? SMC Report, Southwest Florida Water Management District, Brooksville, Florida.
- Ghile, Y., X. Chen, D.A. Leeper, C. Anastasiou, and K. Deak. 2021. Recommended Minimum Flows for the Lower Peace River and Proposed Minimum Flows for Lower Shell Creek, Final Draft, Southwest Florida Water Management District, Brooksville, Florida.
- Hamrick, J.M. 1992. A Three-Dimensional Environmental Fluid Dynamics Computer Code: Theoretical and Computational Aspects, Special Report 317. The College of William and Mary, Virginia Institute of Marine Science, Gloucester Point, VA. 63 pp.
- Hamrick, J.M. 1996. User's Manual for the Environmental Fluid Dynamics Computer Code. Special Report No. 331, The College of William and Mary, Gloucester Point, Virginia.
- Herrick, G., X. Chen, C. Anastasiou, R. Basso, N. Mendez-Ferrer, N. Ortega, D. Rogers, and D.A. Leeper. 2019a. Reevaluation of Minimum Flows for the Homosassa River System – Final Draft. Southwest Florida Water Management District, Brooksville, Florida.
- Herrick, G. X. Chen, C. Anastasiou, R. Basso, N. Mendez-Ferrer, N. Ortega, D. Rogers, and D.A. Leeper. 2019b. Reevaluation of Minimum Flows for the Chassahowitzka River System – Final Draft. Southwest Florida Water Management District, Brooksville, Florida.
- Huang, W. and X. Liu. 2007. Hydrodynamic Modeling of the Little Manatee River. Prepared by the Department of Civil Engineering, FAMU-FSU College of Engineering, Tallahassee, Florida, for the Southwest Florida Water Management District, Brooksville, Florida.
- Intera and Aqua Terra Consultants. 2006. Estimating the Un-Gaged Inflows in the Little Manatee River Basin, Florida. Prepared for the Southwest Florida Water Management District, Brooksville, FL.

Jacobs Engineering Group (Jacobs) and Janicki Environmental, Inc. (JEI). 2021. Little Manatee River System MFLs Development Support, Task 4.5 Technical Memorandum, Hydrodynamic Modeling. Prepared for the Southwest Florida Water Management District, Brooksville, Florida.

Janicki Environmental, Inc. (JEI). 2018. Draft Recommended Minimum Flows for the Little Manatee River Estuary. Draft Report. Prepared for the Southwest Florida Water Management District, Brooksville, Florida.

Mellor, G.L. and T. Yamada. 1982. Development of a turbulence closure model for geophysical fluid problems. *Reviews of Geophysics and Space Physics* 20:851-875.

Peer Review Panel. 2021. Initial Peer Review Report, Reevaluation of Minimum Flows for the Little Manatee River System. Prepared for the Southwest Florida Water Management District, Brooksville, Florida.

Sherwood, E.T., H. Greening, L. Garcia, K. Kaufman, T. Janicki, R. Pribble, B. Cunningham, S. Peene, J. Fitzpatrick, K. Dixon, and M. Wessel. 2016. Development of an Integrated Ecosystem Model to Determine Effectiveness of Potential Watershed Management Projects on Improving Old Tamp Bay. In: Stringer, C.E.K., W. Ken, and J.S. Latimer (eds.), *Fifth Interagency Conference on Research in the Watersheds, Headwaters to Estuaries: Advances in Watershed Science and Management*, Asheville, North Carolina. U.S. Department of Agriculture Forest Service, Southern Research Station. North Charleston, South Carolina. E-Gen. Tech. Rep. SRS-211.

Smolarkiewicz, P.K. 1984. A Fully Multidimensional Positive Definite Advection Transport Algorithm with Small Implicit Diffusions. *J. Comp. Phys.*, 54, 325-362.

Smolarkiewicz, P.K., and T.L. Clark. 1986. The Multidimensional Positive Definite Advection Transport Algorithm: Further Development and Applications. *J. Comp. Phys.*, 67, 396-438.

Smolarkiewicz, P.K., and W.W. Grabowski. 1990. The Multidimensional Positive Definite Advection Transport Algorithm: Nonoscillatory Option. *J. Comp. Phys.*, 86, 355-375.

Smolarkiewicz, P.K., and L.G. Margolin. 1993. On Forward-in-time Differencing for Fluids: Extension to a Curvilinear Framework. *Mon. Weather Rev.*, 121, 1847-1859.

Sweet, W.V., R.E. Kopp, C.P. Weaver, J. Obeysekera, R.M. Horton, E.R. Thieler, and C. Zervas. 2017. *Global and Regional Sea Level Rise Scenarios for the United States*. NOAA Technical Report NOS CO-OPS 083. Silver Spring, Maryland.

Tetra Tech. 2002. User's Manual for Environmental Fluid Dynamics Code: Hydrodynamics. Prepared for the U.S. Environmental Protection Agency, Region 4, by Tetra Tech, Inc., Fairfax, VA.

Tetra Tech. 2006a. User's Manual for Environmental Fluid Dynamics Code: Water Quality. Prepared for the U.S. Environmental Protection Agency, Region 4, Tetra Tech, Inc., Fairfax, VA.

Tetra Tech. 2006b. The Environmental Fluid Dynamics Code, Theory and Computation: Volume 1: Hydrodynamics. Tetra Tech, Inc., Fairfax, VA.

Tetra Tech. 2006c. The Environmental Fluid Dynamics Code, Theory and Computation: Volume 2: Sediment and Contaminant Transport and Fate. Tetra Tech, Inc., Fairfax, VA.

Tetra Tech. 2006d. The Environmental Fluid Dynamics Code, Theory and Computation: Volume 3: Water Quality and Eutrophication. Tetra Tech, Inc., Fairfax, VA.

Tetra Tech. 2007. The Environmental Fluid Dynamics Code User Manual US EPA Version 1.01 Tetra Tech, Inc., Fairfax, VA.

Tyler, D., D.G. Zawada, A. Nayegandhi, J.C. Brock, M.P. Crane, K.K. Yates, and K.E.L. Smith. 2007. Topobathymetric data for Tampa Bay, Florida: U.S. Geological Survey Open-File Report 2007-1051 (revised).

Wang, P. 2006. Bathymetric Survey at Anclote River System and Little Manatee River System. Submitted to Southwest Florida Water Management District, Tampa, Florida.

Zarbock, H., A. Janicki, D. Wade, D. Heimbuch, and H. Wilson. 1994. Estimates of Total Nitrogen, Total Phosphorus, and Total Suspended Solids Loadings to Tampa Bay, Florida. Technical Publication #04-94. Prepared by Coastal Environmental, Inc. Prepared for Tampa Bay National Estuary Program. St. Petersburg, FL.

Zarbock, H., A. Janicki, and S. Janicki. 1996. Estimates of Total Nitrogen, Total Phosphorus, and Total Suspended Solids Loadings to Tampa, Bay, Florida. Technical Appendix: 1992-94 Total Nitrogen Loads to Tampa Bay. Technical Publication #19-96. Prepared by Coastal Environmental, Inc. Prepared for Tampa Bay National Estuary Program. St. Petersburg, FL.

ATTACHMENT 1

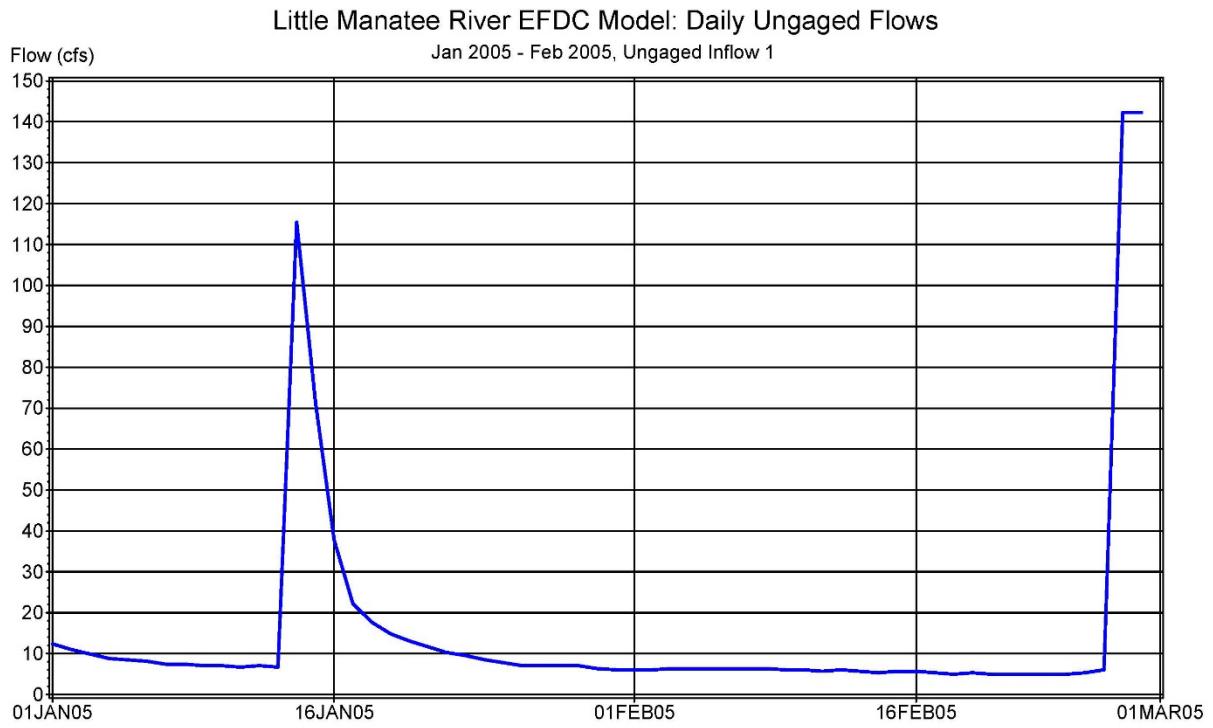


Figure A1-1. Inflows from ungaged location 1 for calibration period January-February 2005.

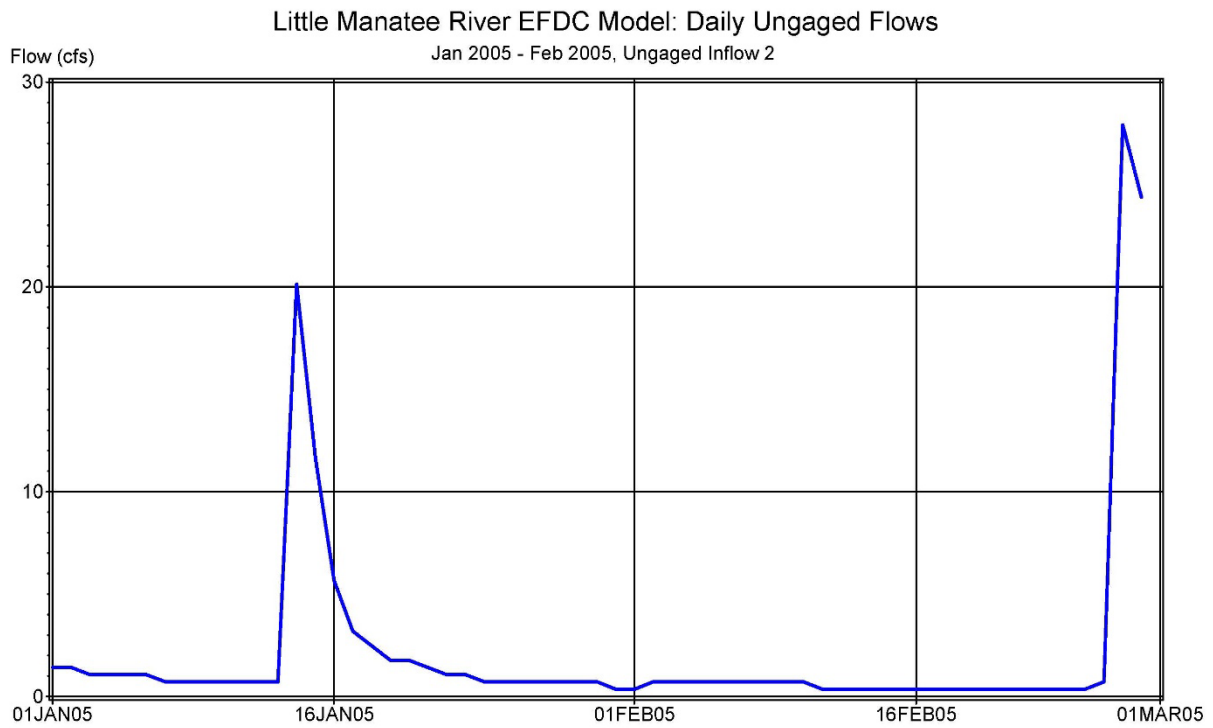


Figure A1-2. Inflows from ungaged location 2 for calibration period January-February 2005.

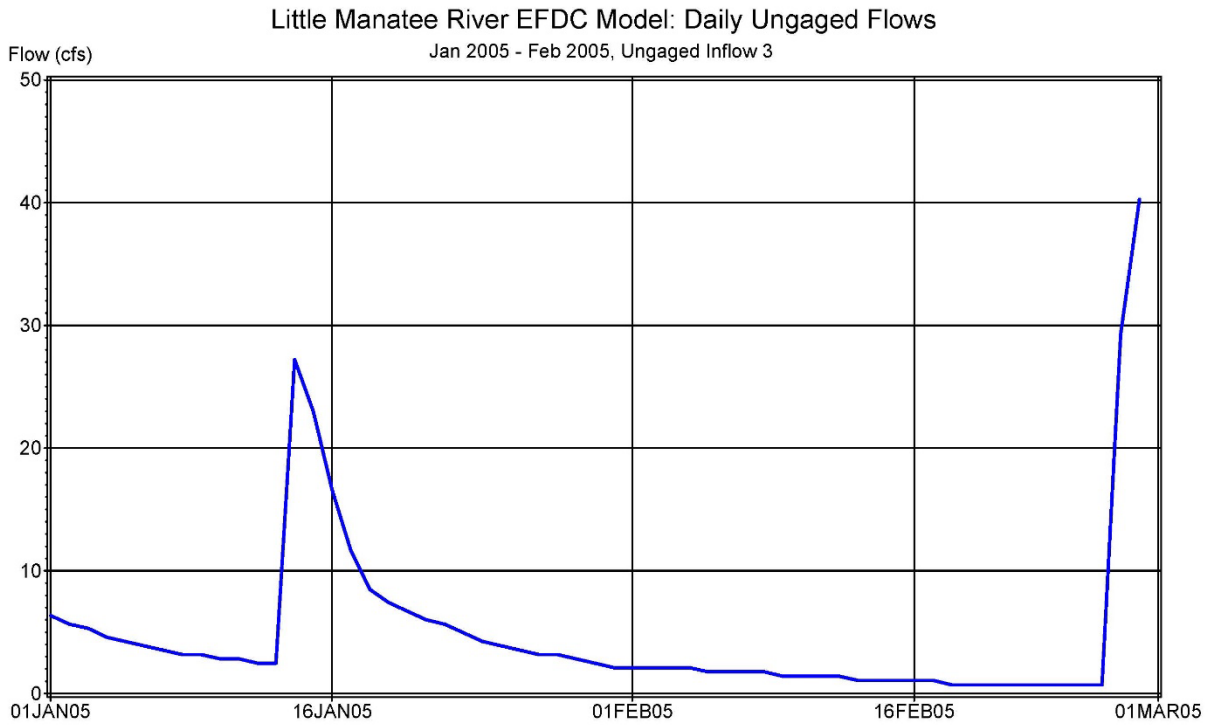


Figure A1-3. Inflows from ungaged location 3 for calibration period January-February 2005.

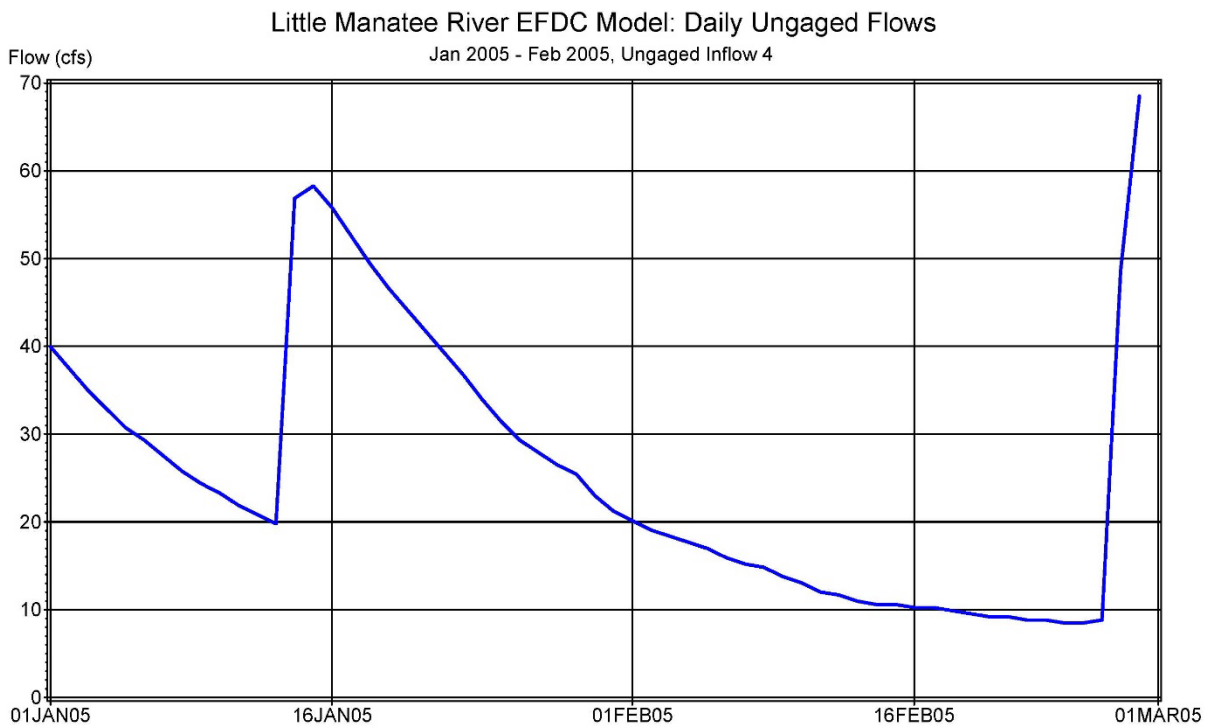


Figure A1-4. Inflows from ungaged location 4 for calibration period January-February 2005.

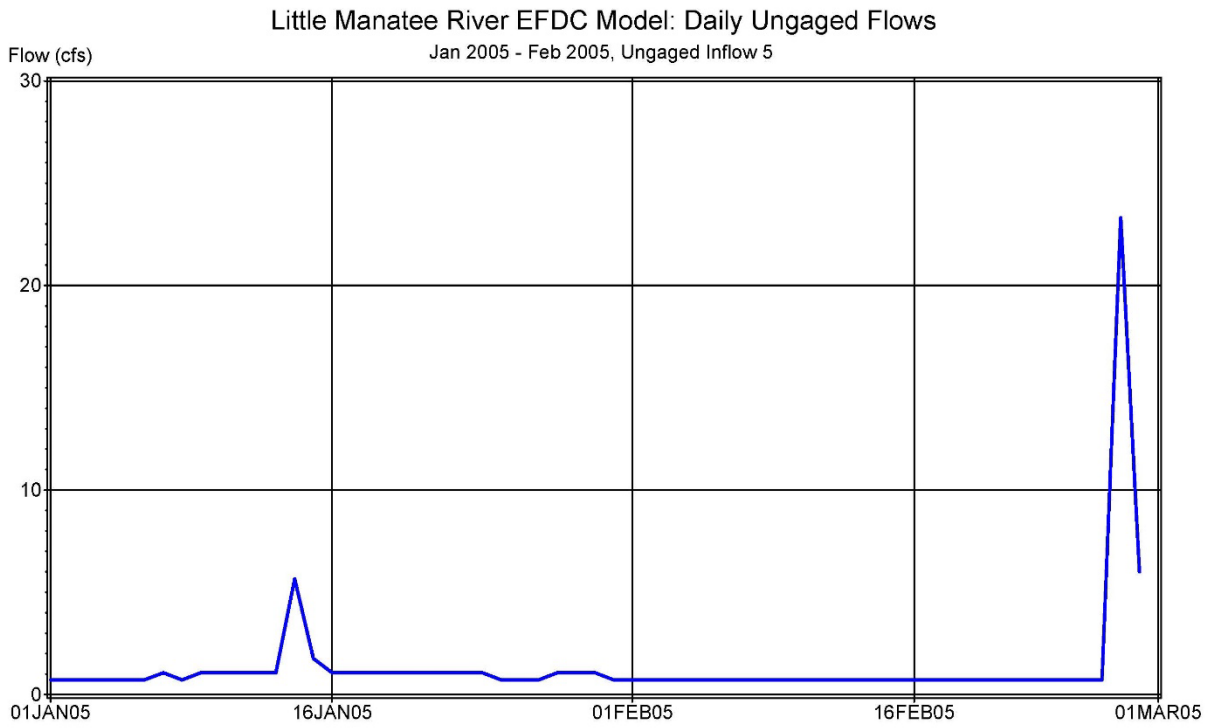


Figure A1-5. Inflows from unaged location 5 for calibration period January-February 2005.

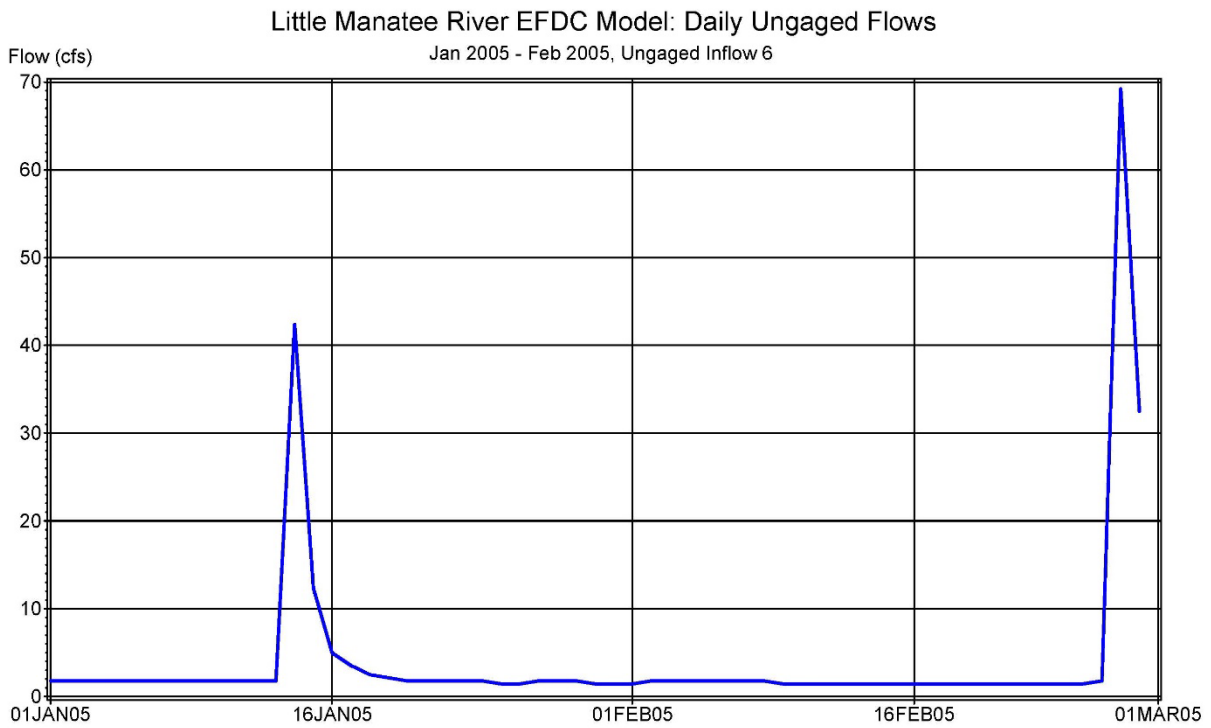


Figure A1-6. Inflows from unaged location 6 for calibration period January-February 2005.

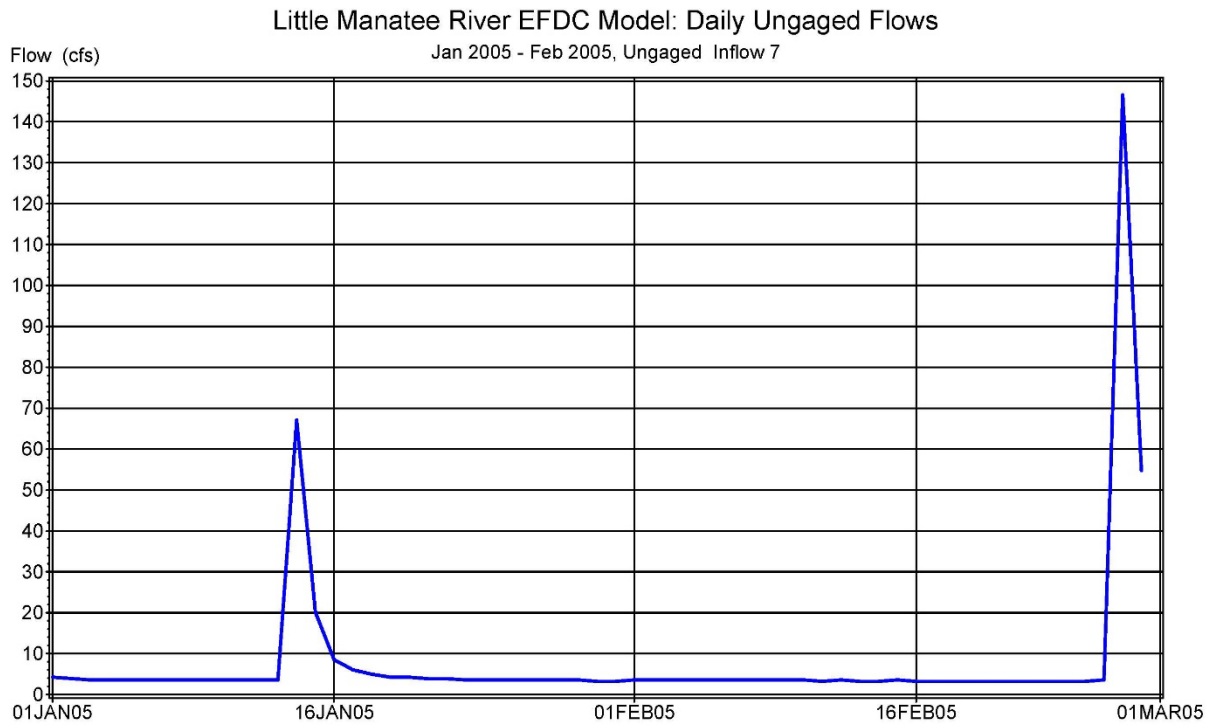


Figure A1-7. Inflows from unaged location 7 for calibration period January-February 2005.

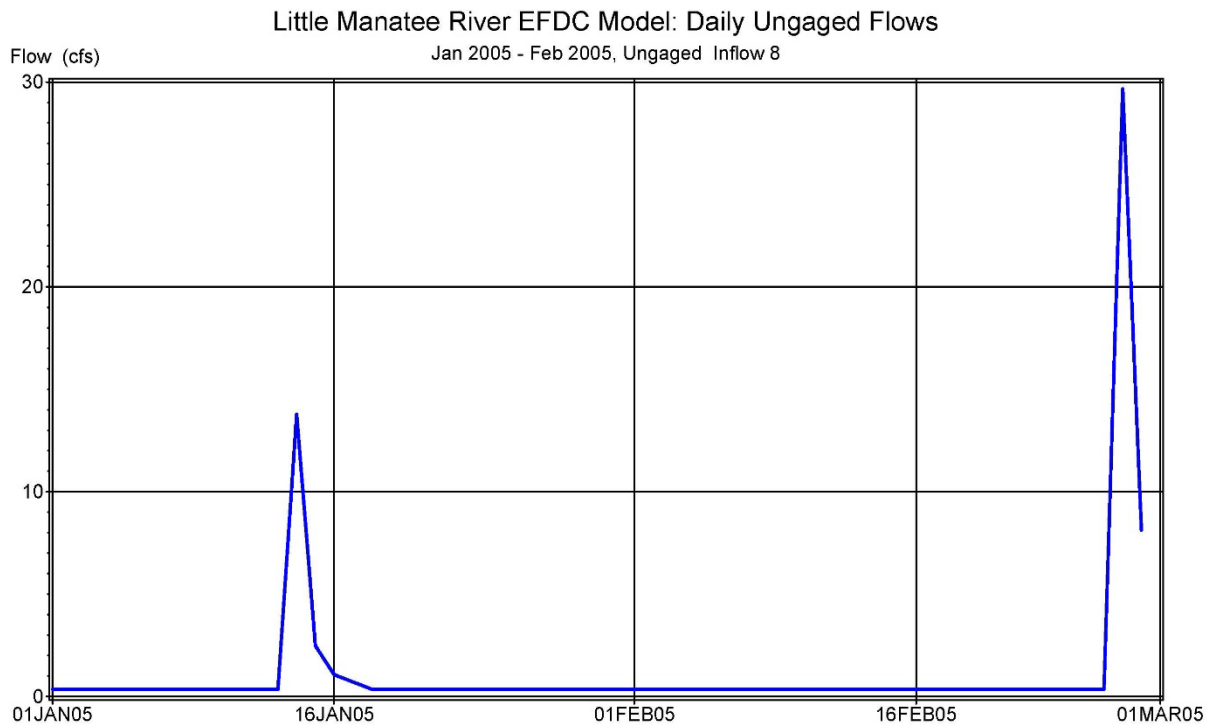


Figure A1-8. Inflows from unaged location 8 for calibration period January-February 2005.

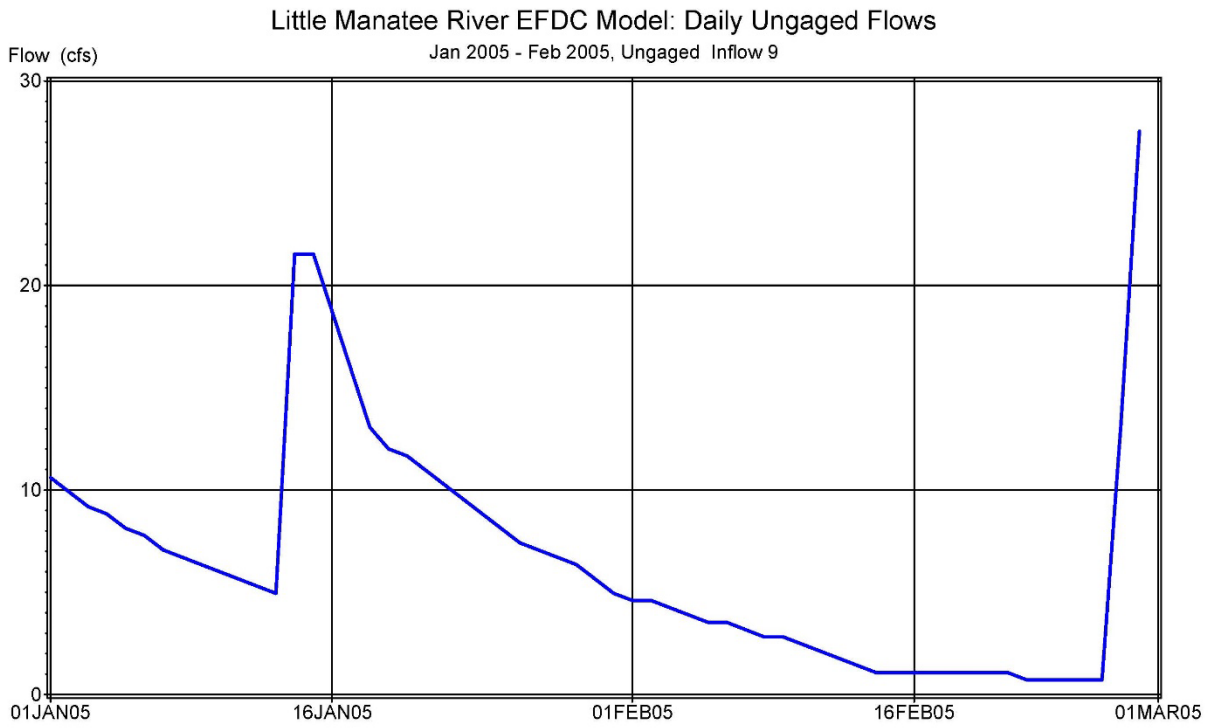


Figure A1-9. Inflows from ungaged location 9 for calibration period January-February 2005.

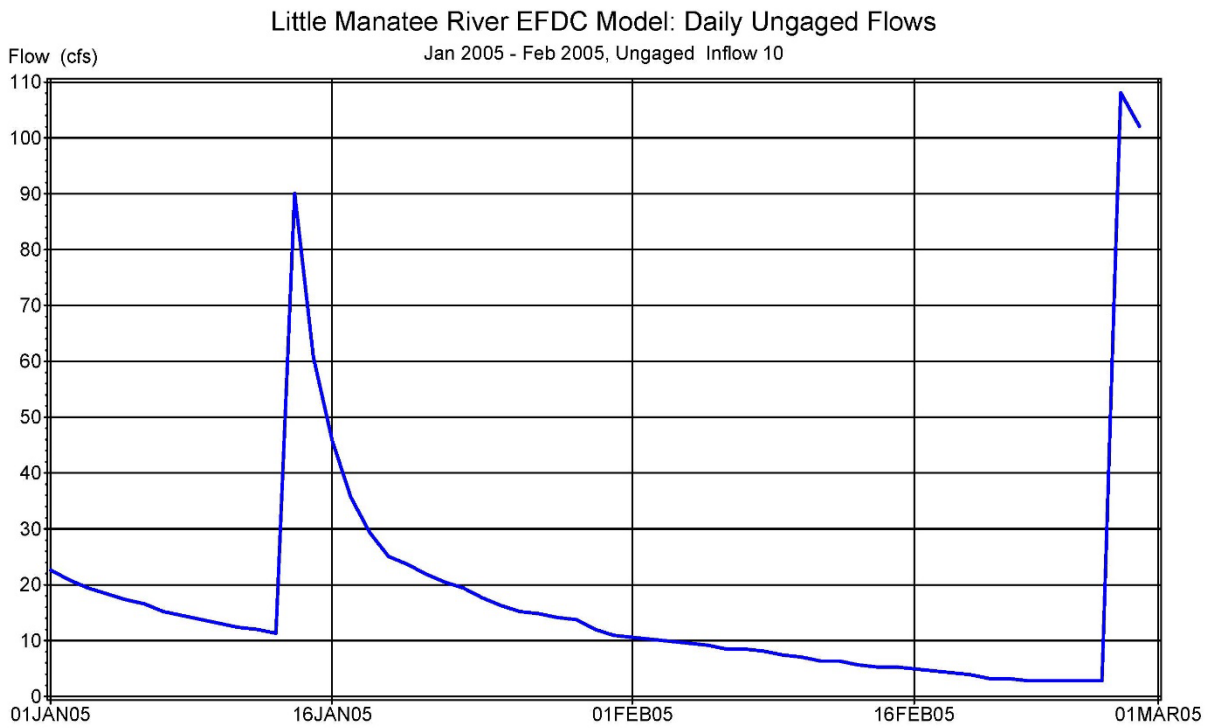


Figure A1-10. Inflows from ungaged location 10 for calibration period January-February 2005.

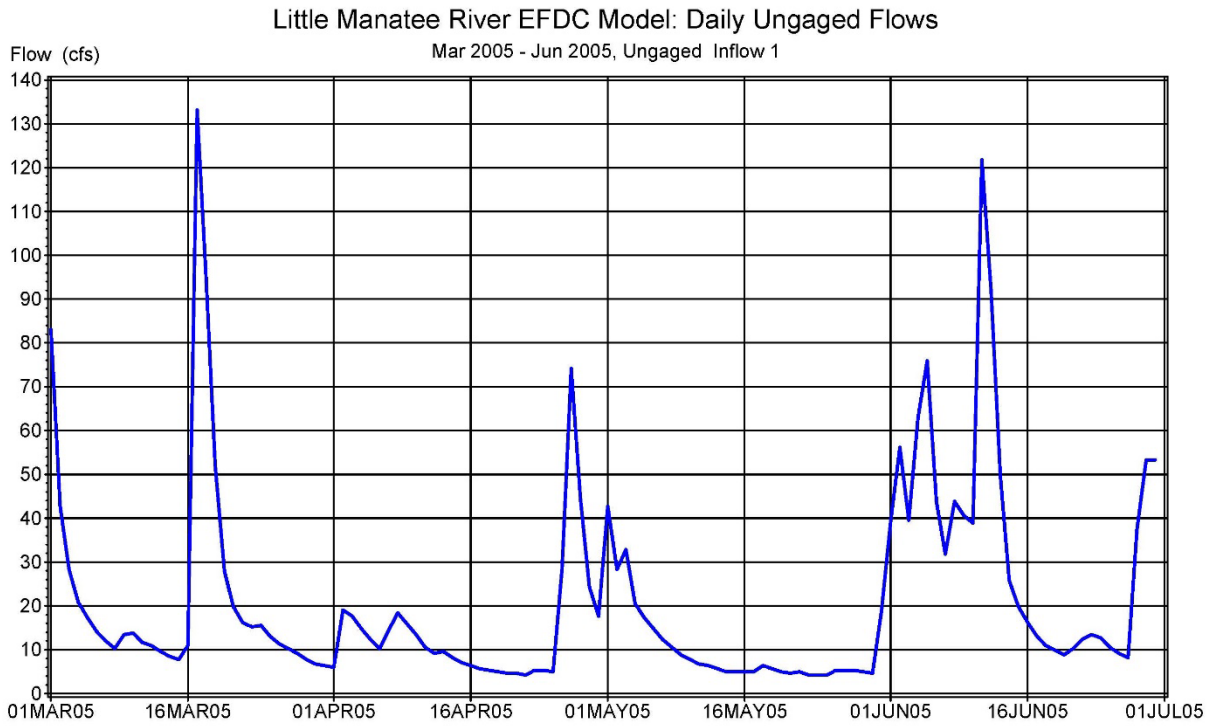


Figure A1-11. Inflows from ungaged location 1 for verification period March-June 2005.

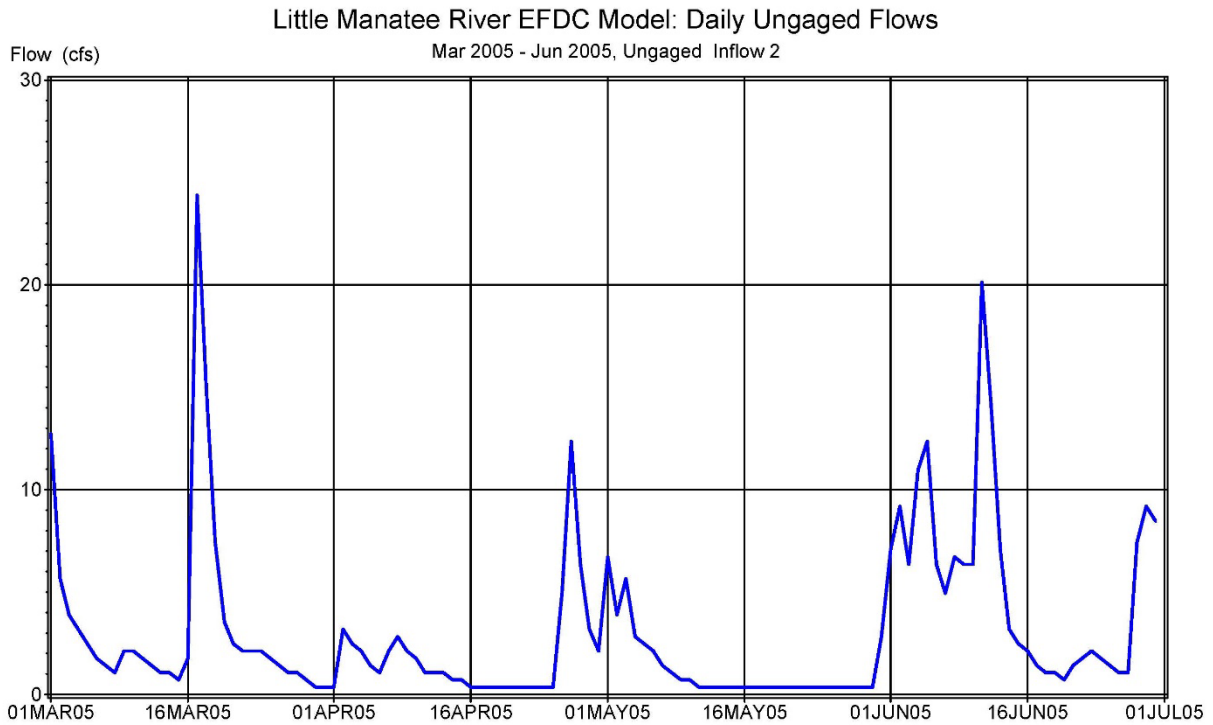


Figure A1-12. Inflows from ungaged location 2 for verification period March-June 2005.

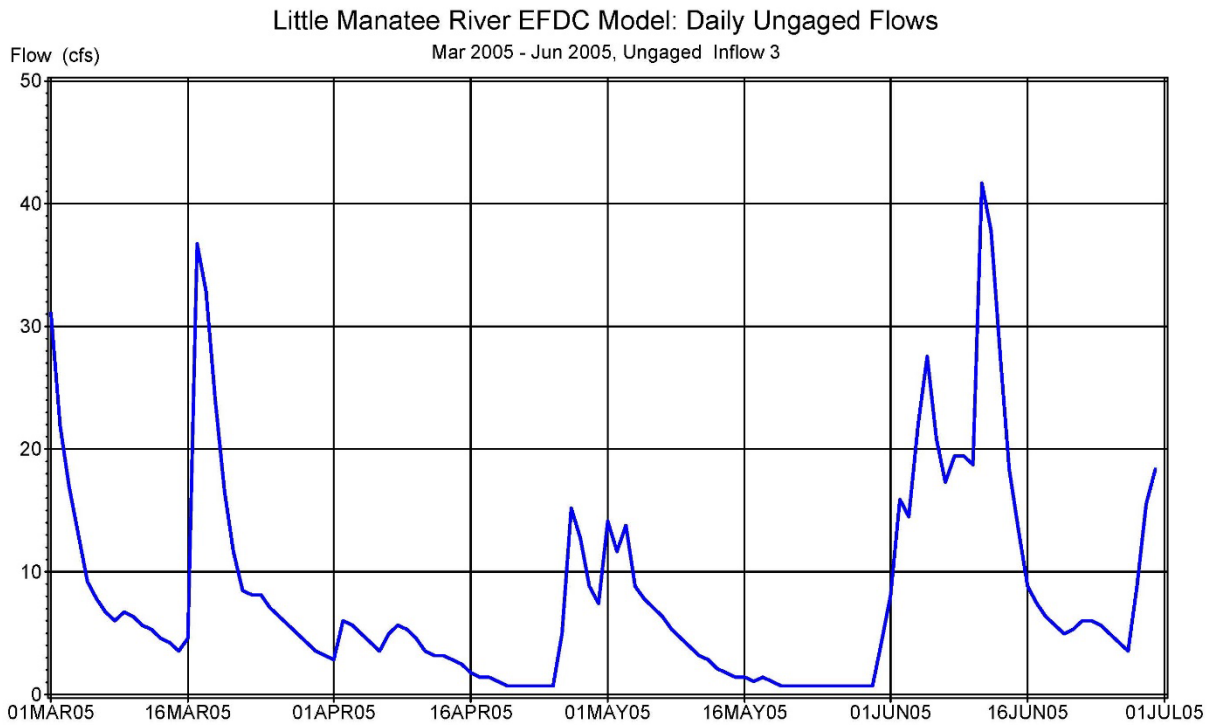


Figure A1-13. Inflows from unaged location 3 for verification period March-June 2005.

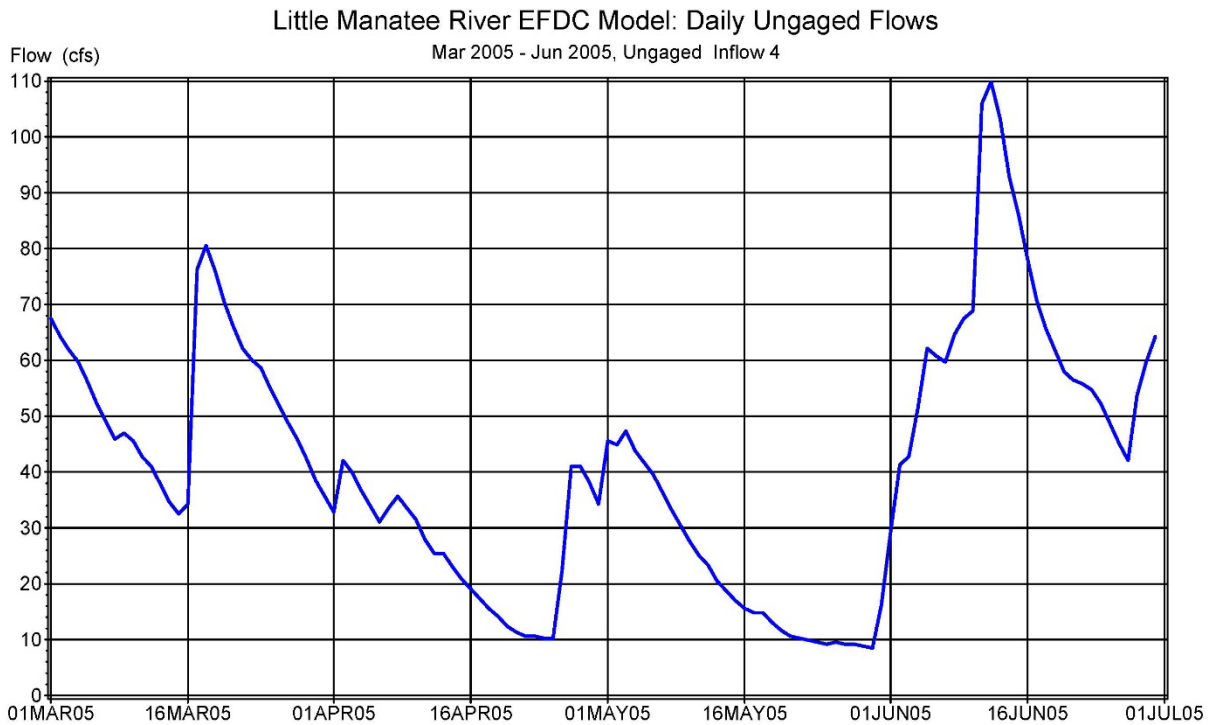


Figure A1-14. Inflows from unaged location 4 for verification period March-June 2005.

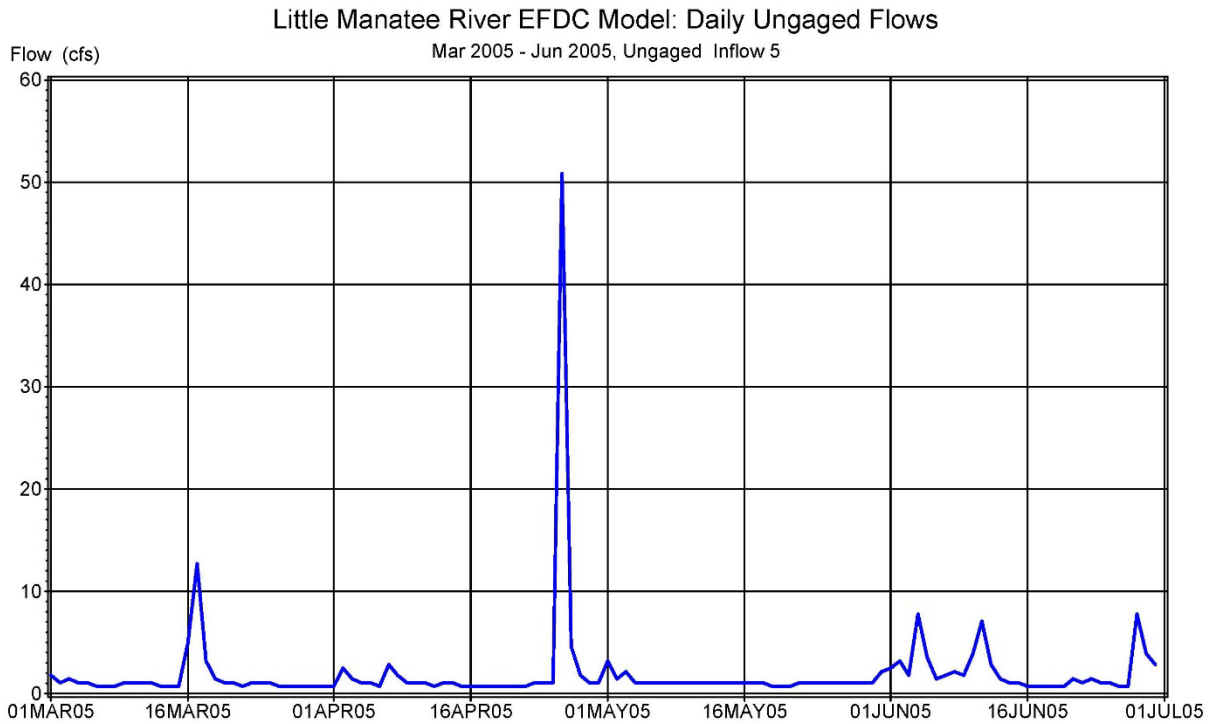


Figure A1-15. Inflows from ungaged location 5 for verification period March-June 2005.

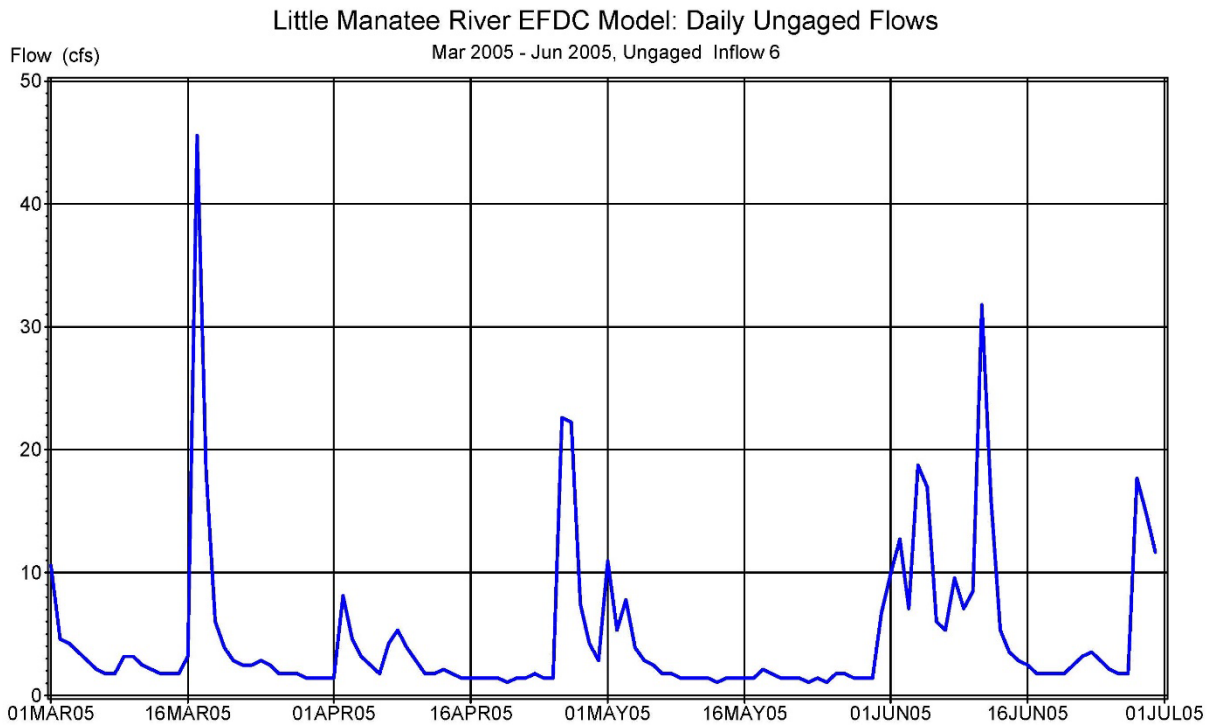


Figure A1-16. Inflows from ungaged location 6 for verification period March-June 2005.

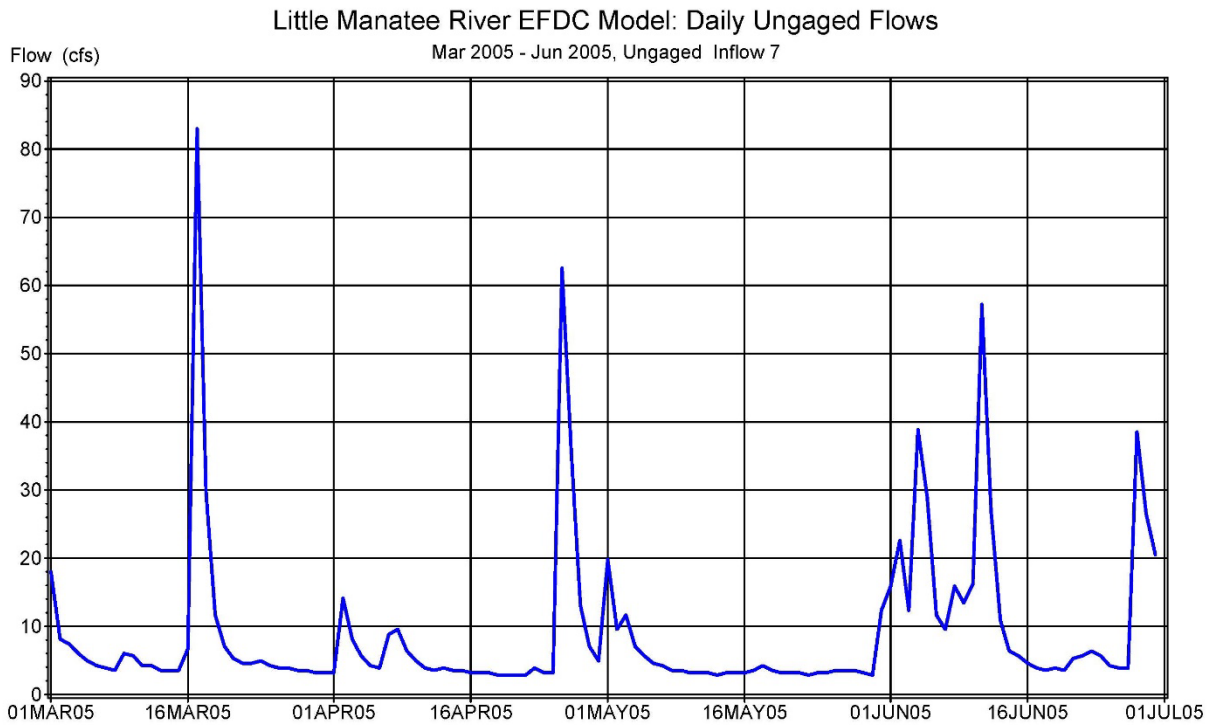


Figure A1-17. Inflows from unaged location 7 for verification period March-June 2005.

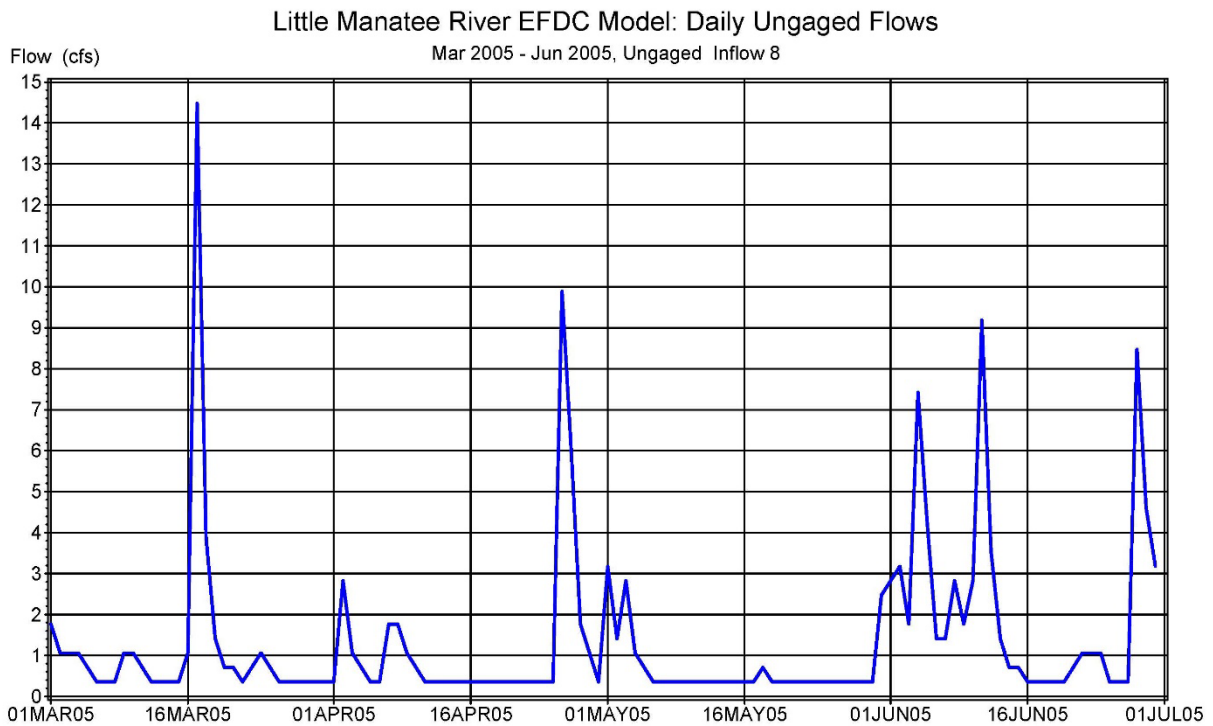


Figure A1-18. Inflows from unaged location 8 for verification period March-June 2005.

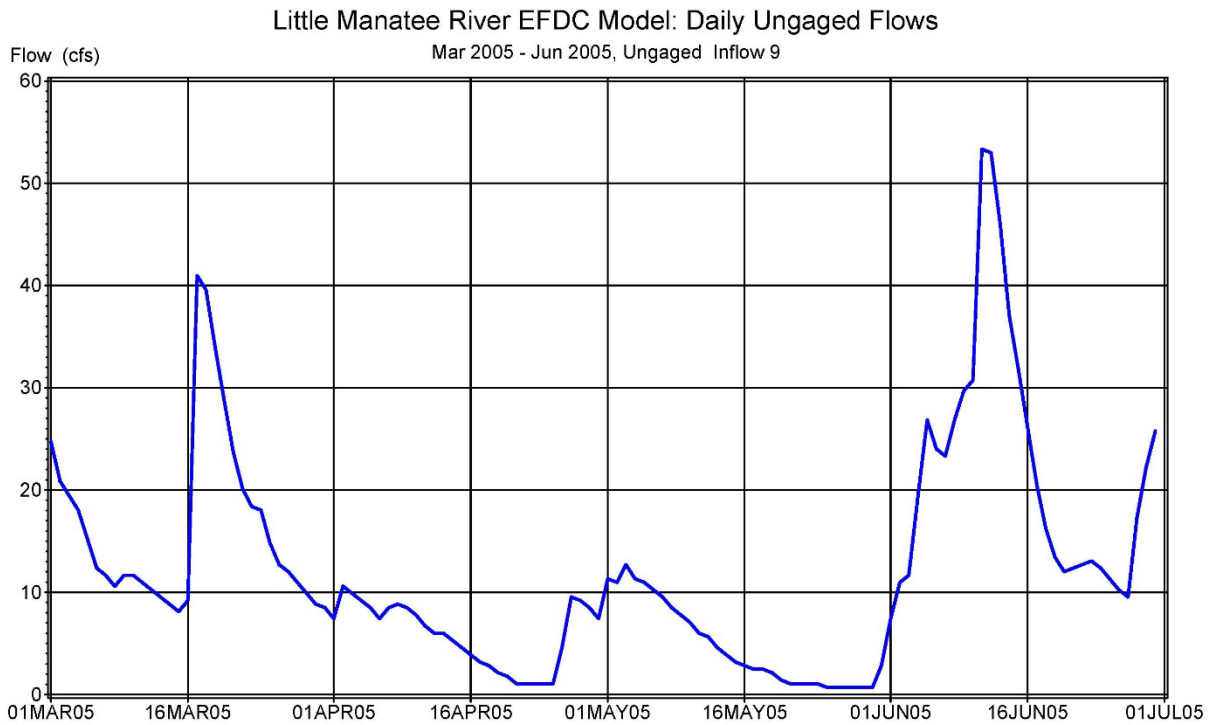


Figure A1-19. Inflows from ungaged location 9 for verification period March-June 2005.

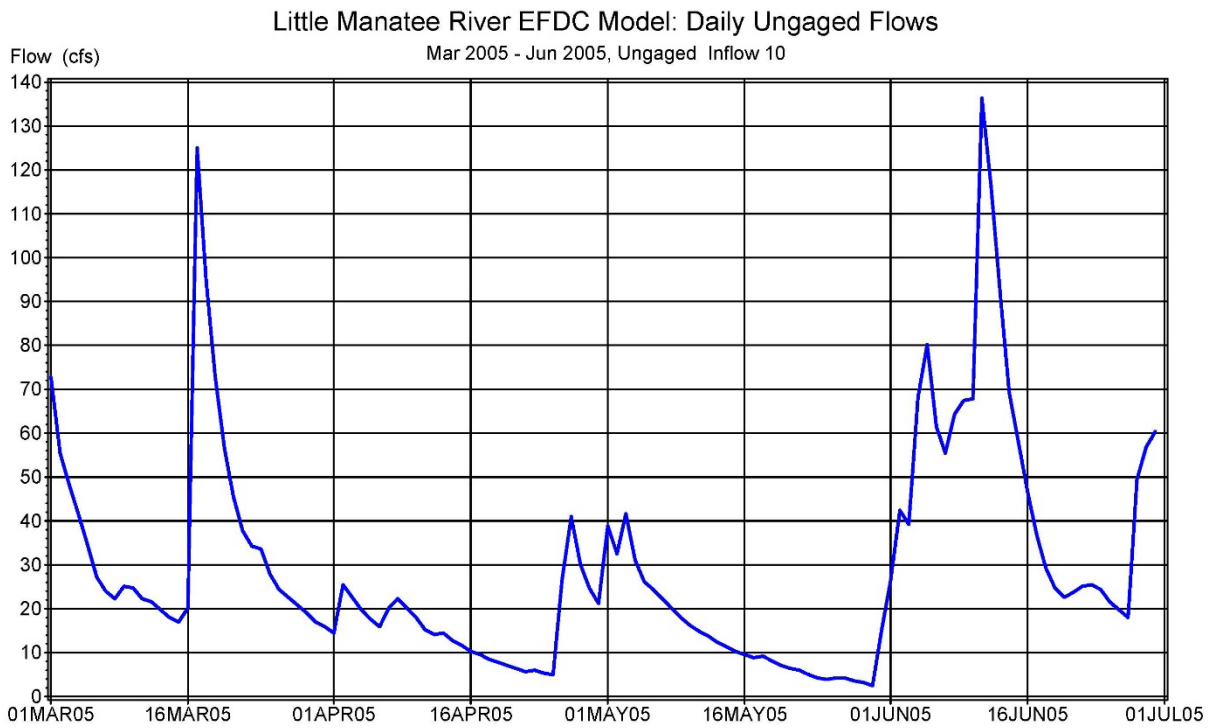


Figure A1-20. Inflows from ungaged location 10 for verification period March-June 2005.